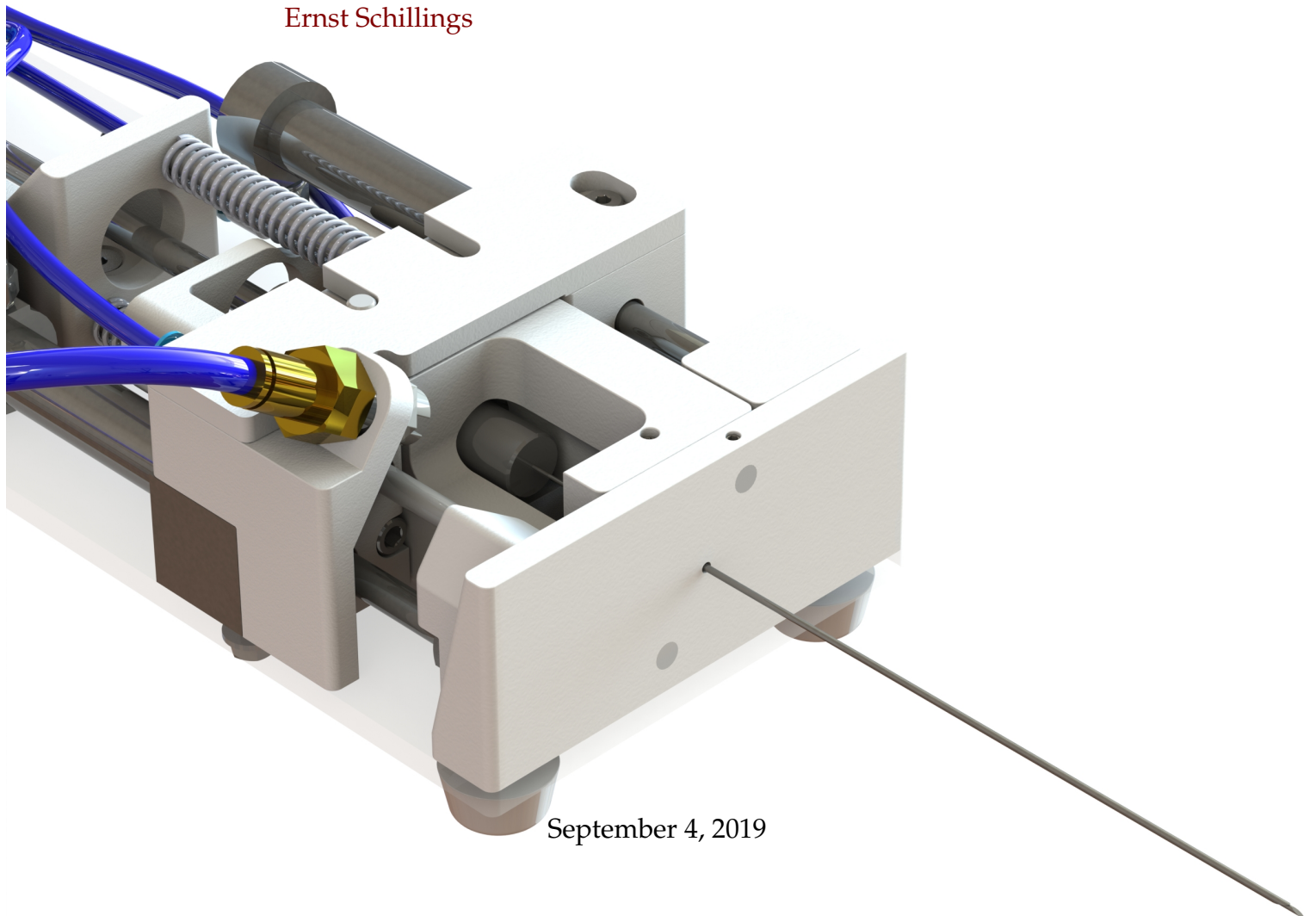TU Delft

Master Thesis

A biopsy system that can automatically sample and remove prostate biopsy samples

---

Author:
Ernst Schillings

September 4, 2019

Supervisors

Dr. John van den Dobbelsteen

Pieter Wiskerke

Committee

Dr. John van den Dobbelsteen	Department of Biomedical Engineering
Pieter Wiskerke	Business Development Manager at Demcon
ir. Jo Spronck	Department of Precision and Microsystems Engineering
Martijn de Vries	Department of Biomedical Engineering

Summery

Suspicion of prostate cancer is based on diagnostic tests such as Prostate-Specific-Antigen (PSA) screening or a Digital-rectal-exam. Prostate needle biopsy can be performed to confirm the diagnosis and determine the stage of the disease. The golden standard in prostate biopsy is the trans-rectal biopsy under ultra-sound guidance (TRUS). TRUS is a relative cost-effective approach, though it has the limitation of having a low prostate cancer detection rate (PCa). Several approaches have been introduced into the clinical practise with the goal of increasing the PCa. A succesfull alternative approach is the trans-perineal (TP) biopsy under MRI guidance [1]. Physicians often use this approach for rebiopsies. A patient requires a rebiopsy if the initial biopsy gave a negative result, while the PSA-screening test remained showing positive result. In contrast to TRUS, TP under MRI guidance is quite expensive. The costs differ about five-fold [2]. Reducing the procedure time might result in a cost reduction. One of the more time-consuming parts of a biopsy under MRI guidance is the biopsy needle insertion, tissue sampling and needle retraction. Currently, the physician performs these steps manually, which can only be done when the patient is removed from the MRI-bore. An MRI-safe biopsy system that can automatically sample, remove and store multiple biopsy samples can make TP procedure under MRI guidance more time-efficient.

This thesis tackled several challenge related to the development of such an automatic biopsy system. First of all, the tissue sample should be removed from the biopsy needle without human intervention. The State of the Art research showed that vacuum-suction was the dominant removing technique in breast biopsy. Automatic sample removing techniques used for prostate biopsy were non-existent. In this thesis, vacuum-suction was not used for the automatic biopsy system. On the grounds that vacuum-suction only proved to be viable with 13G needles and not with 18G or smaller needles. The fragmentation rate of vacuum-suction proved to be already higher than with the manual technique [3]. Decreasing the diameter of the biopsy needle could raise the fragmentation rate even more, which could lead to tissue loss and perhaps lost diagnostic information. Therefore, a novel technique to remove a tissue samples from a biopsy needle was developed. Flushing with saline showed to have potential during several pilot tests. The samples were removed properly while ensuring a low fragmentation rate.

The second challenge was to fire and reload the biopsy needle without human intervention. A concept was created that implemented both the first and second challenge. Here, a pneumatic cylinder both fired and reloaded the stylet. A compression spring fired the cannula while two pneumatic cylinder ensured automatic reloading. The concept scored high in criteria such as inducing no MRI distortion, ensuring a high cannula velocity and low costs.

The concept was realized in a Proof of Principle prototype. Requirements such a 'MRI-conditional' and 'position accuracy' were discarded during this phase for

the sake of cost and lead-time reduction. The prototype was verified against the product specifications (PS). The most important PS could only be verified by testing. These PS were related to the stylet and cannula velocity, the tissue sample quality and the removing of the tissue sample. As sampling on live human prostate was not possible at this stage of the product development, sampling was done on raw chicken breasts. The samples were compared to the ones taken with a standard 18 biopsy needle

The results showed that the velocity of the stylet was acceptable, while those of the cannula was insufficient. This did not result in a reduction of the sample quality though. Surprisingly, the results showed the exact opposite. The samples taken with the automatic biopsy system were significantly longer that the ones taken with the standard biopsy needle. A tissue sample might appear to be longer if the parts of a fragmented samples are compressed together. This could be a explanation for the surprisingly increase of sample length. 93.4% of all the tissue sample were entirely removed from the biopsy needle. Flushing with more liquid could remove the remaining waste. Furthermore, 4.4% of the removed samples were deposited in the container.

Samples taken with a vacuum-assisted 11G biopsy needle were fragmented in 43% of the cases [3]. The automatic biopsy system presented in this thesis project had a fragmentation rate of 20%. This figure is already twice as low compared the vacuum technique. All this was accomplished with a two times smaller diameter. This thesis project showed the potential of the automatic biopsy system that uses flushing to remove the tissue sample from the biopsy needle. Other techniques such as vacuum-suction cannot be discarded as its potential with smaller diameter needles is unknown. Making substantiated conclusions can only be done if both methods were tested on similar specimens and with the same diameter needle.

Contents

viii

List of Abbreviations

ASTM	American Society for Testing and Materials
CT	Computer Tomography
DCEI	Dynamic Contrast-Enhanced Imaging
DWI	**Diffusion** Weighted Imaging
DRE	Digital Rectal Exam
EC	End-Cut
IGTpB	Image Guided Targeted Prostate Biopsy
mpMRI	**m**ulti-**M**parametric Magnetic Resoance Imaging
MR	Magnetic Resoance
MRI	Magnetic Resoance Imaging
MRSI	Magnetic Resoance Spectroscopy Imaging
PCa	Prostate Cancer detection rate
PLA	PolyLacticAcid
PS	Product Specifications
PSA	Prostate Specific Antigen
RF	Radio-Frequency
SAR	Specific Absorption Rate
SC	Side-Cut
T2WI	T 2 Weighted Imaging
TP	Trans Perineal
TPUS	Trans-Perineal Uultra-Sound guided
TR	Trans Rectal
TRUS	Trans-Rectal Uultra-Sound guided
UR	User Requirements

List of Symbols

a	Acceleration	$\mathrm{m\,s^{-2}}$
A	Surface area	m
C_d	Drag coefficient	
C	Spring constant	$\mathrm{Nm^{-1}}$
d	Diameter	m
F	Force	N
m	Mass	Kg
P	Pressure	Bar
Q	Flow rate	$\mathrm{l\,s^{-1}}$
u	Extended distance	m
V	Velocity	$\mathrm{m\,s^{-1}}$
ρ	Density	$\mathrm{Kg\,l^{-1}}$
η	Efficiency	
θ	Angular velocity	$\mathrm{Rad\ s^{-1}}$

Thesis outline

This graduation report is divided into four parts (see Figure 1). The first part introduces the problem definition and scope. This includes finding background on prostate needle biopsy and compiling the clinical workflow. Part B describes the process of developing a method to automatically remove the tissue sample from a biopsy needle. Part C reports the development of an automatic biopsy system. The sample removing method developed in Part B will be implemented in the design of an automatic biopsy system. First, requirements and specifications are defined. Then, several concepts are created and the most promising is selected. A more elaborated design is realized in a Proof of Principle prototype. Finally, the prototype is verified against the product specifications in Part D.
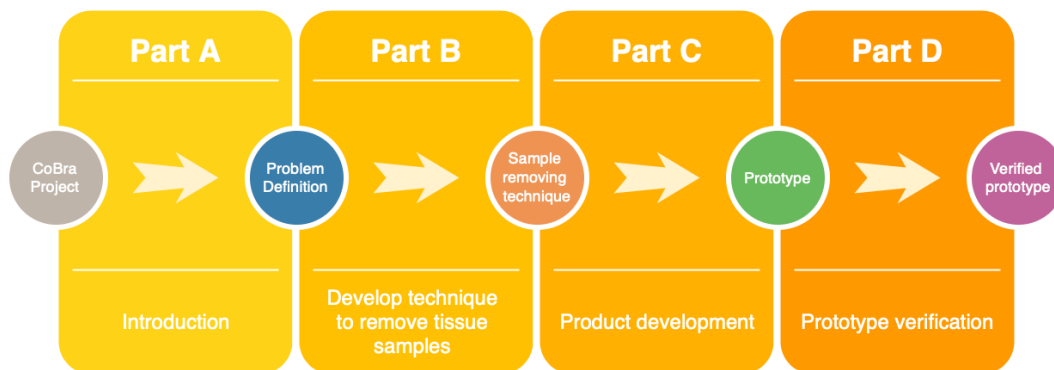
FIGURE 1: This figure shows the outline of this thesis project.

Part A

Introduction

Chapter 1

Project information

This chapter gives an introduction into the thesis project (Section 1.1). The background of the project and the involved parties are discussed in subsequent sections.

1.1 Project introduction

Prostate cancer is the second most common cancer among men around the world (see Figure 1.1)[4]. It is diagnosed by microscopically evaluating prostate tissue samples, which are retrieved with a biopsy needle. The golden standard of prostate biopsy needle is the trans-rectal approach under ultra-sound guidance (TRUS). However, TRUS has the limitation of having a low prostate cancer detection rate (up to 40%) [1]. MRI-guided prostate biopsy has been introduced into the clinical practice to increase the accuracy of prostate cancer detection up to 98% [1]. However, a procedure with MRI imaging is on average 5 times more expensive than one that uses conventional ultra-sound (US) imaging. The mean charge per procedure for MRI and US is, respectively, ±$2000 and $400 [2]. A MRI-safe system that can automatically sample, remove and store tissue samples can make a biopsy procedure under MRI-guidance more time-efficient and, therefore, less expensive.
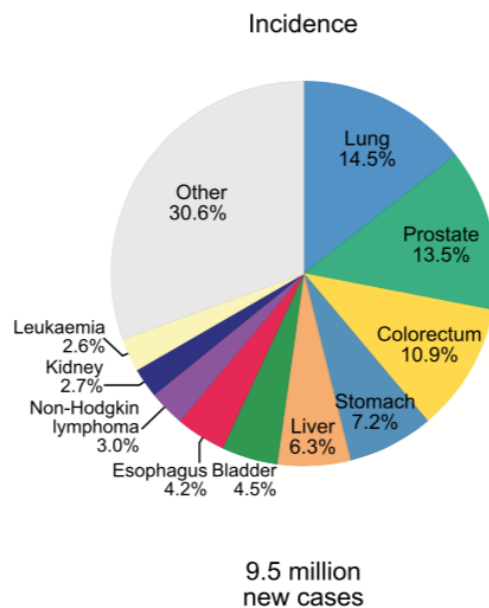
FIGURE 1.1: Distribution of cases and deaths for the 10 most common cancers in men in 2018. Image retrieved from [4].

1.2   Demcon

This graduation project is commissioned by Demcon, which is a high-end technology supplier of medical and other mechatronic systems. Demcon was founded in 1983 as a mechatronic engineering firm. The company has an in-house product facility. Therefore, they can provide services from proof of principle prototype to preproduction and serial production [5]. Besides the head office in Enschede, Demcon is represented in other offices in Best, Munster, Groningen and Delft. Demcon has over 600 employees and is still growing vastly. The ambition of Demcon is *'to realize further growth by addressing new and challenging projects, surveying new international markets and further expanding its production expertise and capacity'* [5].

1.3   CoBra

Demcon takes part in a subsidiary project called 'CoBra'. This project is a collaboration between companies and universities in the 2 Seas region (see Figure 1.2). The project was launched in January 2018 and the planned end date is set at September 2022.

FIGURE 1.2: The 2 Seas region is highlighted in this figure. Figure retrieved from [6].

The CoBra project *'aims to improve quality of both diagnosis and treatment of localized cancers, by developing a new medical robot prototype for brachytherapy and biopsy under*

guidance of MRI' [6]. The involved parties are shown in Figure 1.3. The entire project was divided into sub-tasks. Demcon is responsible for the development of an automatic biopsy system that can be used in CT and MRI environment.

FIGURE 1.3: Lead partners, partners and observers that participate in the CoBra project. Figures retrieved from [6].

Chapter 2

Problem definition and scope

The problem of this thesis project is defined in Section 2.1. The boundaries of the project are determined in Section 2.2.

2.1 Problem definition

Trans-rectal ultrasound guided (TRUS) prostate biopsy is the golden standard for diagnosing prostate cancer in men with elevated Prostate-Specific-Antigen (PSA) levels. PSA is a bio marker for prostate cancer. However, sometimes the initial biopsy can be labelled as negative while the PSA levels remains elevated. In these cases, the physicians perform a rebiopsy . Although TRUS is relatively cost-effective, it has its limitations that can lead to requiring such a rebiopsy. One of the limitations of TRUS is that cancer tissue only appears as a dark spot on the US-image if it is hypoechoic. Usually only 20-30% of cancer tissue is hypoechoic, while up to 40% is isoechoic [7][8][9]. This means that TRUS is unable to detect a significant part of the cancer tissue. Besides that, TRUS has a cancer detection rate between 27-40% [1], which is rather low. Performing prostate biopsy with the TRUS approach can cause underestimation of high risk prostate cancer or overestimation of clinically insignificant cancer [10][11].

Another disadvantage of the TRUS approach is that the anterior, midline and apex of the prostate are hard to sample via the trans-rectal route. Entering the prostate via the perineum results in the detection of significant more cancer tumours in these areas [12][13]. Therefore, the current practice is to perform a rebiopsy under MRI guidance. Using the trans-perineal approach under MRI guidance improved the cancer detection rate and the accuracy of the disease grading significantly [14].

Here, the patient is positioned in the MRI bore, while a MRI-scanner takes an image to locate the lesion. Subsequently, the patient is removed from the MRI bore and the physician inserts the biopsy needle manually into the lesion. To check the position of the needle, the patient is moved back into the scanner and additional MRI-scans are taken.

Taking into account that sometimes up to 20 samples can be taken per patient, such a trans-perineal procedure under MRI guidance is often quite time-consuming and can lead to increased costs. Especially in comparison to conventional TRUS biopsy. Whereas the mean charge per procedure for MRI and US is, respectively, ±$2000 and $400 [2]. A MRI-safe biopsy system that can sample, remove and store a tissue sample of a biopsy needle without human intervention can make the procedure more time-efficient. This means that the patient remains positioned in the MRI-bore during the entire procedure. MRI-scanning, needle insertion and tissue sampling can be performed consecutively with such an automatic biopsy system. MRI-safe biopsy

guns are widely available but they require manual loading and sample must be removed by hand. Therefore, a method must be developed to remove the sample from the biopsy needle without human intervention.

2.2 Scope of thesis

As described in the problem definition, a biopsy system that can automatically sample, remove and store a tissue sample is considered to make a trans-perineal biopsy under MRI guidance more time-efficient. Designing such an automatic biopsy system poses several challenges.

The main challenge is to remove the tissue sample from the biopsy needle without human intervention. Failing to remove the tissue sample from the biopsy needle can result in not being able to take multiple samples, which is considered to be one of the main added values of the system in comparison to the standard biopsy needles. Therefore, developing a method that can remove a tissue sample from a biopsy needle has the highest priority. This method will be tested by constructing a proof of principle prototype.

Removing the tissue sample from the biopsy needle can only be done after the tissue sample is automatically retrieved. Taking a tissue sample with a standard needle is done by firing the biopsy mechanism. When taking subsequent tissue samples, manual reloading of this mechanism is required. Automating this manual reloading process is the second challenge that will be tackled in this thesis project and implemented in Proof of Principle prototype.

Accurately positioning and inserting the needle into the lesion without human intervention is outside the scope of this thesis project. Ideally, the tissue samples should be stored under certain conditions and sorted with respect to their sample location. Again, this is outside the scope of this project. Also, at this stage of the development, the prototype does not have to be MRI-safe yet. Although, it must be kept in mind during the design process. Aspects that are out of the scope of this project should be addressed in future projects.

Chapter 3

Prostate needle biopsy

This chapter provides background on prostate needle biopsy. The anatomy of the prostate is discussed in Section 3.1. The second section introduces needle biopsy. A needle biopsy procedure can be performed according to different biopsy approaches. Their advantages and disadvantages are explained in Section 3.3. Section 3.4 discuses the handling of tissue sample after sampling. Then, the criteria that determine the quality of the tissue sample are mentioned in Section 3.5. Finally, Section 3.6 discuses the different type of biopsy needles.

3.1 Prostate zones

The prostate has four zones: peripheral zone, central zone, transitional zone and anterior fibromuscular stoma (anterior region). Only the last zone, does not contain glandular tissue [15]. Prostate cancers develops in glandular tissue. Figure 3.1 shows the zones of the prostate. The urethra and ejaculatory ducts run through the prostate gland. These tracts should be avoided during biopsy needle insertion.
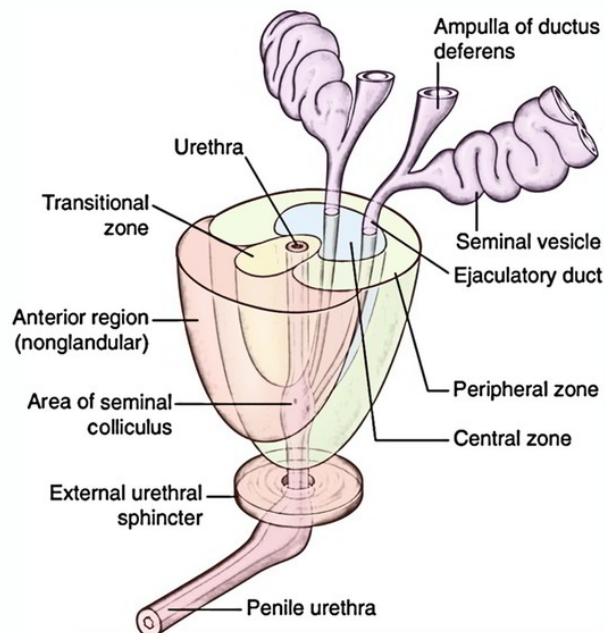

FIGURE 3.1: This figure shows the four zones of the prostate gland. Here, green is the peripheral zone, orange the anterior fibromuscular stoma, yellow the transitional zone and blue the central zone. Figure retrieved from [16].

Most prostate cancers develop in the peripheral zone (75%) and only a small portion develop in the transition zone (20%) [15][17]. The cancers in the former zone are often more aggressive [15].

3.2   Diagnosing prostate cancer

Early detection of significant prostate cancer can avert the related death or prevent the disease to progress. Prostate cancer is diagnosed by microscopically evaluating prostate glandular tissue. Prostatic glandular tissue, which makes up for 70% of the prostate, is examined and screened for adenocarcinomas (cancer or tumour tissue) [18].

Biopsy of the prostate was introduced into the clinical practice in the early 1900s [19]. At this time, the open technique was the only option. Here, an incision made in the perineum revealed the prostate. Some decades later, the needle based approach with finger guidance through the rectum replaced the open technique. Guidance with the finger was in this time the only option because ultrasound, x-rays or MRI were not discovered yet.

A positive Digital Rectal Examination (DRE) or elevated Prostate-Specific Antigen (PSA) levels, which is a biomarker for prostate cancer, leads to a prostate needle biopsy procedure. The goal of screening for PSA is to determine the stage of the disease. The benefit of PSA-screening has been disputed though but it is still the test to determine whether a patient requires a prostate biopsy [20].
Sometimes the initial biopsy is negative whilst the PSA levels remain elevated. In these cases, rebiopsy is necessary. Often, these rebiopsies are performed using alternative scanning techniques or needle insertion points.

3.3   Biopsy approaches

Needle biopsy of the prostate can be performed via different approaches. Finger guided trans-rectal (TR) prostate biopsy has been part of the clinical practice since 1937 [21]. The control of the needle in combination with the guidance of the finger was considered to be good. However, faecal contamination is a serious problem.

During the 1970s, finger-guided prostate biopsy was replaced by ultra-sound guided biopsy [22]. This approach is known as trans-rectal ultrasound (TRUS) guided prostate biopsy (see Figure 3.2a). Here, a probe with an ultrasound transducer is inserted into the rectum. The output of this probe is used to make ultrasound images. These images are used to locate the prostate and possible lesions. A biopsy needle is guided through the biopsy probe to the desired location in the prostate. The location of the needle is real-time visible on the ultrasound images.

Two type of probes are used: end-fire and side-fire. Meaning that the biopsy needle exits the probe from the end or from the side. Studies showed that the type of probe is positively correlated with the detection rate of cancer [23][24]. The superior performance of the end-fire compared to the side-fire was most dominant at the lateral and apical regions of the peripheral zone (the squares in Fig. 3.3).

(A)   (B)
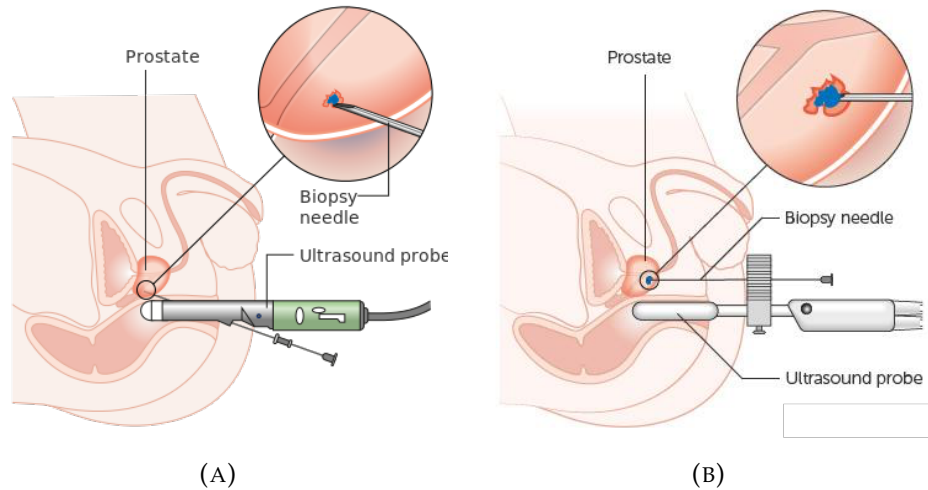
FIGURE 3.2: These figures illustrate the trans-rectal (A) and trans-perineal (B) ultrasound guided prostate biopsy approach. Figures retrieved from [25].
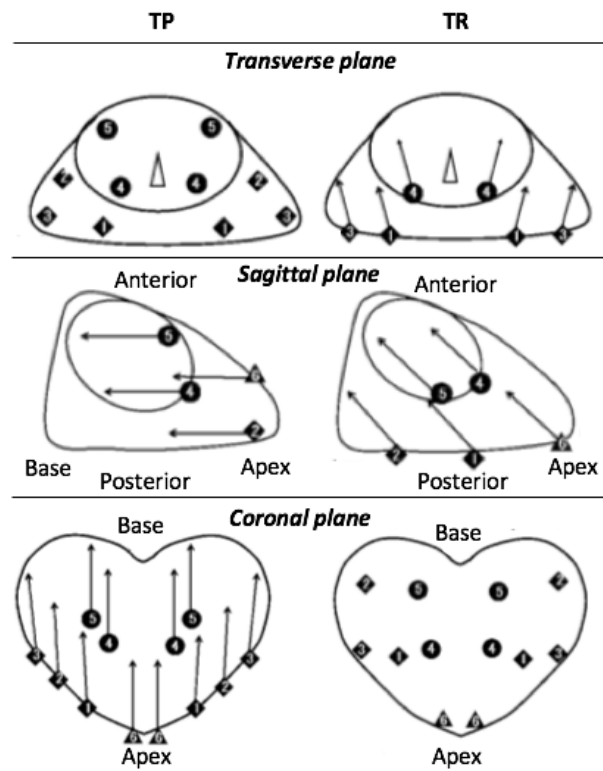
FIGURE 3.3: This figure shows the sample location for 12-core prostate biopsy with the trans-perineal (TP) and the trans-rectal (TR) approach. The sampling locations (squares, circles, triangles) and direction of sampling (arrows) are drawn in the transverse, sagittal and coronal plane. The squares, circles and triangles represent, respectively, sample locations in the peripheral zone, transition zone and apex. Figure retrieved from [13].

Another approach is the trans-perineal biopsy procedure (see Figure 3.2b). Here a biopsy needle is inserted through the perineum into the prostate under transrectal ultra-sound guidance. This approach is known as trans-perineal ultrasound (TPUS) guided prostate biopsy. Studies have shown that TP resulted in significantly higher detection rates, mainly for anterior tumours, and has clinical advantages

over TRUS guided biopsy [12][13]. Figure 3.3 shows the direction of sampling of 12 cores for both the TP and TR approach. TPUS allowed for better sampling of the anterior side of the peripheral zone.

A more recent accepted approach is the prostate biopsy using multiparametric MRI (mpMRI) scanning. Although, this technique was initially tested in the beginning of the 1980's, the clinical applications were limited because the magnetic field was insufficiently strong [26]. This resulted in poor image quality. Nowadays, standard MRI-scanners can have a magnetic field strength of up to 3T, meaning that also the image quality improved considerably over the years.

mpMRI can be defined as obtaining a 3D prostate image by combining T2-weighted (T2WI), diffusion weighted (DWI), dynamic contrast enhanced (DCEI) and MRI spectroscopy (MRSI) images [26]. There are three different kinds of biopsy approaches under MRI-guidance: (1) Cognitive fusion biopsy, (2) Image-guided targeted prostate biopsy (IGTpBx) and (3) In-Bore biopsy.

With cognitive fusion biopsy, the practitioner combines mpMRI images with real-time TRUS imaging without the use of software. Pech et al. showed that with Cognitive fusion biopsy more clinical significant prostate cancer tumours were detected.
In contrast to cognitive fusion biopsy, IGTpBx does use software to merge pre-processed MRI-images with real-time ultrasound images. This resulted in a significant increase of the cancer detection rate [27].
Finally, with In-Bore biopsy the patient is positioned inside the MRI-bore and real-time imaging can be performed. As several MRI-images are taken to localize the lesion and confirm the position of the needle, the procedure time is considerably longer than with conventional TRUS or TPUS. The limited space inside a MRI-bore is considered to be a drawback as well. Often, the patient is removed from the MRi-bore to be able to insert and fire the biopsy needle. Besides that, biopsy in an MRI-environment requires specialized equipment.
The gain in detecting more clinical significant cancer with In-Bore clearly outweighed these drawbacks. Pokorny et al. showed that MRI In-Bore biopsy increased detection of intermediate or high-risk prostate cancer detection rate by 17.7% compared to TRUS biopsy. Similar results were reported in [28]. A significant difference in cancer detection rate of 14% was observed. These studies showed that mpMRI In-Bore biopsy has a high potential. All three mpMRI methods outperformed the standard TRUS biopsy procedure [29].

3.4 Handling of tissue samples

Sampled prostate tissue is manually removed from the biopsy needle. This is done with the following two techniques: (1) wiping the needle on a saline soaked sponge or (2) passing the needle over the edge of a biplicated filter paper. Tissue samples are removed with care to prevent deformation or fragmentation [30]. Prostate biopsy samples are often, immediately after removing, embedded and flattened in filter paper or saline socked sponges [30].

The samples are stored in a container and brought to the pathology department for screening. On arrival in the laboratory, the samples are straightened, fixated in

formalin, embedded in paraffin and cut into slices with a maximum thickness of 4μ. Van der Kwast et al, explained the processing of prostate biopsy samples [31]. The pathologist microscopically evaluates the slices and reports the type of cancer, grading of cancer and if possible, the staging. Grading of cancer is done using the Gleason score, which is composed of the dominant grade and the worst grade present. The Gleason score can range from 6 to 10 [32].
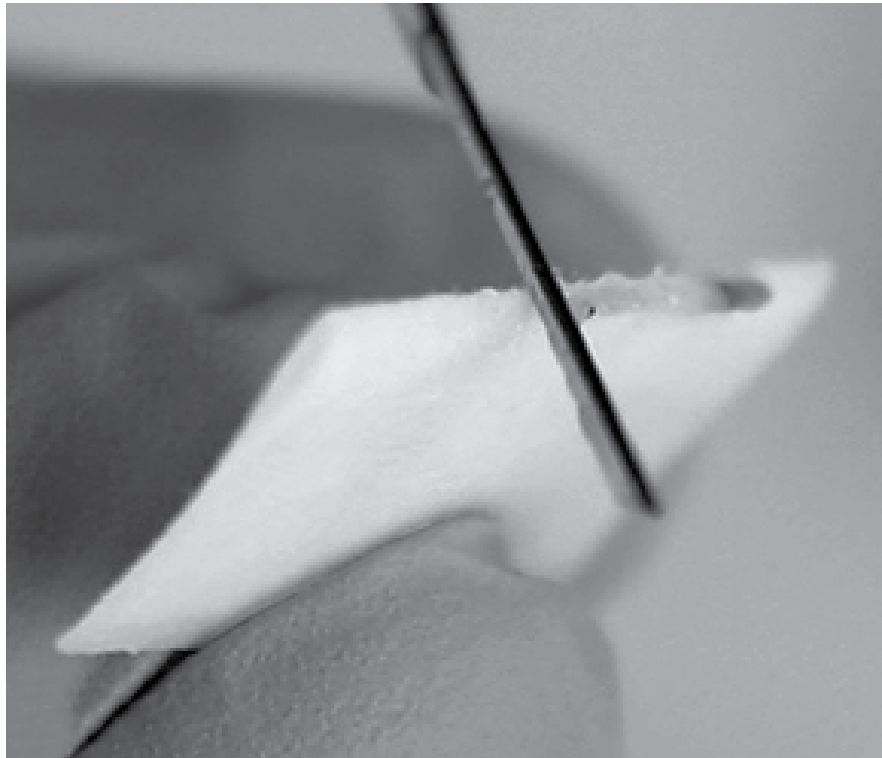
FIGURE 3.4: Figure illustrates the manual removal of tissue sample from a biopsy needle by wiping it on the edge of a biplicated paper. Figure retrieved from [30].

3.5   Evaluating the quality of a tissue sample

The quality of tissue sample is obviously an important factor in the histopathological process. The urologist or radiologist who performs the procedure is responsible for determining the quality of the specimens. Processing of samples (e.g. embedding, cutting) can directly influence the quality [31]. Factors that determine the quality of the biopsy samples are length, amount of prostate glandular tissue or absence of extraprostatic connective tissue and degree of fragmentation [31]. A fragmented tissue sample is defined as a sample that is broken in two or more parts [32]. Tissue samples without glandular tissue are considered to be inadequate [32][31][33]. The presence of glandular tissue can only be defined by microscopic histologic evaluation, which is not always directly possible after sampling [33][34]

The length of a biopsy sample is a quality parameter that can be determined more easily. Tissue samples that are shorter than a certain length, also known as the cut-off length, are often marked as being of inadequate quality. The value of this cut-off length varies between studies. Some cut-off values are based on clinical data, others on expert opinions. Boccon-Gibod et al. [33] Bertaccini et al. [34] and Van der

Kist et al. [32] based their cut-off value of 10 mm on expert opinions. Other studies using clinical data reported somewhat higher values, 12,9 mm [35] and 12 mm [36]). According to Obek et al., retrieved samples longer than 11,9 mm resulted in a 2.5 times higher chance of prostate cancer detection.

3.6 Biopsy needles

Though needle biopsy has been part of the clinical practise for quite some time, the fundamental sampling mechanism of a biopsy needle has not evolved that much over the years. The sampling mechanism defines both the fundamental mechanism that is used to fill the sampling space with target tissue and the mechanism that separates the tissue from surrounding tissue. Several studies have compared the performance of different kind of sampling mechanisms. Two type of sampling mechanisms are reported in literature: the side-cut (Fig. 3.5) and the end-cut (Fig. 3.6). The side-cut mechanism is the golden standard, while the end-cut mechanism was proposed as an alternative in 1996 by Ascendia AB in Sweden [37]. The mechanisms will be briefly discussed.

(A) (B)
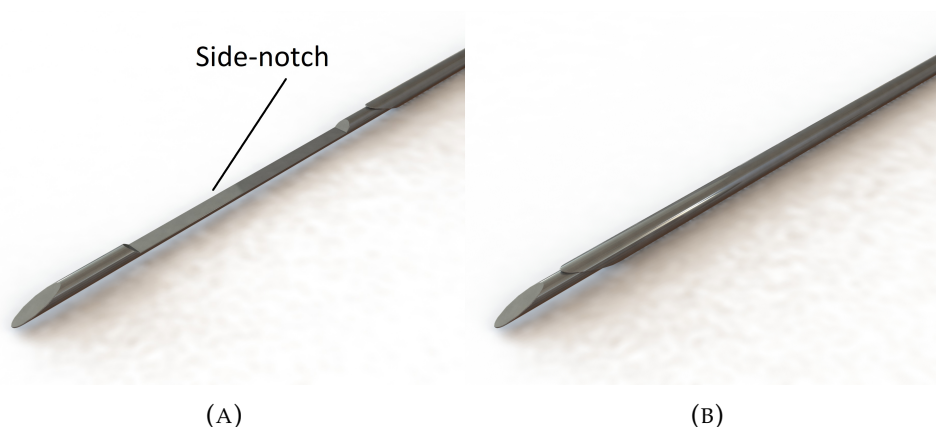
FIGURE 3.5: Mechanism of the side-cut biopsy needle in the open (a) and in the closed (b) position.

(A) (B)

FIGURE 3.6: Mechanism of the end-cut biopsy needle in the open (a) and in the closed (b) position.

Most of the biopsy instruments use the side-cut method to cut the tissue and retrieve the sample (see Fig. 3.5). A side-cut instrument consists of an inner needle (stylet) with a notch that is pushed through an outer sheath (cannula). The inner

needle can axially translate through the outer sheath. A biopsy sample is retrieved by pushing the stylet out of the cannula into the target tissue. The notch is fi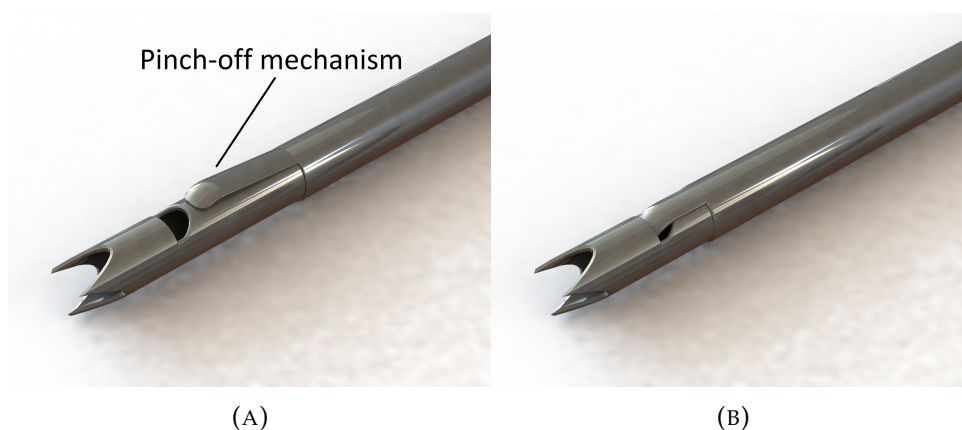lled with the target tissue. The tissue is then cut by moving the cannula over the stylet at a high speed. This linear movement is actuated by releasing a loaded spring. The entire needle is pulled from the body and the sample can be collected by manually reloading the cannula and pushing the inner needle out. The available side-cut biopsy instruments have a cutting length of 17 - 30 mm [38].

The side-cut technique has two disadvantages. First of all, only the notch is filled with tissue, meaning that not the entire diameter of the outer sheath is used. Secondly, the tip of the inner needle cuts without being filled with tissue [39].

Why the first point is claimed to be a disadvantage was not explained nor supported by literature or clinical data. No other studies were found that mentioned this disadvantage. Three other studies mentioned the need for a higher cancer detection rate as motivation [38][40][41]. They hypothesized that more tissue resulted in a higher detection rate. This supports the second disadvantage that is mentioned in Haggarath et al. More tissue can aid the pathologist in sample evaluation and resulted in a higher cancer detection rate.

The end-cut technique has been developed to overcome these disadvantages. Again, the instrument consists of two parts, a hollow inner needle and an outer sheath. The outer sheath has a pinch-off mechanism at the end (see Fig. 3.6). The hollow inner needle is pushed into the target tissue. After the hollow needle is filled with tissue, the outer sheath is fired over the inner needle. The pinch-off mechanism is actuated by releasing a loaded spring and cuts the tissue at the end of the inner needle. The entire instrument is pulled back and reloaded to retrieve the sample. The instrument has three settings for the cutting length: 13, 23 and 33 mm.

The end-cut instrument was claimed to have three advantages over the side-cut method. Firstly, a fully cylindrical specimen can be sampled. Secondly, the specimen is cut from point of fire (at the end of needle). Thirdly, the stronger stroke force can cut the tissue more cleanly [42] and can decrease fragmentation [40].

Several studies have compared the performance of the side-cut and end-cut instruments in terms of mean length of samples, percentage of the maximum length, mean weight of samples, failed biopsy rate, pain, fragmentation rate, presence of small samples and cancer detection rate. The available literature on the side-cut and end-cut mechanism was compared in (see literature study in Appendix A). The type of sampling mechanism did not correlate with the cancer detection rate. Both needles sampled similar quality samples and caused equally amount of complications. However, the end-cut needle showed more failed biopsies. The side-cut method seems to be more suitable than the end-cut method.

There are strong indications that increasing the cutting length of side-cut biopsy needles resulted in an increased cancer detection rate. This was not the case with end-cut biopsy needles. A side-cut needle with a cutting length of 25 mm is recommended. This recommendation can be more substantiated after the influence of the cutting length on sample quality have been studied.

Finally, the diameter of the biopsy needle (16G, 18G or 20G) did not correlate with the cancer detection rate. There are indications that a large calibre needle increased the core quality, although hard evidence was not found in literature. No biopsy needle diameter was preferred over the other.

Chapter 4

Clinical workflow

As described in Chapter 2, an automatic biopsy system will be developed for In-Bore trans-perineal prostate biopsy under real-time MRI guidance. In order to determine the requirements of the automatic biopsy system, an overview of the clinical workflow of the above mentioned procedure is drafted. In section 4.1, the environment, in which the procedure is performed, is described. The medical personnel or staff involved in the procedure are mentioned in Section 4.2. The tasks that the medical personnel execute are mentioned and visualized in Section 4.3.

4.1 Clinical environment

The procedure is performed in an operating room that is equipped with a closed-bore-MRI-scanner (See Figure 4.1). The operating room can be divided in two separate spaces: one for the MRI-scanner and one for controls of the MRI-scanner. These rooms are shielded from one another to avoid interference and to meet safety guidelines. A MRI-bore has diameter of 60 cm.
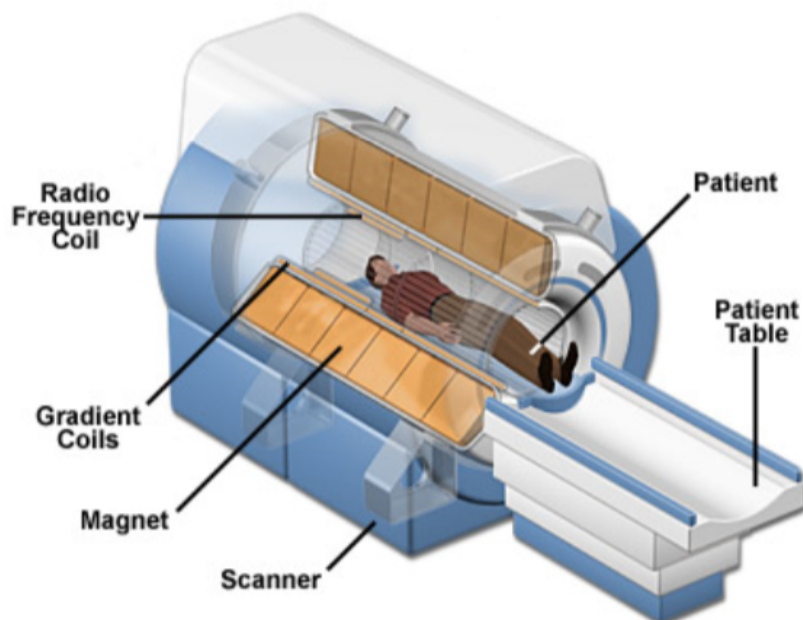
FIGURE 4.1: Cutaway of a MRI-scanner that is used for MRI-guided trans-perineal prostate biopsy. Figure retrieved from [43].

An MRI-scanner generates three major magnetic fields that can pose a risks for patient and staff [44]. The largest magnetic field B_0 is between 0.2 and 3T. The attracting forces generated by this field can accelerate large objects in the direction of the MRI-scanner. This attracting force depends on the distance between object and scanner. The second magnetic field is the radio-frequency field (RF), which is in the order of μT. The last magnetic field is the gradient field with amplitudes in the order of $100\frac{mT}{m}$. Low magnetic susceptible magnetic metals can be heated up by the RF field and gradient switching and can cause tissue damage. The allowed amount of heating is expressed in a Local Specific Absorption Rate (SAR) and is, according to the IEC standard, $10\frac{W}{Kg}$ [45].

The surroundings of a MRI-scanner can be divided into four different zones (see Figure 4.2) [46].

Zone I: The area outside the MRI environment that is freely accessible for the general public.

Zone II: Area between the freely accessible and controlled zones (III and IV). Patients are not freely to move without supervision of MR personnel.

Zone III: Contains for instance the MRI control room. This zone is only accessible through code protected doors.

Zone IV: This zone is in the room where the MRI-scanner is located. The walls of this room contain the five 0.5 mT, or 5 Gauss, line. Beyond this border, the magnetic field could affect metallic objects.
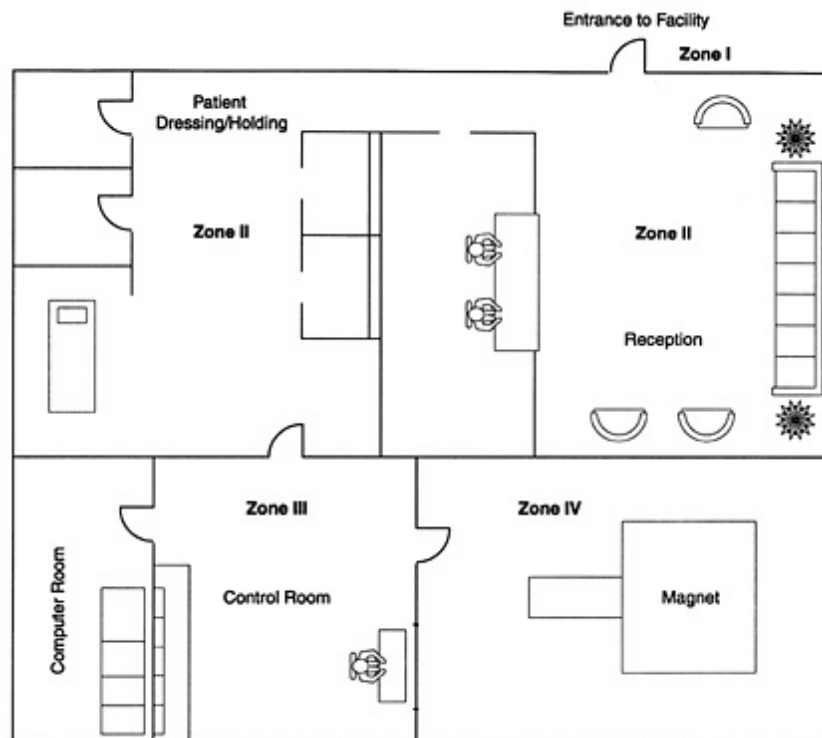
FIGURE 4.2: This figure shows the four zones (I to IV) surrounding a MRI scanner. Figure retrieved from [47]

Medical procedures that are performed under MRI-guidance require specialized equipment, which is considered safe to use in an MRI-environment. Medical devices can be labelled in terms of the hazards they pose in a MRI environment. Three different classes can be distinguished according to the ASTM standard [48]:

> *MRI-safe*: Medical device does not contain metallic, conducting or magnetic materials. The device does not pose any hazards in MRI environment of any strength.

> *MRI-conditional*: Medical device does not pose any hazards in a predefined MRI environment. The following parameters should be specified: static magnetic field strength, radio frequency (RF) fields, spatial gradient, time varying magnetic fields and specific absorption rate (SAR).

> *MRI-unsafe*: Medical device poses hazards in all MRI environments.

4.2 Involved staff

At least five people are involved in a standard MRI-guided prostate biopsy procedure. There is at least one physician, one anesthesiologist, one assistant, one MRI operator, and the patient. The physicians, the assistant and the MRI operator execute the procedure, although they all have different tasks. The entire staff is allowed to be in both the control and MRI-scanner room.

The tasks of the physician are to select the target lesion from the MRI-scan, insert and fire the biopsy needle, remove the tissue sample from the biopsy needle and determine whether additional sample are required. The anesthesiologist injects the anaesthetics. The MRI operator is responsible for taking the MRI-scans. The assistant performs all supporting tasks such as patient positioning, preparing patient, preparing operating equipment, disposing of operating equipment, and more.

4.3 Clinical workflow

The Clinical work-flow describes the order of tasks that are performed during a standard MRI-guided prostate biopsy procedure. A flow chart of the clinical workflow was shown in Figure 4.3. A standardized work-flow is non-existent. Literature [30], user-input of the CoBra project [49] and common knowledge were used to determine the main tasks and their sequence during the procedure. Therefore, in some hospitals additional tasks (extra scanning, etc.) can be added or tasks can performed in a different order. This is not expected to lead to different or additional design input.

As previously mentioned in section 2.1 of Chapter 2, the patient was slide in and out of the MRI bore several times (red boxes in Figure 4.3). At least twice, once before needle insertion and once after tissue sampling. These tasks are time consuming and need to be repeated when taking an extra sample. The flowchart shown in Figure 4.3 illustrated the need for a biopsy system that could automatize some tasks of the physician. These tasks were shown as green boxes in the flowchart.

FIGURE 4.3: This is a flowchart of the clinical workflow during a standard manual MRI-guided trans-perineal prostate biopsy procedure.

Chapter 5

Discussion Part A

In-bore trans-perineal prostate biopsy under real-time MRI guidance significantly increased the cancer detection rate and improved the accuracy of the disease grading. During such a procedure, the physician performs the sampling part manually. This requires the patient to be removed from the MRI-bore for several times. Taking into account that sometimes up to 20 samples can be taken per patient, the manual approach was considered to be time-consuming and, consequently, expensive. A biopsy system that can automatically sample, remove and store a tissue sample is considered to make a trans-perineal biopsy under MRI guidance less time-consuming. This thesis project mainly focuses on two challenges.

First of all, a technique will be developed to remove a tissue sample from a biopsy needle without human intervention. Automating the reloading of the biopsy needle is the second challenge that will be tackled in this thesis project. Both challenges shall be realized in a proof of principle prototype. Accurately positioning and inserting the biopsy needle is beyond the scope of this thesis.

Background on prostate biopsy was provided in the present part. For instance, prostate anatomy, biopsy approaches, tissue sample handling and tissue sample quality were discussed. Also, two type of biopsy needles were introduced: the side-cut and the end-cut biopsy needle. Literature indicated that the former is preferred over the latter.

In the last chapter of this part, the clinical workflow of a manual trans-perineal prostate biopsy procedure under MRI guidance was discussed. Once again, the clinical workflow chart demonstrated the flaws of the manual approach and, thus, provided more evidence for the need of an automatic biopsy system. This chart was not constructed in collaboration with the medical staff, meaning that it should be considered with a degree of caution. Nonetheless, several user requirements can be extracted from this chart.

Part B

Developing a technique to remove tissue samples

Chapter 6

Analyses

In Chapter 2, the scope of this thesis project was introduced. One of the objectives is to develop a technique to remove a tissue sample from a biopsy needle without human intervention. This objective is analyzed in the present chapter. First the objective is analyzed by describing the State of the Art in Section 6.1. Then, the requirements for such a technique are discussed in Section 6.2.

6.1 State of the Art on automated tissue sample removing techniques

The state of the art on medical devices that can automatically remove or collect a tissue samples is researched before the requirements are determined. Here, the focus is not only on prostate needle biopsy but also on biopsy procedures of other organs. Because, removing a tissue sample from a biopsy needle is not only done in prostate biopsy but in all needle biopsies. Widening the search area is expected to lead to a better overview of what the State of the Art is. Both a literature and patent search are performed. Finally, the commercially availability of above described medical devices is described.

6.1.1 Literature search in Pubmed

A literature search was done in Pubmed using the following search query: biopsy AND needle AND (automat*) AND (collect* OR remov*). This resulted in 114 papers (results last checked on 8 July 2019). Papers were excluded on the following criteria: evaluated instrument could not remove sample from needle without human intervention or paper was not focused on needle biopsy. By using these exclusion criteria, only five relevant papers were found [50][51][52] [53][3].

All five papers discussed the performance of the same vacuum-assisted biopsy device in breast biopsy procedures. The Mammotome elite (see Figure 6.1) was used during these procedures. This device has a stylet, which is hollow instead of solid, with an opening that can be filled with tissue (see Figure 6.1b). Similar as with standard side-cut biopsy needles, a cannula is fired over the stylet to cut the tissue. The sample is moved from the distal to the proximal end of the device by vacuum suction. The samples are collected in a collecting chamber at the proximal end of the device. The Mammotome Elite can only be equipped with a 10 to 13G needle. The added diagnostic value of a vacuum-assisted biopsy is the ability to sample an adequate amount of tissue and complete removal of some clusters of microcalcifications [53]. Larger samples are required for imaging-discordance lesions of the breast. The traditional technique is surgical excision or biopsy with a standard core biopsy needle [52]. Vacuum-assisted biopsy has been introduced as an alternative to

these techniques for the reason of sampling more tissue in a less radical procedure.

(A)   (B)

FIGURE 6.1: Figure shows an iso-view (A) and a tip close up (B) of the Mammotome
Elite. Figures retrieved from [54].

Kim et al. showed that vacuum-assisted biopsy was a valuable alternative compared to standard 14G core breast biopsy [50]. In this study, 26 breast lesion were sampled under ultra-sound guidance. In 2011, Kim et al. reported a newer paper were they sampled 230 papillary breast lesions [51]. They concluded that standard 14G core breast biopsy was associated with significantly higher false-negative rates compared to vacuum-assisted breast biopsy. Sohn et al. had similar conclusion when researching 161 breast lesions in re-biopsy procedures [52]. Tothova et a. showed that vacuum-assisted biopsy outperformed the standard 14G needle biopsy [53]. However, the lower disease estimation, sensitivity and false-negative rate was not statistically significant. So there are strong indications that the clinical outcome of 13G vacuum-assisted breast biopsy improved compared to standard core needle breast biopsy. Whether this statement can be extended to smaller diameter needles is up for debate.

Here, a study that researched the influence of needle diameter with respect to tissue loss and fragmentation rate is important. Khoury et al. researched the issue of possible loss of valuable diagnostic tissue (debris) in the vacuum tubing system and collecting chamber [3]. The results demonstrated that sampling with a 11G vacuum-assisted biopsy needle indeed lead to tissue lost in aforementioned spaces. However, the debris did not add any significant diagnostic information. The authors concluded that fragmented samples were predictors of tissue loss. The 11G vacuum-assisted needle sampled fragmented cores in 44% of all cases.
Combining an 18G biopsy needle, which is required for prostate biopsy, with vacuum-assistance is considered to increase the fragmentation rate and, therefore, possible reduce the diagnostic information significantly. On that account, using vacuum to automatically remove the tissue sample from the 18G biopsy needle during a prostate biopsy procedure is not considered to be a viable option.

These few papers found on this subject indicated that automatically removing a tissue sample from a biopsy needle was uncommon. According to the researched literature, only one technique, the vacuum suction technique, was introduced into the clinical practise.

6.1.2 Patent search in Espacenet

A patent search was conducted in Espacenet by using the following search query: biopsy AND needle AND (automat*) AND (collect* OR remov*). This resulted in 32

patents (results last checked on September 4, 2019). Patents were excluded using the same criteria that were used during the above mentioned literature search and some additional criteria: biopsy devices used to sample a tissue surface, biopsy devices without a needle and devices that only focused on the storing of biopsy samples. Three relevant patents were found [55][56][57]. They are briefly discussed in the following paragraphs.

Patent US2018242959A1 described a biopsy device including a body, a needle, a cutter and a tissue sample holder [55]. Vacuum was used to remove the sample from the stylet (#114 in Figure 6.2) and storing in a collecting chamber (#300 in Figure 6.2).
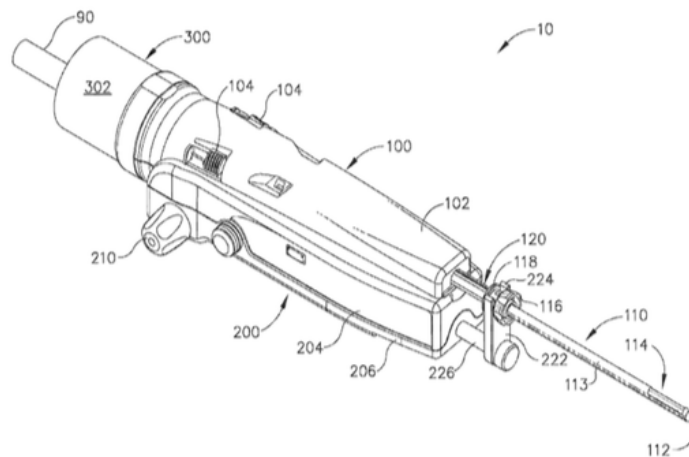
FIGURE 6.2: Patent US2018242959A1[55]

In patent WO2018127848A1 an alternative sample removing technique was described [56]. Here, after sampling, the stylet (#18 in Figure 6.3) was pulled back to the distal side of the cannula and a manipulator (#93 in Figure 6.3) pushed the tissue sample (#62 in Figure 6.3) from the stylet notch into a collecting tray (#78 in Figure 6.3). The removing or unloading mechanism was not described in detail. For instance, the technique of actuation was not mentioned.
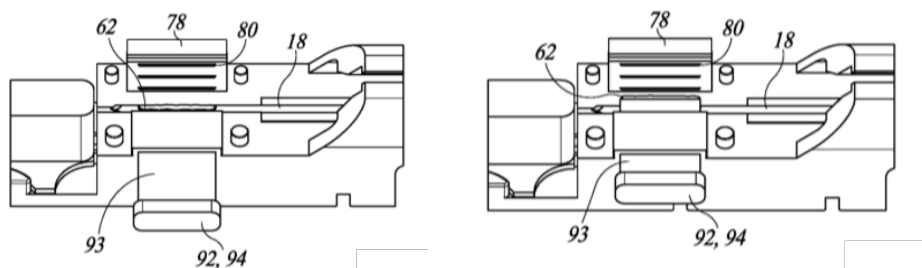
FIGURE 6.3: Patent WO2018127848A1 [56]

The last patent (WO2018087367A2) described several different tissue sample removing techniques [57]. The similarity between these techniques was that they all make use of a carrier medium to which the tissue sample adheres to. The techniques are categorized into ones that can be integrated into the biopsy device (Figure 6.4A to D) and ones that are standalone (Figure 6.4E and F). The latter can only remove a tissue sample when a biopsy instrument is inserted into the device.

In figures 6.4A to D a drum or wheel is equipped with a carrier medium and rolls against the stylet. The tissue sample (#2 in Figure 6.4A to D) adheres to the

(A)   (B)

(C)   (D)
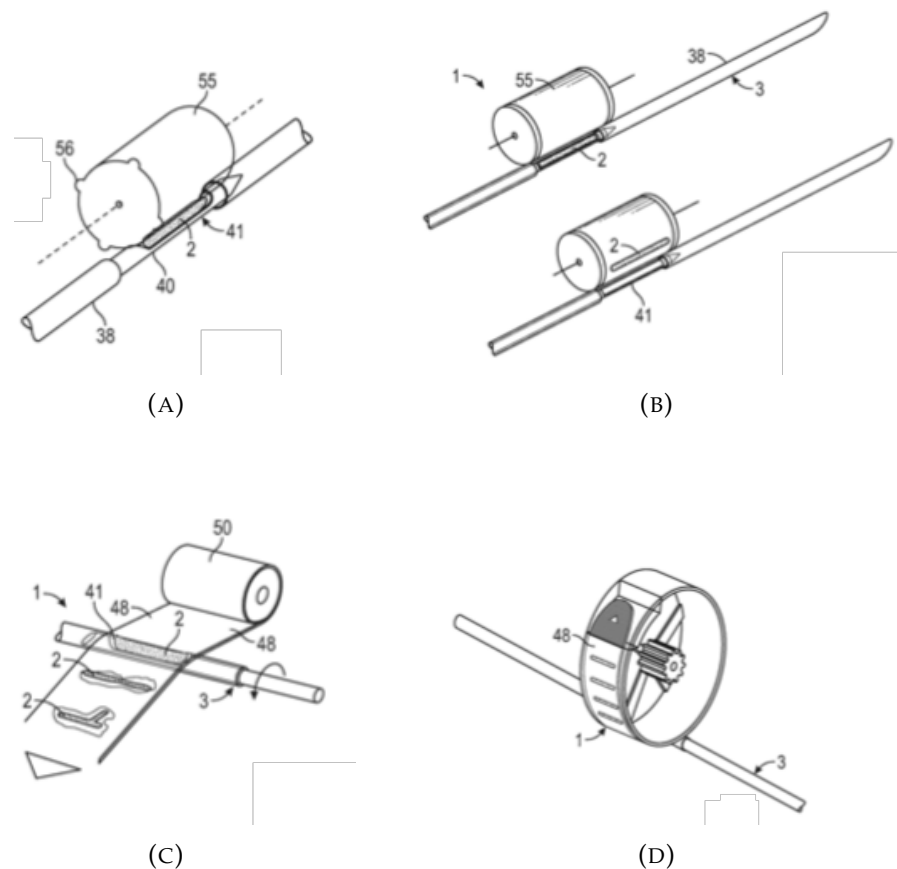
FIGURE 6.4: Patent WO2018087367A2 [57]

carrier medium when in contact, which results in the sample to be removed from the stylet. The technique shown in 6.4A also collects tissue waste that remains on the stylet. Both the techniques shown in 6.4C and D remove multiple samples with a removable carrier medium.

Figure 6.4E consists of a rotating sample holder (#43 in Figure 6.4) with compartments that can be moved towards the sample. The compartments are lined with a carrier medium (#6 in Figure 6.4E). The tissue sample adheres to the carrier medium when in contact. This results in the sample to be removed from the stylet.

Again, figure 6.4F shows a removing technique that makes use of a carrier medium (#48 in Figure 6.4F) to remove the sample from the stylet. In this technique, the carrier medium is pushed against the sample using a piston (#54 in Figure 6.4F). Then, the tissue sample is transported to the storing compartment by rotating the sample holder (#51 in Figure 6.4F).

The relevant patents described three different techniques to remove the tissue sample from the stylet: (1) vacuum suction, (2) manual pushing with a manipulator and (3) adhesion to a carrier medium. Only the vacuum assisted biopsy technique has been reported in literature and was shown to be feasible. Pushing the tissue sample from the stylet or using a carrier medium was not clinically tested. Whether these two techniques were feasible in practice was unknown.

(E)

(F)
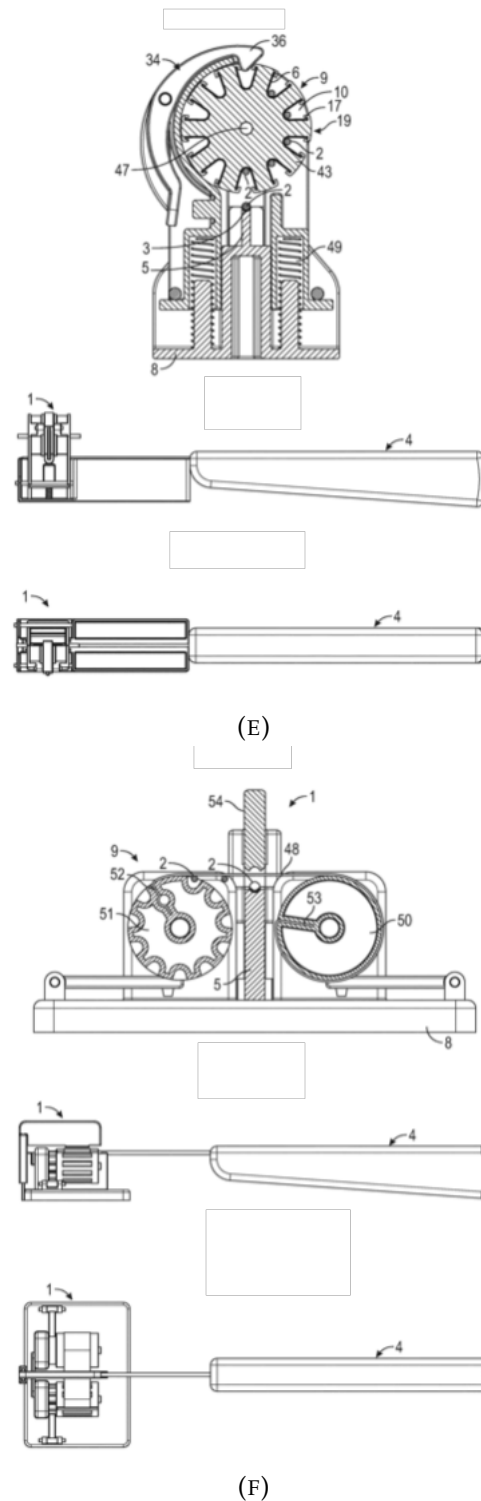
FIGURE 6.4: Patent WO2018087367A2 [57]

6.1.3 Commercially available devices

Besides the Mammotome, which was evaluated in the papers found in the literature search, a few other biopsy devices that could automatically remove a tissue sample were commercially available. Four alternatives were found: the Encor, the Atec, the Teesuvac and the Brevera (see Figure 6.5). The specifications of these devices were listed in Table 6.1. Similar to the Mammotome, vacuum suction was used in these

medical devices to remove the sample from the needle and for transportation to the collecting chamber. Also, all found devices were developed for breast biopsy and were equipped with a needle that had a diameter between 7 and 13G. The difference between the devices was that some had an internal vacuum pump, while others required an external vacuum supply. Some devices were MRI-safe and others were not.

(A)

(B)

(C)

(D)
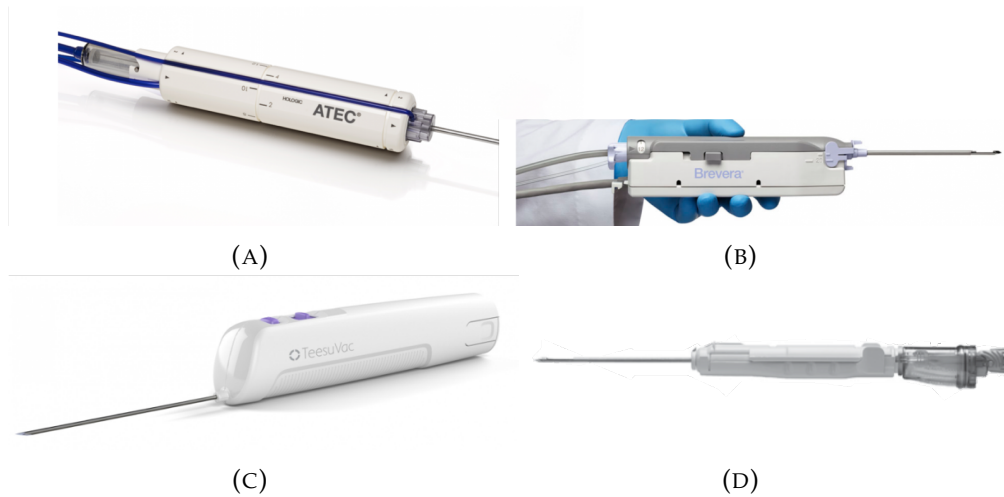
FIGURE 6.5: Commercially available biopsy devices that can automatically sample and remove a tissue sample. Where (A) is the ATEC **2012ATEC** (B) the Brevera [58], (C) the Teesuvac [59] and () the Encor [60].

TABLE 6.1: This table list the specifications of several vacuum-assisted biopsy devices.

Medical device	Removing technique	MRI-safe	Supported needle diameter
Mammotome Elite	Vacuum suction	No	10 or 13G
Encor	Vacuum suction	Yes	7, 10 or 12G
Atec	Vacuum suction	Yes	9 or 12G
Teesuvac	Vacuum suction	Unknown	Unknown
Brevera	Vacuum suction	Yes	10G

6.1.4 Conclusion on the State of the Art

The literature and patent search showed that automatically removing a tissue sample from biopsy needle was uncommon. Manually removing the tissue sample from the biopsy needle is still the common practice. Two patents were found that described a technique other than vacuum suction to remove the tissue sample from the stylet. However, the performance was unknown. The few commercially available devices that were found all used vacuum suction to remove the tissue sample. Vacuum-assisted devices were proven to be comparable to standard biopsy needles. However, these vacuum-assisted devices could only be equipped with needles up to 13G. Sampling more amount of tissue such as in breasts biopsy can be done with larger diameter needles. But a smaller organ, like the prostate should be sampled with a much smaller needle, often 18G or smaller. Tissue samples taking with a 18G needle had a diameter that was at least twice as small compared

to a 13G needle. Smaller diameter samples of equal length were considered to be more fragile and prone to fragment when removed with vacuum suction. Khoury et al. already showed a fragmentation rate of 43% with 11G vacuum-assisted biopsy needles, which is already a significant increase compared to standard biopsy needles (36% [61]). Higher fragmentation rate meant that automatically the quality was reduced as well. This figure is expected to raise with decreasing needle diameter, which could lead to more tissue loss and lost diagnostic information. This problem introduced the need for an alternative tissue sample removing technique.

6.2 Requirements

The next step in developing a technique to remove a tissue sample from a biopsy needle without human intervention was setting up requirements. The to be developed tissue sample removing technique will replace the manual technique. Therefore, it should perform equally good. As described in Chapter 3, the manual removing technique started by retracting the biopsy needle from the body entirely. Followed by pushing the stylet out of the cannula to reveal the tissue sample. The tissue sample was removed from the stylet by wiping it onto a saline socked sponge, on a filter paper or on the edge of a biplicated paper [30]. The latter was shown in Figure 6.6.
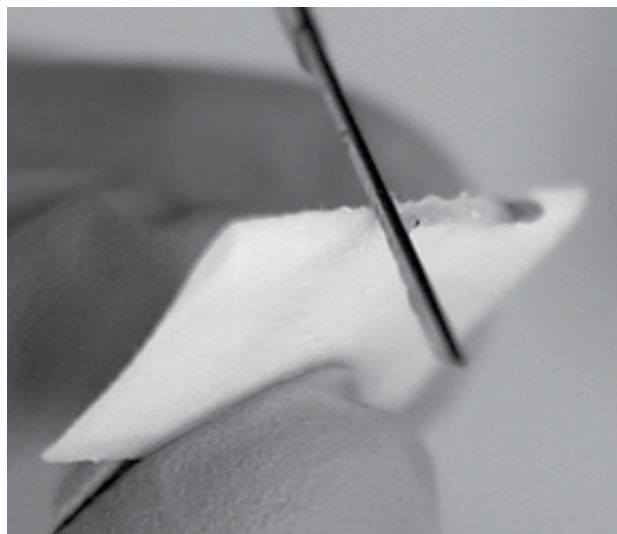
FIGURE 6.6: Figure illustrates the manual removal of tissue sample from a biopsy needle by wiping it on the edge of a biplicated paper. Figure retrieved from [30].

Whether a tissue sample was removed in a correct manner was determined by evaluating three criteria. First, the stylet was checked to ensure that the entire tissue sample was removed.
Secondly, the tissue sample was checked for fragmentation. Fragmentation of tissue samples into smaller parts was undesired. Tissue samples that were shorter than a certain length, also known as the cut-off length, were often marked as being of inadequate quality. The value of this cut-off length varies between studies (see Chapter 3 of Part A). The highest reported cut-off value (>13 mm) was chosen as acceptance criteria because tissue samples longer than this value were marked as an adequate quality sample in all the discussed studies.

Finally, the removing process was only marked as successful when the tissue sample was placed on the carrier (sponge, filter paper, etc). The carrier was then placed in the container and sent to the pathology department.

As the to be developed tissue sample removing technique will replace the manual technique, it should at least meet the three requirements that were mentioned above. The requirements and their acceptance criteria were listed in Table 6.2.

TABLE 6.2: This table lists three requirements of the tissue sample removing technique.

#	Requirement	Acceptance criteria
1	Amount of removal	No obvious parts of tissue sample left on stylet notch
2	Fragmentation	Part of a fragmented tissue sample should be >13 mm
3	Control of depositing	Tissue sample deposited on carrier

Chapter 7

Creating novel techniques

The next step in the development process is to create alternative techniques that can remove a tissue sample from a biopsy needle without human intervention. First, a sketch of the problem is provided (Section 7.1). Based on this sketch, four tissue sample removing techniques are identified: blowing, flushing, wiping and pushing. These techniques are illustrated and explained in the subsequent sections.

7.1 Problem sketch

A sketch of the problem is shown in Figure 7.1. A tissue sample taken with a 18G needle usually has a cutting length of 20 mm. It is assumed that the tissue sample had a cross section surface area of about half the size of the stylet cross section surface area (0.5 mm^2). The volume of a tissue sample is estimated to be ±5 mm^3. Prostate tissue has a density of a about 1.0 g/mL [62]. Therefore, the mass of a tissue sample is estimated to be ±0.005 grams. The force required to move such a mass is expected to be very low, about 0.03 mN, which is almost negligible. Generating these low forces is not considered to be a problem. However, as the tissue sample contained body fluids such as extra-cellular fluids, a fluid film might be created between the tissue sample and the stylet notch surface. Such a fluid film can create a surface tension. Meaning that the tissue sample can adhere to the stylet notch surface. Because of the extremely low mass of the sample, the influence of adhesion forces is also considered to be negligible.
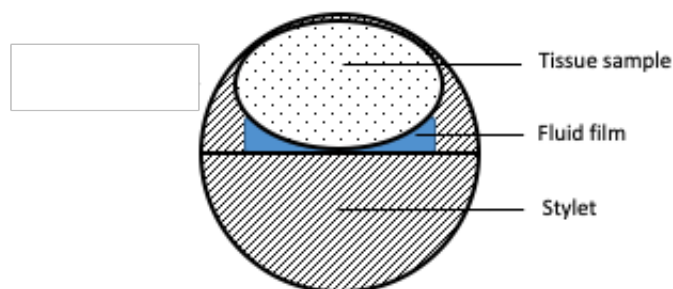
FIGURE 7.1: Cross-section sketch of a tissue sample on a stylet that was taken with a biopsy needle. Gravitational field was facing downwards.

In Chapter 6, three tissue sample removing techniques were already mentioned: removing by vacuum suction, removing by pushing and removing by adhesion to a carrier medium. Only the former was clinically tested in a prototype or commercial

device. While vacuum suction was only proven to be feasible with 7 to 13G needles, the performance with 18G to 20G needles is unknown. During the identification of tissue sample removing techniques, the fragility and the small size of the tissue sample is taken into account. Vacuum suction with 18 to 20G is not considered to be a viable technique (see Section 6.1). The feasibility of the 'removing by pushing' and 'removing by adhesion to a carrier medium' is unknown. Besides that, the actuation of the former technique is not clearly described, meaning that removing a tissue sample by pushing in an automated manner is still an option. The claim on the latter technique is very extensive. The patent describes six different mechanisms to remove a tissue sample with the use of a carrier medium. This limits the freedom to operate tremendously. Using a carrier medium to remove the tissue sample will most likely resemble one of these mechanisms. Therefore, removing the tissue sample by adhesion to a carrier medium is not considered to be an option.

Besides the 'removing by pushing' technique, other techniques are created. There are two categories. The first category grouped the techniques that use a flowing fluid to exert a drag force on the sample. Such a drag force might cause the tissue sample to be removed from the stylet. The techniques in the second categories apply a mechanical force on the sample to remove it from the stylet. The identified tissue sample removing techniques in the first category are: removing by blowing air and removing by flushing with a liquid. Those in the second category are: removing by wiping.

7.2   Blowing

An air flow aimed at the tissue sample creates a drag force that can result in the removal of the tissue sample. Figure 7.2 shows a sketch of the technique. Here, the dotted lines represent the air flow. An advantage of this technique can be that removing a tissue sample is done without physical contact, which decreases the chance on cross-contamination. The air flow can be created by for instance a fan or compressed air.

FIGURE 7.2: Cross-section sketch of a tissue sample on a stylet that was taken with a biopsy needle and removed by blowing air. Gravitational field was facing downwards.

The required drag force be calculated using the following equation:

$$F_D = \frac{1}{2}\rho V^2 C_D A_{front} \tag{7.1}$$

Where ρ is the density of air (1.25 $\frac{kg}{m^3}$), C_D the drag coefficient ($C_D = 1.0$), A_{front} the frontal area ($A_{front} = 12.5\ mm^2$) and V the velocity of the flow. As described in the previous section a force of about 0.03 mN was estimated to be sufficient to remove the tissue sample. This required the velocity of the stream to be about 2.5 $\frac{m}{s}$. Whether this technique could remove the tissue sample in a controlled manner should be tested in an experiment.

7.3 Flushing

This technique is similar to the blowing technique but instead of air, a liquid is used to create the drag force. The liquid flow can be created by single or multiple jets. The jet can have all sort of shapes (e.g. straight, flat, cone, etc). A suitable liquid could be saline, because it poses no harm to the patient. Cross-contamination is, similar to the blowing technique, not expected to be an issue.
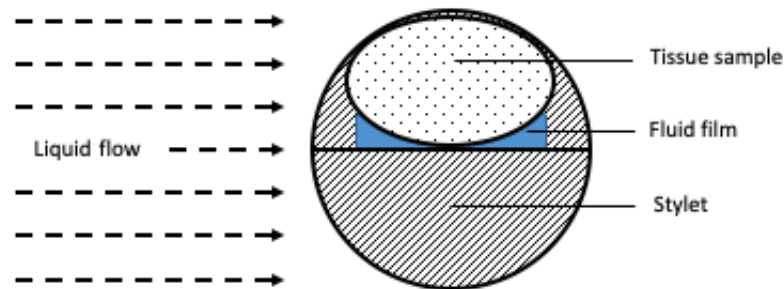
FIGURE 7.3: Cross-section sketch of a tissue sample on a stylet that was taken with a biopsy needle and removed by flushing with a liquid. Gravitational field was facing downwards.

Equation 7.1 can be used to determine the required velocity. Here, the density of water is 997 $\frac{kg}{m^3}$. This results in a flow velocity of 0.04 $\frac{m}{s}$. The velocity of the liquid flow is estimented to be 30 times lower than the air flow velocity, which was calculated for the blowing technique. Again, this should be tested in an experiment.

7.4 Wiping

The wiping technique is based on the currently used manual technique, which was explained in Chapter 3. In figure 7.4 the wiping technique is illustrated. A wiper rotates around a certain point, which results in the end of the wiper to move along the surface of the stylet notch and force the sample from the stylet. The orientation of the wiper and stylet in Figure 7.4 is just one of many. For instance, rotating the entire system for a quarter turn around the center of the stylet resulted in the gravitational force to be in the direction of the stylet notch surface.

Ideally, the tissue sample should fall from the stylet on to, for instance, a carrier. However, the low mass and the fluid film might cause the tissue sample to stick to the wiper. This can be resolved by moving the wiper along the carrier so that it sticks to the carrier instead of the wiper. Coating the wiper with a low-friction coating can
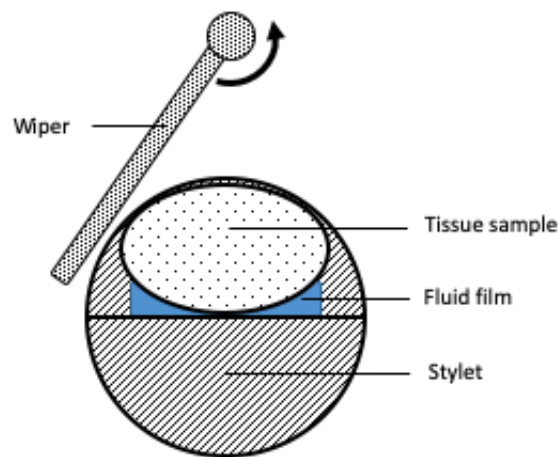
FIGURE 7.4: Cross-section sketch of a tissue sample on a stylet that was taken with a
biopsy needle and removed by wiping. Gravitational field was facing downwards.

be another option.

Another disadvantage of this technique is that tissue of previous samples that remained on the wiper could be wiped on the stylet and inserted in to the patient when taking subsequent samples. This problem is often called cross-contamination. Experiments should be done to test whether these disadvantages occurred.

7.5 Pushing

This technique was previously described in a patent (Section 6.1). Although, in the present technique, the pusher is automatically actuated by for instance a pneumatic cylinder or piezo motor.
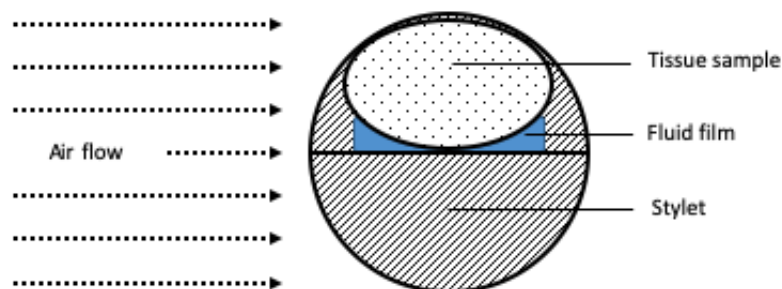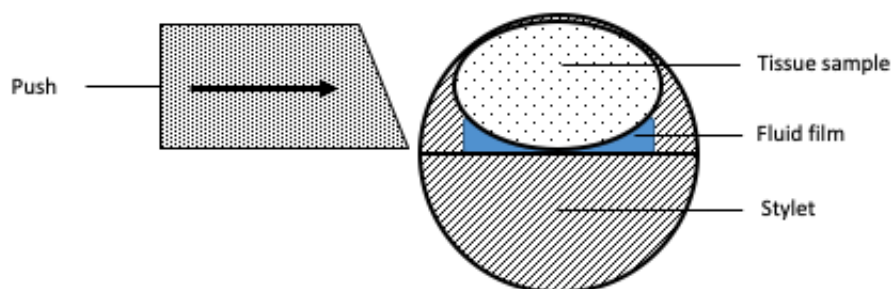

FIGURE 7.5: Cross-section sketch of a tissue sample on a stylet that was taken with a
biopsy needle and removed by wiping. Gravitational field was facing downwards.

Ideally, the pusher moves over the stylet notch surface. When this can not be accomplished, a gap will appear between the pusher and the stylet notch surface. Worst case, the gap can be filled with tissue, which damages the tissue sample. Fabricating a precise mechanism can be a problem because the dimensions of the needle are quite small.

Removing the tissue sample from the biopsy needle by pushing has the similar problem of cross-contamination, which is also considered to be a problem of the 'removing by wiping' technique.

Chapter 8

Selecting the most promising technique

In Chapter 7, four tissue sample removing techniques were identified: 'removing by blowing', 'removing by flushing' 'removing by pushing' and 'removing by wiping'. Whether a technique can result in the removal of a tissue sample from the biopsy needle in conformance to the requirements is tested in this chapter. In section 8.1, the test plan for each technique is described. The results are shown in section 8.2. Finally, the most promising technique is selected in Section 8.3.

8.1 Test Plans

The tissue sample removing techniques are evaluated by removing a tissue sample taking with a standard 18G biopsy needle from a raw chicken breast. Each technique is tested in two set of test. The variable that is considered to have the most influence on the results, varies between the two set of tests. Such a set consisted of 5 runs.

Only tissue samples that have a length >5 mm are used during these tests. The performance of the technique is determined by evaluating the requirements that were described in Section 6.1. However, the acceptance criteria of the 'Fragmentation' requirement is updated. This is done because instead of sampling life human prostate tissue, raw chicken was used. Whether sampling of raw chicken produced similar length tissue samples compared to sampling a life human prostate is unknown. The length of the sample after removing is compared to the length before removing. Therefore, the acceptance criteria is changed to a percentage of the length after removal compared to before.

The goal of these tests is to determine the potential of a tissue sample removing technique. A positive or negative value is attributed to the requirements during each run (see Table 8.1). Here, positive means that the test passed the acceptance criteria and negative that it did not.

TABLE 8.1: This table lists three requirements of the tissue sample removing technique.

#	Requirement	Acceptance criteria
1	Amount of removal	No obvious tissue waste on stylet
2	Fragmentation	Tissue sample length after removal was ≥80% of length before removal
3	Control of depositing	Tissue sample deposited on carrier

8.1.1 Test Plan: Blowing

A test tool (see Figure 8.1) is developed to test whether blowing can remove the tissue sample from the stylet in a proper manner. A cooling fan is used to generate the air flow. The cooling fan is connected to a rectangular shape funnel to direct the air flow in the direction of the stylet.

According to the fan specifictions, the cooling fan can displace 3 $\frac{m^3}{hr}$. The cross-section area of the funnel near the stylet can be changed. Decreasing this area results in a higher air flow velocity and vise versa.

Variables that are expected to have an influence on the results are listed below:

- Air flow velocity

- Funnel shape

- Direction of gravitational force w.r.t air flow

The airflow velocity is considered to have the most influence on the result. In theory, higher velocity results in larger drag forces. Therefore, two set of test are performed. One with a low (2.5 $\frac{m}{s}$) and one with a high air flow velocity (13$\frac{m}{s}$).

The remaining variables are the same in both set of tests. The direction of gravitation is chosen to be parallel to the air flow. The designated depositing surface is the horizontal surface directly below the stylet and is shown in Figure 8.1a.

The tests are performed according to the test protocol that is described in Appendix B. The results are shown in Section 8.2.
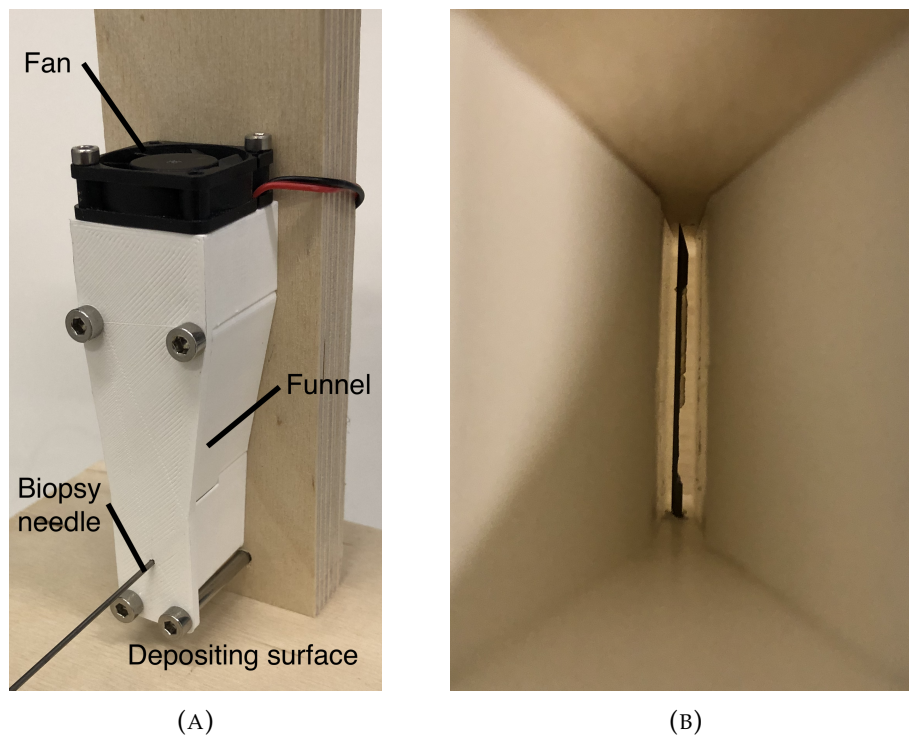
FIGURE 8.1: Test tool used to test the blowing technique. (A) is an overview of the tool and (B) a a view from the top through the funnel.

8.1.2 Test Plan: Flushing

A test tool is developed for the flushing technique as well (see Figure 8.2). The flushing technique is tested by spraying a flat shape water jet over the stylet notch

and tissue sample. A container is placed under the stylet notch to collect the tissue sample.

The water jet is created with a syringe that is connected via a tube to a flat spray nozzle. The flow through nozzle is parallel to and in the direction of the stylet notch surface. This is done to control the depositing direction. Changing the force applied on the syringe, changes the pressure and, therefore, the velocity of the water jets.
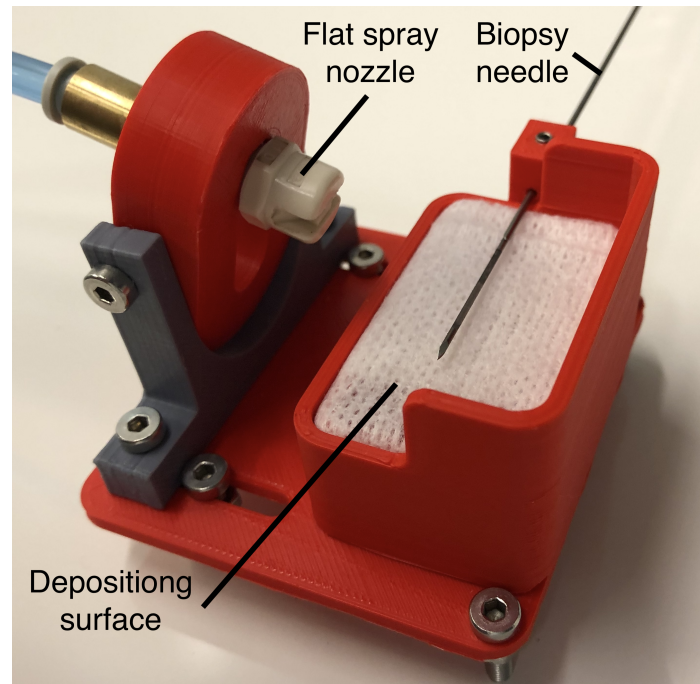
FIGURE 8.2: Test tool used to test the flushing technique.

The variables that are expected to have an influence on the results are listed below:

- Water flow velocity

- Distribution of jet along the tissue sample

- Total contact area between water flow and tissue sample

- Direction of flow

The contact area between the water flow and the tissue sample is distributed more uniform across the tissue sample by using a flat shape jet that is aimed at the center of the tissue ample. Distributing the water flow more even across the tissue surface with the flat V-shaped spray should result in a more uniform distribution of the drag force created by the water flow on the tissue sample.

Same as with the airflow, described in the previous test, the drag force is determined by the velocity of the flow. The exact value of the water flow velocity is unknown. However, the velocity of the flow at the contact area between the water flow and tissue sample can be varied by changing force applied on the syringe. Increasing this force, increases the water flow velocity at impact and, thus, increases the drag force on the tissue. A higher drag force is expected to increase the chance of sample removal.

The flow velocity is considered to have the most influence on the removing of the tissue. Therefore, the test was performed twofold. One with a low syringe force

(± 5 *N*) and one with a high (± 50 *N*) syringe force.

The same amount of water (60mL) is used for both test runs. The tests are executed as described in the flushing test protocol (see Appendix C). The results are shown in Section 8.2.

8.1.3 Test Plan: Wiping

A test tool (see Figure 8.3) is developed to test whether the wiping technique resulted in the removal of the tissue sample from the stylet. The test tool consists of a base and a wiper with a thin blade (see Figure 8.4a). The thin blade has about the same width as the stylet notch width, which is about 20 mm (see Figure 8.4b). The wiper and blade can rotate causing the blade to wipe closely, within 0.3 mm (thickness of paper), along the stylet notch surface.
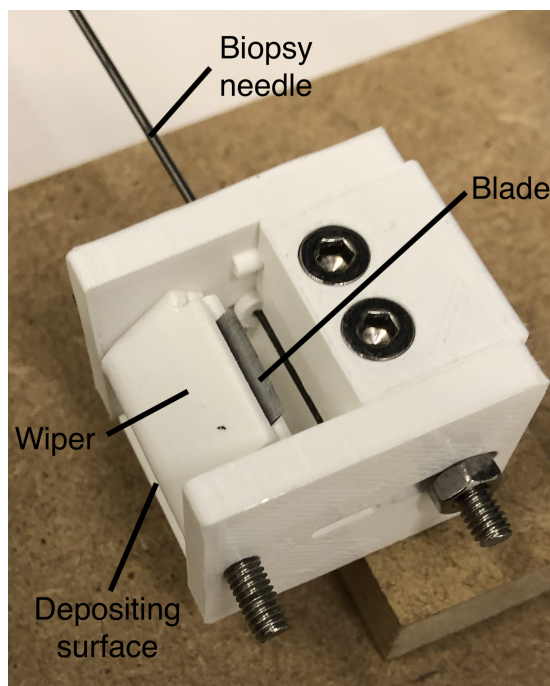
FIGURE 8.3: Test tool used to test the wiping technique.

The velocity and angle of rotation is controlled using a stepper motor that is connected to the shaft of the wiper. The angle of rotation is 120°. A curved surface with the radius of the wiper and blade, is created. This surface is the depositing surface. The following variables were expected to have in influence on the outcome:

- Wiper angular speed
- Minimum distance between blade and stylet notch surface
- Blade width
- The location and orientation of the depositing surface

The angular wiper speed is expected to have the most influence on the outcome. Therefore, the test is performed twofold. The first set of test runs is performed with a low (8.4 $\frac{rad}{s}$) and the second with a fast (50.4 $\frac{rad}{s}$) wiper angular speed. The other variables remained constant.

The tests are executed as described in the wiping test protocol (see Appendix 6.4f). The results are shown in Section 8.2.

8.1.4 Test Plan: Pushing

The potential of the pushing technique is tested using the test tool shown in Figure 8.4). The test tool consists of a linear moving pusher or shovel and a base, in which the biopsy needle is fixed with the stylet notch surface facing upwards. The shovel is equipped with a thin blade and is connected to a linear stage that can move only along one axis. This axis is parallel to the stylet notch surface and perpendicular to the biopsy needle.

The linear speed of the pusher is controlled by connecting the moving part of the linear stage to a belt, which is on its turn actuated by a stepper motor. The pusher can be rotated to ensure that the far edge of the blade moves closely, within 0.3 mm (thickness of paper), along the stylet notch surface.

The angle between the blade and the stylet notch surface is approximately 40 °. On both sides of the stylet notch surface a co-linear adjacent surface is created. This surface is the surface at which the sample is deposited. Variables that are expected to have an influence on the results are:

- Pusher linear speed
- Push angle w.r.t. stylet notch surface.
- Minimum distance between blade and stylet notch surface
- Blade width
- The location and orientation of the depositing surface

The pushing linear speed is expected to have the most influence on the results. Therefore, the test is performed wit a high 42 $\frac{mm}{s}$ and with a low 10 $\frac{mm}{s}$ linear speed. The other variables remained constant.

The tests are executed as described in the shoving test plan (see Appendix E). The results are shown in Section 8.2.

(A)   (B)
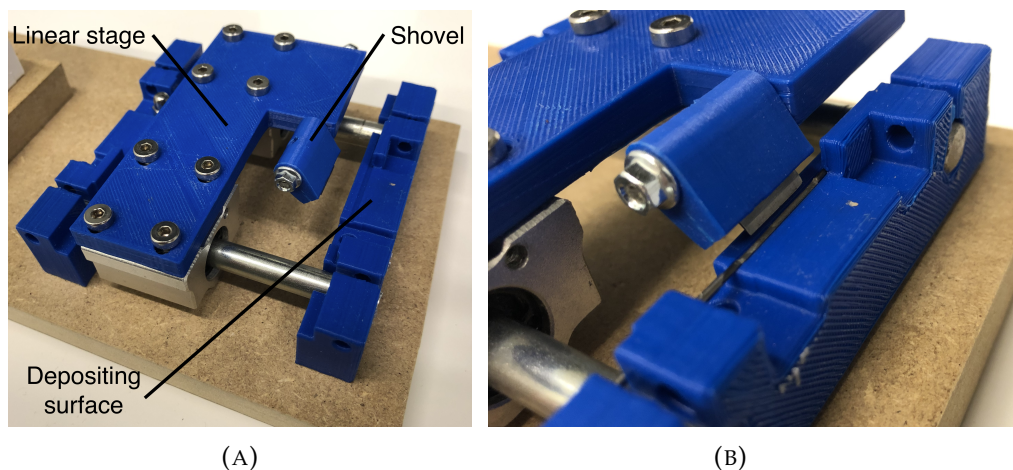
FIGURE 8.4: Test tool used to test the pushing technique. (A) is an overview of the tool and (B) a close up of the blade that moves across the stylet notch surface.

8.2 Results

8.2.1 Results: Blowing

The results of the blowing tests are shown in Table 8.2. Removing a tissue sample from a biopsy needle by blowing failed with both a lower and higher velocity airflow. In two out of the five runs, a high velocity air flow resulted in the tissue sample to fragment. As none of the tissue samples were removed, also none were deposited on the designated surface.

TABLE 8.2: This table lists the results of the blowing tests. Here, V_{low} meant low velocity and V_{high} the high velocity of the air flow. The three type of results were explained in Table 8.1.

Run	Amount of removal		Fragmentation		Depositing	
	V_{low}	V_{high}	V_{low}	V_{high}	V_{low}	V_{high}
1	-	-	+	-	-	-
2	-	-	+	+	-	-
3	-	-	+	+	-	-
4	-	-	+	-	-	-
5	-	-	+	+	-	-

8.2.2 Results: Flushing

The results of the flushing tests were shown in Table 8.3. The tissue sample was entirely removed in nine out of the ten runs. The higher water flow velocity resulted in all of the tissue samples to be removed. However, the higher flow velocity of the flat spray jet resulted in more fragmented tissue samples. When a tissue sample was removed properly, it was consistently deposited on the designated surface.

TABLE 8.3: This table lists the results of the blowing tests. Here, V_{low} meant low velocity and V_{high} high velocity of the water flow. The three type of results were explained in 8.1.

Run	Amount of removal		Fragmentation		Depositing	
	V_{low}	V_{High}	V_{Low}	V_{High}	V_{Low}	V_{High}
1	+	+	+	-	+	+
2	+	+	+	+	+	+
3	-	+	-	+	-	+
4	+	+	+	-	+	+
5	+	+	+	+	+	+

8.2.3 Results: Wiping

The results of the wiping tests were shown in Table 8.4. A slow angular wiper speed resulted in the tissue sample to be removed only two out of the five times and only one was deposited on the designated surface. The tissue sample adhered to the

wiper blade instead of falling onto the depositing surface. Better results were obtained when a six times faster angular speed was used. Another problem problem was that a too large distance between the blade and stylet notch surface resulted in the samples to be crushed before they were removed. Crushing damaged and sometimes fragmented the tissue sample. Decreasing the distance between the blade and the stylet notch surface was unsuccessful because the blade often crashed in to the stylet notch, which made it impossible to remove the tissue sample.

TABLE 8.4: This table lists the reported outcomes (positive or negative) of the wiping tests. Here, V_{low} is the low angular speed (8.4 rad/s) and V_{fast} the fast angular speed (50.4 rad/s). The three type of results were explained in Table 8.1.

Run	Amount of removal		Tissue damage		Depositing	
	V_{Slow}	V_{Fast}	V_{Slow}	V_{Fast}	V_{Slow}	V_{Fast}
1	-	+	-	+	-	+
2	-	+	+	+	-	+
3	+	+	+	+	-	+
4	+	-	+	-	+	-
5	-	+	-	+	-	+

8.2.4 Results: Pushing

The results of the 'pushing' tests were shown in Table 8.5. These tests showed that the tissue sample was only removed in half of the cases. Similar as with the wiping tests, failing to remove the entire tissue sample was probably caused by the too large distance between pushing blade and the stylet notch surface. The thin blade only pushed against the top part of the tissue sample and caused the tissue sample to fragment. Ideally, this distance should be decreased so that shovel blade touches the surface of the stylet notch. However, in practice this resulted in the shovel blade to crash into the depositing surface. The linear speed of the shovel did not seem to have in influence on the results.

TABLE 8.5: This table lists the reported outcomes of the shovel tests (positive or negative). Here, V_{low} is the low linear speed (10 mm/s) and V_{fast} the fast linear speed (42 mm/s). The three type of outcomes were explained in Table 8.1.

Run	Amount of removal		Tissue damage		Depositing	
	V_{Slow}	V_{Fast}	V_{Slow}	V_{Fast}	V_{Slow}	V_{Fast}
1	+	-	-	+	+	-
2	-	+	+	+	-	+
3	-	-	-	-	-	-
4	+	-	+	-	+	-
5	+	+	-	+	+	+

8.3 Test discussion

In the previous sections of this chapter, four different tissue sample removing techniques were evaluated by means of tests. The results of the requirements 'Amount of removal', 'Fragmentation' and 'Control of depositing' were reported (see Table 8.1). The results should be considered with a degree of caution because the test setups were not optimized and could therefore not show its optimal performance. The tests gave only an indication of the potential of a tissue sample removing technique. Meaning that a technique that did not score the best in these tests could still be a viable option.
The tests showed that removing a tissue sample by blowing was unsuccessful in all the runs. Increasing the velocity might have better results. Although, fragmentation rates will probably increase as well. Whether the tissue sample could be deposited on the designated surface was still unknown because no tissue samples were removed. This technique was not considered to be a feasible option.

Wiping already performed better but still failed in about half of the runs. Rotating the wiper at a higher velocity showed that removing a tissue sample from a biopsy needle was feasibly with a low fragmentation rate. Also, most samples were deposited on the designated depositing surface. However, crushing was considered to be a problem. This could be solved by using, for instance, a flexible wiper instead of a solid blade. This could result in more tissue samples to be removed while ensuring a low fragmentation rate.

Removing a tissue sample by pushing was successful in half of the runs. The linear speed of the pusher did not have an influence on the results. The too large distance between the stylet notch surface and the shovel blade might have caused the failures. Manufacturing a system that optimized this distance could solve this problem. Besides crushing, fragmentation was also a problem, which had probably a similar cause. In the successful cases, the tissue sample was deposited correctly on the designated surface.

The 'removing by flushing' technique had by far the most promising results. All but one tissue sample was removed from the biopsy needle and deposited on the designated surface. Only two of them were fragmented. The optimal velocity of the water flow, which ensured high removal and low fragmentation rate, should be reconsidered.

Based on these tests, only 'removing by blowing' was considered to be not feasible. Removing a tissue sample by wiping and shoving showed to have potential, but required some sort of optimization to increase the performance. Whether this resulted in a more successes was just a theory. More testing should be done to substitute this claim.

An advantage of the 'removing by flushing' technique could be that remaining tissue can be removed by flushing with more liquid. This was considered to be harder to accomplish with a wiper or pusher because they could only move in a predefined range, which is done to prevent cross-contamination. Tissue sample waste that remained on the stylet could be inserted into the patient during subsequent sampling passes. This increased the chance on cross-contamination, which is a serious risk.

There is concluded that removing a tissue sample by flushing with, for instance saline, was the most promising option. Saline is a common used fluid for medical applications. Besides that, the potential tests showed that all but one sample was removed and deposited correctly, while ensuring a low fragmentation rate and low chance on cross-contamination.

Chapter 9

Discussion Part B

In Part B, a novel technique was developed to remove a tissue sample from a biopsy needle without human intervention. First the State of the Art on automated tissue sample removing techniques was established. Vacuum-assisted breast biopsy with a 9 to 13G needle was the dominant removing technique in literature and among commercially available devices. There were strong indications that this technique was a viable option compared to standard needle biopsy of the breasts. Vacuum-assisted biopsy was introduced to increase the amount of sampled tissue without using radical procedures. This contrasted with the goal of a prostate needle biopsy. Biopsy devices developed for prostate biopsy were non-existent.

Using vacuum to remove a tissue sample from a biopsy needle was viable with biopsy needles down to 13G. However, needles of 18G or smaller are used for prostate biopsy. Such diameter needles yield at least two times smaller diameter samples. Vacuum-assisted biopsy was not developed for this purpose. Smaller diameter samples are considered to be more fragile and prone to fragment when removed with vacuum suction. Khoury et al. already showed that the fragmentation rate with 11G vacuum-assisted biopsy needles was higher compared to standard needle biopsy (43% vs. 36%) [3]. This figure will probably raise with decreasing needle diameter, which could lead to more tissue loss and perhaps lost diagnostic information. This problem introduced the need for an alternative tissue sample removing technique.

The found patents described two other type of techniques, which were 'removing by pushing' and 'removing by adhesion to a carrier medium'. The latter was extensively patented, while the former lacked a clear description. The patent on adhesion to a carrier medium described six different mechanisms to remove a tissue sample with the use of a carrier medium. The freedom to operate with this method was limited. Therefore, removing the tissue sample by adhesion to a carrier medium was not considered to be an option. This was not the case with the pushing technique.

Four tissue sample removing techniques were identified: blowing, flushing, wiping and pushing. The performance of these techniques were measured by removing tissue samples taken with a standard 18G biopsy needle from a chicken breast. In chapter 8 the techniques were evaluated in terms of the requirements.

Finally, flushing showed to be the most promising technique. In the evaluation tests all but one sample were removed and deposited correctly, while ensuring a low fragmentation rate. Other techniques showed to have problems like crushing or promoting cross-contamination. With flushing on the other hand, cross-contamination

is mostly prevented because it is a non-physical removing techniques. Flushing should be done with saline because of its safe use in medical applications.

One adjustment to the initial concept should be implemented. In the initial concept, the tissue sample was on the top part of the stylet notch surface. In the final concept, the stylet notch surface will be facing downwards. This can be realized by rotating the stylet over 180°. Now the gravity will aid in sample removal.

Part C

Product development

Chapter 10

Requirements and specifications

The design process starts by defining the requirements of the user in Section 10.1. Based on the User Requirements (UR), Product Specifications (PS) are determined (Section 10.2). These PS restate the UR in terms of measurable parameters. Finally, main- and sub-functions are identified in the last section.

10.1 User requirements

The user requirements describe the needs of the stakeholders with respect to the to be designed device. It specifies what the device should do or in what way it should be constrained. The requirements are unambiguous and specific. Table 10.1 shows a list of the user requirements. Whether the requirement must be realized in the design or are only seen as a wish, is noted as well.

TABLE 10.1: User requirements for the automatic biopsy system and their acceptance level. The source of the requirement is noted in the last column.

UR	User Requirements	Must/wish	Acceptance criteria	Source
1.0	*General*			
1.1	Procedure time	Must	The total procedure time should be similar or less compared to a manual approach.	Clinical workflow
1.2	Reusable	Wish	The biopsy system, except for the biopsy needle, should be reusable.	CoBra user-input [49]
1.3	Standard parts	Wish	The device should be manufactured of standard parts.	
1.4	Costs	Wish	The costs should be minimized.	
1.5	Interface positioning robot	Wish	The biopsy system should interface with the positioning robot.	CoBra user-input [49]
1.6	Stability	Must	The biopsy system should function properly during the entire procedure	CoBra user-input [49]
2.0	*Scanning*			
2.1	MR conditional	Must	The biopsy can be performed in an 3T MRI environment, meaning that the entire system should not pose any hazards to the patients or operator.	CoBra user-input [49][45]
2.2	Ultrasound compatible	Wish	The biopsy can be performed using ultrasound (US), meaning that the entire system should be US-compatible.	CoBra user-input [49]
2.3	Artifacts magnetic susceptibility	Wish	Non-ferromagnetic or low magnetic suspectible materials should be used to prevent artifacts on the MRI image.	[63][64]
2.4	Artifacts electrical conductivity	Wish	Materials with low conductivity should be used near the isocenter of the MRI image to prevent artifacts on the MRI image.	[63]

TABLE 10.1: User requirements for the automatic biopsy system and their acceptance level. The source of the requirement is noted in the last column.

UR	User Requirements	Must/wish	Acceptance criteria	Source
2.5	RF and gradient heating	Must	Limit of the local Specific Absorption Rate < 10 W/kg to prevent tissue damage due to RF and gradient heating.	[65][66]
3.0	*Dimensions*			
3.1	Maximum operating dimensions	Must	The biopsy system is used within the bore of a MRI scanner and between the legs of the patient (in lithotomy, semi-lithotomy or lateral decubitus posistion). The system should fit between the legs of the patient in these positions.	Clinical workflow
3.2	Maximum transportation dimensions	Must	The device must fit through a normal size door and within the footprint of a sterile cart.	Clinical workflow
3.3	Maximum weight	Must	Positioning device should be able to lift the system	CoBra user-input [49]
4.0	*Biopsy Needle*			
4.1	Biopsy needle	Wish	The biopsy system should be fitted with a standard biopsy needle estalished on the market.	CoBra user-input [49]
4.2	Core length	Must	Core length should be long enough to sample sufficient part of the prostate (large and small prostates).	Literature study Appendix A
4.3	Variable core length	Must	The core length should be variable.	CoBra user-input [49]
4.4	Needle diameter	Must	Needle diameter should be similar to currently used biopsy needles.	CoBra user-input [49]
4.5	Shaft length	Must	Length of shaft should be comparable to currently used biopsy needles and sufficient to sample entire length of prostate.	Literature study Appendix A
4.6	Dismountable biopsy needle	Must	The biopsy needle should be dismountable.	Clinical workflow
5.0	*Sampling*			
5.1	Actuating sampling mechanism	Must	Sampling mechanism should be actuated without manual intervention.	CoBra user-input [49]
5.2	Biopsy sampling mechanism	Wish	Side-cut favored over end-cut because of the low failed biopsy rate.	Literature study Appendix A
5.3	Sampling multiple tissue samples	Must	The biopsy system should be able to sample multiple tissue samples.	Clinical workflow
5.4	Sampling same lesion	Wish	The biopsy system should be able to sample multiple tissue samples from same lesion without the need to remove the biopsy needle.	Clinical workflow
5.5	Sample quality	Must	Sample quality should be good (length of sample >13 mm)	Literature study Appendix A
5.6	Cross contamination	Must	Only sampling of one lesion with same biopsy needle.	Clinical workflow
6.0	*Removing*			
6.1	Tissue sample removing	Must	Tissue sample should be removed from biopsy needle without manual intervention	CoBra user-input [49]
6.2	Tissue sample waste	Must	No obvious portion of the tissue sample should remain in or on the biopsy needle	Clinical workflow
6.3	Tissue sample damage	Wish	Fragmentation and crushing of tissue sample should be minimized.	Literature study Appendix A
7.0	*Safety*			

TABLE 10.1: User requirements for the automatic biopsy system and their acceptance
level. The source of the requirement is noted in the last column.

UR	User Requirements	Must/wish	Acceptance criteria	Source
7.1	Emergency stop	Must	System should have an emergency stop.	CoBra user-input [49]
7.2	Manual retraction	Must	System should deactivate after failure to be able to manually retract.	CoBra user-input [49]
7.3	Remember position needle	Wish	The biopsy system should remember the position of the needle in real-time.	CoBra user-input [49]
8.0	*Sterile*			
8.1	Sterilization	Must	The device should be sterile.	ISO 11737-2:2009 [67]
8.2	Cleaning	Must	The device should be clean.	ISO 11737-2:2009 [67]

10.2   Product specifications

Product specifications are a list of criteria that are to be satisfied by the design. Acceptance criteria that were found in literature and user-input are assigned to the product specifications (see Table 10.2. The specifications are based on the requirements, meaning that they are user-driven. Also, they are quantifiable, verifiable, specific and solution-neutral.

TABLE 10.2: The product specifications of the automatic biopsy system, their acceptance criteria and rationale behind it are listed in this table.

PS	Product Specifications	Related to UR	Accectance Criteria	Rationale
1.0	*General*			
1.1	Sampling time	1.1	Moment of insertion to storing sample in container <1 min	Similar to manual sampling time
2.0	*Scanning*			
2.1	MR conditional	2.1	No hazards in MRI environment with static magnetic field strength up to 3T, spatial gradient up to 45 mT/M and RF up to 128 mHz.	1.5T and 3.0T MRI scanners, with a RF signal of up to 128 mHz, are used most for prostate biopsy. The maximum spatial gradient of MRI scanners is 45 mT/m [45].
2.2	Ultrasound compatible	2.2	Biopsy system poses no hazard in US environment.	Using ultrasound results in no limitations to the device.
2.3	Local SAR	2.5	<10 W/kg	Limit of the local Specific Absorption Rate determiend by regulations prevents tissue damage due to RF and gradient heating [45].
3.0	*Material*			
3.1	Magnetic susceptability	2.1	X-Xwater	<10^-2	Materials that meet this specification do not experience easily detectable magnetic forces or torques [68].
3.2	Chemical stability	1.7	No significant change in chemical composition of materials that are in contact with tissue or blood for 3 hours.	A prostate biopsy procedure can take up to 1.5 hours. This is the longest time interval in which the biopsy system is in contact with tissue or blood. For safety reasons, twice this value is chosen.
3.3	Mechanical stability	1.7	No significant change in mechanical performance of the biopsy system after being in contact with tissue or blood for 3 hours.	A prostate biopsy procedure can take up to 1.5 hours. This is the longest time interval in which the biopsy system is in contact with tissue or blood. For safety reasons, twice this value is chosen.
3.4	Sterilization	8.1	No significant change in mechanical performance of parts or in chemical composition of materials after being sterilized by 25kGy during their lifetime.	25kGy is commonly used to sterilize a surgical device [67].
4.0	*Dimensions*			

TABLE 10.2: The product specifications of the automatic biopsy system, their acceptance criteria and rationale behind it are listed in this table.

PS	Product Specifications	Related to UR	Acceptance Criteria	Rationale
4.1	Maximum operating dimensions	3.1	550 x 150 x 300 mm	Device used within the bore of a MRI scanner (D:60 cm) and operates between the legs of the patient (lithotomy, semi-lithotomy or lateral decubitus posistion). Height from bed to MRI scanner is approximately 60% of bore size.
4.2	Maximum transport dimensions	3.2	2210 x 1000 x 1000 mm	Overall dimensions of the device must not exceed a conventional small trolley bed. The trolley bed with the biopsy system should fit through a normal sized door (2 m height).
4.3	Maximum weight	3.3	2 kg	Positioning robot can lift 2kg [49].
5.0	*Biopsy Needle*			
5.1	Cutting length biopsy needle	4.2 and 4.3	from 15 mm up to 30 mm	Biopsy needles with different cutting lengths are used for prostate biopsy.
5.2	Needle diameter	4.4	From 14G up to 20G	Biopsy needles with different needle diameters are used for prostate biopsy. Based on currently used biopy needles.
5.3	Shaft length	4.5	<200 mm, >100 mm	Maximum length prostate is 50 mm [69]. Twice this value is chosen to compensate for skin thickness and safe distance between proximal end of needle and skin. Shorter length favourable to minimize needle tip deflection.
5.4	Dismountable	4.6	Biopsy needle can be dismounted from the biopsy system in maximum of 3 actions.	For each lesion a different biopsy needle is used to prevent cross-contamination. (Dis)mounting of the needle should not be time consuming.
6.0	*Tissue sampling*			
6.1	Fire cannula	5.1	Without manual intervention	Main function of system
6.2	Fire stylet	5.1	Without manual intervention	Main function of system
6.3	Reload cannula	5.1	Without manual intervention	Main function of system
6.4	Reload stylet	5.1	Without manual intervention	Main function of system
6.5	Stylet insertion velocity	5.4	>50 mm/s	Higher axial needle insertion velocity (up to 50 mm/s) reduces the development of rupture events that can occur when the stylet transits between different tissue layers [70][71].
6.6	Cannula firing velocity	5.4	>5 m/s	For fully automatic biopsy needles the cannula velocity should be higher than 5 m/s to obtain tissues samples of sufficient quality [72].
6.7	Multiple samples	5.5	Able to take multiple samples from same lesion without removing of needle.	Main function of system
6.8	Cross contamination	5.6	A biopsy needle is only used for sampling one lesion.	Sampling multiple lesions with same biopsy needle can result in cross contamination.
6.9	Sampling quality	5.4	Tissue sample has a length of >13 mm	Tissue sample with a length >13 mm has been considered to be of sufficient quality (Appendix A).
6.10	Detect stylet position	7.3	The axial position of the stylet is measured relative to the positioning robot with an accuracy of +/- 0.05 mm.	The positioning robot measures the orientation of the biopsy system in 3D relative to the MRI table [49]. Within the biopsy system the position of the stylet should be known.
6.11	Axial position accuracy of stylet	7.3	Axial accuracy position of stylet <1.0 mm.	The entire length of the stylet notch (up to 50 mm [69]) is to be positioned into the target lesion. An accuracy of +-2% of the longest possible stylet notch length was considered to be sufficient.
6.12	Detect cannula position	7.3	The axial position of the cannula is measured relative to the stylet with an accuracy of ±0.05 mm.	The positioning robot measures the orientation of the biopsy system in 3D relative to the MRI table [49]. Within the biopsy system the position of the cannula should be known to determine whether the cannula is fired entirely over the stylet notch.
6.13	Axial position accuracy of cannula	7.3	Axial accuracy position of cannula <1.0 mm.	The entire length of the stylet notch (up to 50 mm [69]) is to be covered with the cannula. An accuracy of ±2% of the longest possible stylet notch length was considered to be sufficient.
7.0	*Tissue removing*			

TABLE 10.2: The product specifications of the automatic biopsy system, their acceptance criteria and rationale behind it are listed in this table.

PS	Product Specifications	Related to UR	Accectance Criteria	Rationale
7.1	Removing sample	6.1	Without manual intervention	Main function of system
7.2	Amount of removal	6.2	No obvious parts of tissue sample left on stylet notch	Remaining tissue should not be inserted back into the patient
7.3	Control of depositing	6.1	Tissue sample deposited on carrier surface	Mix-up or loosing tissue sample should be prevented. Quality of sample must be preserved.
7.4	Fragmentation	6.3	Part of a fragmented tissue sample should be >10 mm	Fragmentation should be prevented to ensure quality
8.0	*Safety*			
8.1	Procedure initiation	7.2	Manually	Initiation is responsibility of operator.
8.2	Emergency stop	7.1	System has an emergency stop	Stop system during failure.
8.3	Manual retraction	7.2	System can after failure be manually retracted.	Manual retraction of needle after failure.

10.3   Identifying functions

Concepts that are created in a systematized manner are considered to provide the best solutions. This is accomplished by determining the main-functions that should be realized in the design of the automatic biopsy system. The following two main-functions are introduced:

1. Take a tissue sample with a biopsy needle without human intervention

2. Flush a tissue sample from a biopsy needle

The main-functions are unspecific and can be substituted by several specific sub-functions. Different solution can be created for these sub-functions and be visualized in a morphological chart. Combining different solutions for the sub-functions results in a concept. The following sub-functions were identified:

1a. Firing of stylet without human intervention

1b. Firing of cannula without human intervention

1c. Reloading of stylet without human intervention

1d. Reloading of cannula without human intervention

1e. Cannula firing mechanism

2a. Transportation of tissue sample to removing location without human intervention

2b. Flushing pump

Chapter 11

Conceptualization

This chapter describes the concept selecting process. First, solutions for the sub-functions are determined in Section 11.1 to 11.4. These solutions are visualized in a morphological chart (see Section 11.5). Five concepts are created using this chart. Finally, a Harris profile is constructed in Section 11.7, which is the bases for selecting the final concept in Section 11.8.

11.1 Solutions for function 1a to 1d

The first four sub-functions (1a to 1d) represent the ability to take a sample by firing and reloading the stylet and cannula without human intervention. In a needle biopsy procedure, a small amount of tissue should be separated from the target tissue. As explained in chapter 3, standard biopsy needles achieve this by inserting a stylet into the target tissue. The stylet has a notch that is filled with tissue. An outer sheath, also known as the cannula, is fired over the stylet to sever the tissue in the stylet notch from surrounding tissue. This type of cutting mechanism is known as the side-cut technique and is selected to be implemented in the automatic biopsy system (UR-5.2). Firing and reloading of the stylet and cannula without manual intervention requires some sort of automatic actuation. In this section, several actuation methods are identified. The actuator should move, possible via some sort of transmission, the stylet and cannula in the axial direction. The actuator should, as all the other components of the automatic biopsy system, be MRI-conditional (PS-2.1). The identified actuation methods are: (1) pneumatic cylinders, (2) hydraulic cylinders, (3) piezo-motors and (4) compression springs. They are briefly discussed in the next paragraphs.

11.1.1 Pneumatic cylinders

Pneumatic cylinders consist of a cylinder and a piston. A pressure difference between the sides of the piston causes the piston the move in axial direction. A pressure difference is created by increasing the air pressure at one side of the piston with compressed air or by creating a vacuum at the other side of the piston. Pneumatic cylinders can be divided into double-acting and single-acting pneumatic cylinders.

Only a MRI-conditional version of the former are commercially available (a €200 a piece). A cylinder that is MRI-conditional and single-acting will be a custom design. Besides that, only MRI-unsafe single-acting cylinders with a stroke length up to 50 mm are available. Increasing the stroke of single-acting pneumatic cylinders increased the overall length and costs of the cylinder more than with a similar stroke length double-acting cylinder. This is the case because the length of the spring increases non-linear with respect to the stroke length.

Spanner et al. did research on the influence on the signal-to-noise ratio of pneumatic cylinders used in an MRI bore. They concluded that pneumatic cylinders placed in or around an MRI scanner did not influence the signal-to-noise ratio [73].

The required stroke length of a pneumatic cylinder, which is used to actuate the stylet, depends on the tissue removing location. For example, if the tissue is removed at the proximal end of the cannula, then the stroke should at least be the length of the stylet (at least 100 mm). A single acting would in that case be unsuitable.
In contrast to single-acting cylinders, MRI-conditional double-acting pneumatic cylinders are available in numerous lengths, which makes them more suitable to actuate the firing and reloading of the stylet.
The cannula actuator should only move for a maximum of 30 mm, which is suitable for both a single- and double-acting pneumatic cylinder.

FIGURE 11.1: Figure shows a round-bore double-acting pneumatic cylinder. Figure retrieved from [74].

The advancing and retracting force of pneumatic cylinder depends on the bore diameter and the pressure difference. An estimation of the bore diameter could be determined as follows. The weight of the cannula was expected to be around 0.1 kg. The pressure available in most operation rooms is at least 4.0 bar [75] and is used for these calculations. The efficiency (η) of the cylinder is ±90%.

$$a_{cannula} = \frac{v_{cannula}^2}{2 * x_{velocity}} = \frac{5^2}{2 * 0.01} = 1250 \ \frac{m}{s^2} \tag{11.1}$$

$$F_{cannula} = m_{cannula} * a_{cannula} = 0.1 * 1250 = 125 \ N \tag{11.2}$$

$$A_{cannula} = \frac{F_{cannula}}{\rho * \eta} = \frac{125}{400.000 * 0,9} = 347 \ mm^2 \tag{11.3}$$

$$d_{cannula} = \sqrt{\frac{A_{cannula} * 4}{\pi}} = \sqrt{\frac{223 * 4}{\pi}} = 21.1 \ mm \tag{11.4}$$

The commercially available MRI safe double-acting pneumatic cylinders have a bore size of 9 mm. To be able to reach the required force, two of these cylinders can be used in parallel or a custom one with a bore size of at least 17 mm should be produced.
Whether a pneumatic cylinder is able to move the stylet is possible with a smaller

bore diameter pneumatic cylinder because a lower velocity of a less heavy mass is required.

Using vacuum instead of compressed air introduces the problem of having a maximum pressure difference of only 1 bar. The previously mentioned equations show that with a pressure difference of 1 bar a bore diameter of at least 47 mm is required. Such bore size cylinders are unsuitable for the biopsy system.

Whether a pneumatic cylinder is able to move the cannula with the required velocity of 5 $\frac{m}{s}$ is of interest. The velocity of the piston depends on the flow rate. The required velocity of 5 $\frac{m}{s}$ can be used to calculate the flow rate.

$$Q = V_{piston} * A_{piston} = 5 * 0.000223 = 0.000115 m^2/s = 67 L/min \qquad (11.5)$$

There are lots of affordable flow control valves available that can regulate the flow rate around this calculated value. However, there is another aspect of pneumatic cylinders that has an influence on the velocity. The friction between the piston and bore will prevent the piston from reaching the required speed. Whether the pneumatic cylinder can fire the cannula at a higher velocity is debatable. Though, there was concluded that pneumatic cylinders were suitable for the firing and reloading of the stylet.

11.1.2 Hydraulic cylinders

Hydraulic cylinders are similar to pneumatic cylinders but use a liquid instead of compressed air as working fluid. Compressing the liquid requires a pump, which is not available in the operating room. MRI safe hydraulic cylinders are not commercially available. Using hydraulics required a custom made design.

Pneumatic and hydraulic cylinders are similar in dimension and force output. Although, pneumatic cylinders can have a delay in movement because of the compressible air. Hydraulic cylinders use an in-compressible medium, which results in more direct and precise movement. This phenomenon is more present with higher loads. For the biopsy system low forces are expected, which means that the difference in performance between hydraulic and pneumatic cylinder is expected to be insignificant.

The use of a liquid brings an added risk to the system, which is leakage. Leakage would be a huge problem and could be dangerous for the patient. Compressed air leakage is on the other hand not considered to be a problem. Therefore, hydraulic cylinders are not considered to be a suitable solution for the firing and reloading of the cannula and stylet.

11.1.3 Piezo-motors

Piezo electric motors are able to generate unlimited linear or rotational motion by converting electrical energy charge on a certain material into a mechanical motion. This operating principle is called the inverse piezoelectric effect [73]. A piezo-electric rotary motor is shown in Figure 11.2.
Piezo-electirc motors are self-locking at rest position, have a compact size and provide nano meter accurate positioning. Some versions can be used in magnetic and

vacuum environments. Torques or linear forces of, respectively, 50 mNm and several 100 N can be achieved. However, non-magnetic piezo-electric motors are limited in speed (up to 200 rpm or 70 mm/s) [76][77]. Firing the cannula with the required velocity of 5 $\frac{m}{s}$ is not possible with such a motor.

FIGURE 11.2: Figure shows a non-magnetic rotary piezo-motor that was developed by Piezomotor. Figure retrieved from [77].

Fischer et al. compared MR-compatible actuators to determine the suitability for use in an MRI [78]. They tested a pneumatic actuator and two different piezo-electric actuators in an 1.5T and 3T MRI-scanner. The piezo-electric actuators caused large reduction in Signal-to-noise ratio in both 1.5T and 3T, especially with the controller placed in the scan room. This effect only occurred in real-time imaging. Another study showed that an operating piezo-electric motor interfered with the RF-field and caused motion artifacts [79]. Wang et al. showed that carefully shielding all components of a piezo-electric driven robotic system resulted in an ultra noise free system[80]. Fischer et al. showed that piezo-motors, which are used at a distance of more than 0.3 m, only slightly decrease the signal-to-noise ratio [78].

A piezo-rotary motor and its control hardware are estimated to cost up to 1000 €. There was concluded that piezo-electric motors are suitable for reloading and firing the stylet. However, they are only suitable for reloading the cannula and not firing the cannula because of insufficient velocity output.

11.1.4 Compression spring

A compression spring can be used to fire the cannula and stylet. They come in numerous lengths, diameters and spring constants. Also, springs can be produced from MRI-safe material such as brass or titanium. Although, it should be kept in mind that these materials can induce local heating due to the RF field in the MRI scanner.

Whether a compression spring can move the cannula with the required velocity of 5 $\frac{m}{s}$ after moving over 10 mm (X) [72], was calculated. The cannula had a mass of about 50 $grams$. The maximum sample length was 25 mm

$$a_{cannula} = \frac{V^2_{cannula}}{2X} = \frac{5^2}{2*0.01} = 1250 \ \frac{m}{s^2} \tag{11.6}$$

$$F_{advancing} = m_{cannula}a_{cannula} = 0.05*1250 = 62.5 \ N \tag{11.7}$$

$$C_{Spring} = \frac{F_{advancing}}{u_{max}} = \frac{62.5}{0.025} = 2500 \; \frac{N}{m} \tag{11.8}$$

Compression springs with this spring constant come in numerous lengths and diameters. Therefore, using compression springs as firing actuation is considered to be a viable option.

11.2 Solutions for function 1e

In the previous section, the actuators that could move the stylet and cannula are discussed. In the case of a decoupled fire and reloading actuation, a mechanism is required to couple the two actuation methods. Several of these mechanism are discussed next. Four different options are identified: (1) No mechanism required, (2) a cam roller mechanism, (3) a pinion and rack mechanism and (4) a firing pin mechanism.

11.2.1 No mechanism required

This option is selected when one type of actuator is used. For instance if a pneumatic cylinder is used for both the reloading and the firing of the cannula. Increasing the pressure at one side of the pneumatic cylinder results in moving the piston and, subsequently, firing of the cannula. No extra components were required.

11.2.2 Cam roller

This option can be selected when a piezo-electric rotary motor is used for the reloading and a compression spring for the firing of the cannula. The piezo-electric motor rotates the cam (see Figure 11.3), which on its turn pushes against a spring. The cams diameter increases from 0 to 360°and than returnes to its original diameter. At this point the loaded spring is able to fire the cannula in direction of the dotted arrow in Figure 11.3. The cam roller will be a custom made design.
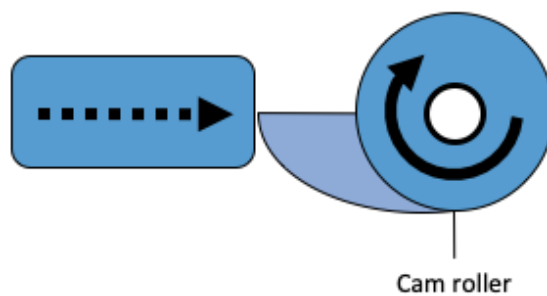

Cam roller

FIGURE 11.3: This figure shows a cannula firing mechanism consisting of a cam roller. The thick-line bordered area was fixed. The box with the dotted line was connected to the cannnula and spring. The dotted line was the cannula firing direction.

11.2.3 Gear pinion and rack

Again, this option can be selected when a piezo-electric rotary motor is used for the reloading and a compression spring for the firing of the cannula. The piezo-electric motor rotates the gear pinion (see Figure 11.4) that moves a gear rack in

linear direction. The gear rack pushes against the spring. The gear pinion is not standard because it is only partly teethed. The gear rack is free to move when the teeth-less part of the gear pinion moves over the rack. The gear pinion is custom made while the gear rack can be a standard part.
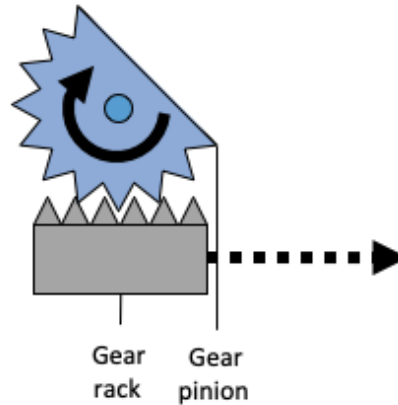
Gear
rack

Gear
pinion

FIGURE 11.4: This figure shows a cannula firing mechanism consisting of a gear pinion and rack. The thick-line bordered area was fixed. The gear rack was connected to the cannnula and spring. The dotted line was the cannula firing direction.

11.2.4 Firing pin

This option can be selected when a piezo-electric rotary motor or pneumatic cylinder is used for the reloading and a compression spring for the firing of the cannula. The cannula is connected to the firing pin and pushes against a compression spring. The firing pin can rotate outwards if not blocked. Figure 11.5 shows this position. The firing pin is rotated outwards and blocked to move in the direction of the dotted arrow. Only forcing the firing pin inwards (solid arrow in Figure 11.5) enables the spring to fire the cannula in the direction of the dotted arrow. The entire mechanism is custom made.
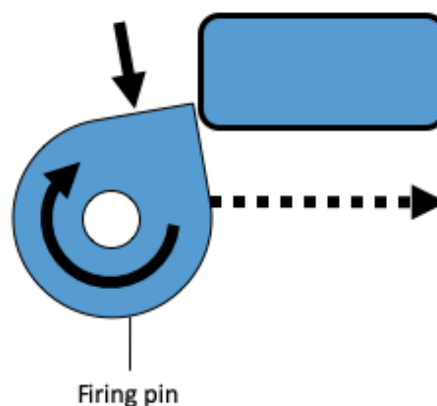
Firing pin

FIGURE 11.5: This figure shows a cannula firing mechanism consisting of a firing pin. The thick-line bordered box was fixed. The shaft of the firing pin was connected to the cannnula and spring. The dotted line was the cannula firing direction.

11.3 Solution for function 2a

After the tissue sample is separated from surrounding tissue, the tissue sample should be removed from the stylet notch. However, the tissue sample is inaccessible because it is still covered by the cannula. Therefore, the stylet should, after reloading both the cannula and stylet, be removed from the cannula to reveal the tissue sample. This could be done in two different ways. The stylet can be pushed out in the direction distal to the cannula or pulled backwards in the direction proximal to the cannula.

11.3.1 Distal end cannula

Pushing the stylet out of the distal end of the cannula to reveal the tissue sample is identical to the currently used technique. However, this would mean that the entire biopsy needle should be removed from the patient before the tissue sample can be removed. Bearing in mind that the system is required to take multiple samples (PS-5.3) from a lesion without retracting the needle, this solution is not an option.

FIGURE 11.6: This figured showed the stylet that was pushed out in the direction distal to the cannula.

11.3.2 Proximal end cannula

The second option is to retract the stylet all the way back to the proximal end of the cannula. With this solution, it is possible to take a tissue sample, remove and reinsert it without retracting the cannula from the lesion. This would mean that the stylet should be able to move over the entire length of the cannula.

FIGURE 11.7: This figured showed the stylet that was pulled back in the direction proximal to the cannula.

11.4 Solution for function 2b

A pump is used to create the pressure that is required to produce the flat spray. The selected flat spray nozzle requires a pressure difference of 1 bar. The spraying liquid should not contaminate the biopsy needle. Liquid pumps can be one of two categories. The liquid can be forced through a pump or an external force on a confined space, such as a syringe or bag, could increase the pressure. The former is considered to increase the risk of contamination because the entire pump should be sterile. With the latter pump category, only the confined space is required to be sterile. Therefore, this category is selected. Two type of pumps are identified: (1) syringe pump and (2) peristaltic pump .

11.4.1 Syringe pump

The working principle of a syringe pump is straightforward. An external force on the syringe plunger increases the pressure in the syringe. MRI-compatible syringe pumps are available. Though, manufacturing a custom one is not considered to be a challenge. The pressure created in the syringe depends on the plunger diameter and external force. The pressure range (up to several bar) of syringe pumps is considered to be sufficient for the application.

11.4.2 Peristaltic pump

A peristaltic pump increases the pressure by constricting a tube in wave-like motion. Figure 11.8 shows a pump where a tube is constricted at three different locations.
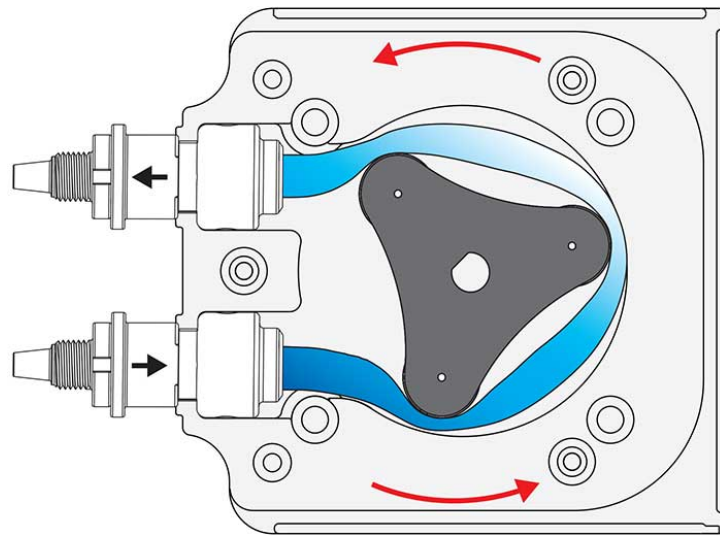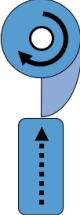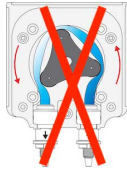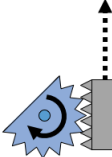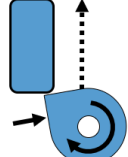

FIGURE 11.8: This figure illustrate the working principle of a peristaltic pump. Figure retrieved from [81].

MRI-safe version of such pumps are available. However, they are not able to reach the required pressure. This makes this type of pump unsuitable for the application.

11.5 Morphological chart

The concepts for subsystem I are created using a morphological chart (see Figure 11.1). Such a chart aided in the concept creating process. The solutions of the subfunctions, which were mentioned in previous sections, are visualized in a morphological chart.

TABLE 11.1: Figure visualizes the different solutions in a morphological chart. Where 1a is 'Firing of stylet', 1b is 'Firing of cannula', 1c is 'Reloading of stylet', 1d is 'Reloading of cannula', 1e is 'Cannula firing mechanism', 2a 'Tissue sample transport to removing location' and 2b is 'Flushing pump'. The solutions with a red cross are excluded because of not fitting the requirements.

#	1a	1b	1c	1d	1e	2a	2b
1	Pneumatics	Pneumatics	Pneumatics	Pneumatics	None	Distal end	Syringe pump
2	Hydraulics	Hydraulics	Hydraulics	Hydraulics	Cam roller	Proximal end	Peristaltic pump
3	Piezo Motor	Piezo Motor	Piezo Motor	Piezo Motor	Pinion and rack		
4	Spring	Spring			Firing pin		

11.6 Concepts

11.6.1 Concept 1

In this concept (see Figure 11.9) the options for the five sub-functions (see Figure 11.1) are, respectively, 1, 1, 1, 1, 1 , 2 and 1. Two double-acting pneumatic cylinders independently actuate the stylet and cannula. The piston-rod of the stylet pneumatic actuator is concentric to the cannula pneumatic actuator and can independently move in axial direction.

Both pneumatic cylinders are discretely controlled by two piezo-valves per cylinder. These type of valves are MRI-safe, which means that they can be placed near the MRI-scanner. The pneumatic cylinder that actuate the firing and reloading of the cannula is custom made. Whether it can fire the cannula at the required speed ($5 \frac{m}{s}$) is debatable (see Section 11.1.1). The stylet and cannula are standard components. The sample can be removed from the stylet notch at the proximal side of the cannula pneumatic cylinder. Pneumatic cylinder are not heavy, which means that the overall weight is estimated to be <2kg.

FIGURE 11.9: This figure shows a front-view sketch of concept 1. The components with a thick border-line were fixed. The remaining components could move with respect to the fixed components. In this sketch, the cannula is reloaded and the stylet is fired. The estimated length was shown at the bottom.

11.6.2 Concept 2

In this concept (see Figure 11.10) the options for the five sub-functions (see Figure 11.1) are, respectively, 1, 1, 1, 1, 1, 2 and 1. Two standard double-acting pneumatic cylinders independently actuate both the firing and reloading of the stylet and cannula. The pneumatic cylinders are orientated co-linear to one another. Similar to concept 1, piezo-valves control both cylinders.

FIGURE 11.10: This figure shows a top-view sketch of concept 2. The components with a thick border-line were fixed. The remaining components could move with respect to the fixed components. In this sketch, the cannula was reloaded and the stylet was fired. The estimated length was shown at the bottom.

Whether a pneumatic cylinder can fire the cannula at the required speed (5 $\frac{m}{s}$) is also debatable in this concept (see Section 11.1.1). The tissue sample is removed by the flat spray at the proximal end of the cannula. This concept is relatively simple because it consisted of only a few standard components . The stylet and cannula are standard components. So were both the pneumatic cylinders. Pneumatic cylinders are not heavy, which means that the overall weight is estimated to be <2kg.

11.6.3 Concept 3

In this concept (see Figure 11.11) the options for the five sub-functions (see Figure 11.1) are, respectively, 1, 4, 1, 1, 4, 2 and 1. A standard double-acting pneumatic cylinders actuate both the firing and reloading of the stylet. Two standard double-acting pneumatic cylinders are used to reload the spring-loaded cannula. Two pneumatic cylinders are orientated in a symmetric manner, which crosses out any undesirable torques. Such torques applied on the biopsy needle can result in bending and, possible, lead to failure.

The spring-loaded cannula and cannula pneumatic cylinders are not connected to one another. A locking mechanism, which is connected to the cannula, consisted of two firing pins. When loaded, the firing pins rotate outwards and prevent the cannula from advancing. Advancing the cannula pneumatic cylinders, forces the firing pins to rotate inwards, which enables the spring to move the cannula forwards. Similar to concept 1, piezo-valves control both cylinders. The tissue sample is removed by the flat spray in between the cannula pneumatic cylinders. This concept is relatively complex because it consisted of, among other, a custom locking mechanism. The stylet and cannula are standard components. So are all the pneumatic cylinders. Once again, the overall weight is estimated to be <2kg.

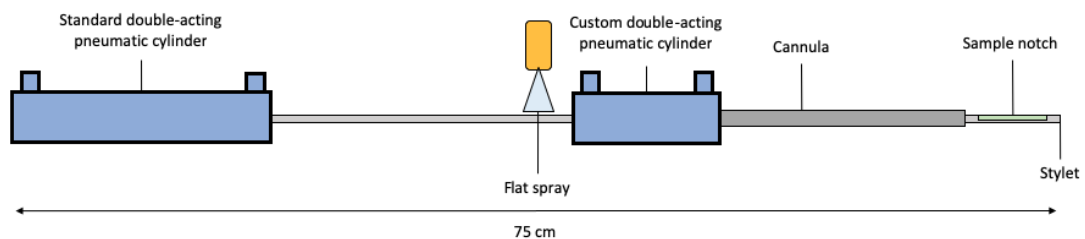FIGURE 11.11: This figure shows a top-view sketch of concept 3. The components with a thick border-line were fixed. The remaining components could move with respect to the fixed components. In this sketch, the cannula was reloaded and the stylet was fired. The estimated length was shown at the bottom.

11.6.4 Concept 4

In this concept (see Figure 11.12) the options for the five sub-functions (see Figure 11.1) are, respectively, 3, 4, 3, 3, 3, 2 and 1. A piezo-electric rotary motor reloads and fires the stylet. The rotational motion of the motor is translated to a linear motion by means of gear pinion and rack combination. Because piezo-electric rotary motors are not able to move the cannula at the required speed, another actuation methods is used. The cannula is fired by a compressed spring. Again, a gear rack and pinion translates the rotational motion to a linear one. The pinion is not standard. A part

the pinions teeth is removed. No contact between gear pinion and rack is present when the teethless part of the pinion is positioned above the rack. This enables the spring to fire the cannula.

The controllers of the piezo-electric motors are not MRI-safe. Therefore, placing them in the control room or shielding is required. The tissue sample is removed by the flat spray at the proximal side of the spring. This concept is relatively complex because it consisted of, among others, two custom gear mechanisms. The stylet and cannula are standard components. So were all the piezo-electric motors. Such motors are not heavy, which means that the overall weight was estimated to be <2kg. However, MRI image distortion is considered to be a problem as the piezo motors are placed within 0.3 m from the iso center of the MRI image (see Section 11.1.3 for an explanation).
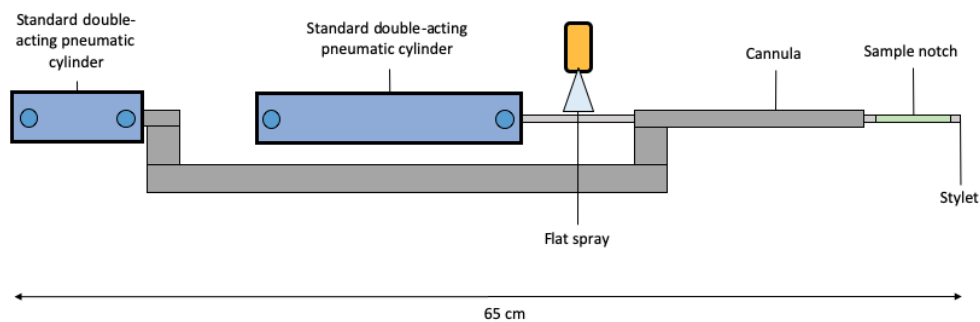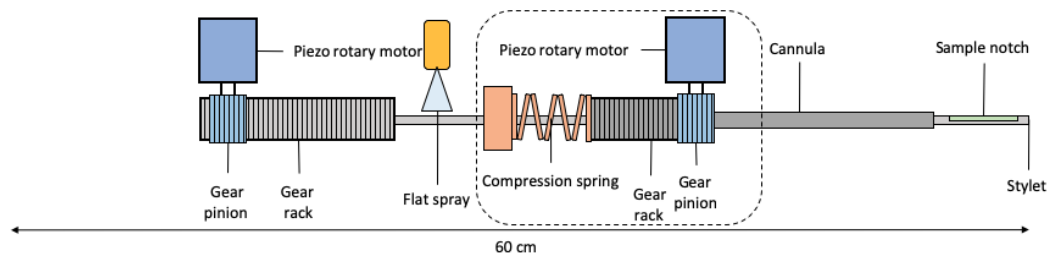

FIGURE 11.12: This figure shows a front-view sketch of concept 4. The components with a thick border-line were fixed. The remaining components could move with respect to the fixed components. In this sketch, the cannula was reloaded and the stylet was fired. The estimated length was shown at the bottom. A top-view sketch of the parts enclosed by the dotted-line box was shown in 11.13.
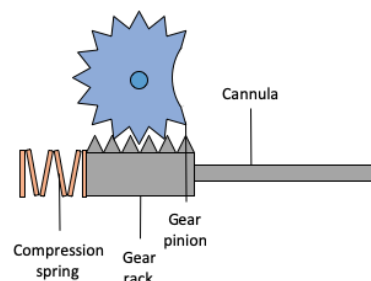
FIGURE 11.13: This figure shows front-view sketch of the parts enclosed by the dotted-line box in Figure 11.12. 11.13.

11.6.5 Concept 5

In this concept (see Figure 11.14) the options for the five sub-functions (see Figure 11.1) are, respectively, 3, 4, 3, 3, 2, 2 and 1. This concept is similar to concept 4. A piezo-electric rotary motor is used to reload and fire the stylet. The rotational motion of the motor is translated to a linear motion by means of gear pinion and rack combination. The cannula is fired by a compressed spring. Here, a cam roller is used to translate the rotational motion to a linear one (see Figure 6.4f). Rotating the cam roller for more than 360 °enables the spring to fire the cannula.

The controllers of the piezo-electric motors are not MRI-safe. Therefore, placing them in the control room or shielding is required. The tissue sample is removed by the flat spray at the proximal side of the spring. This concept is relatively complex because it consisted of, among others, a custom gear cam roller mechanism. The

stylet and cannula are standard components. So were all the piezo-electric motors. Similar to the concept 4, the weight is not sufficient and MRI-image distortion was considered to be a problem.
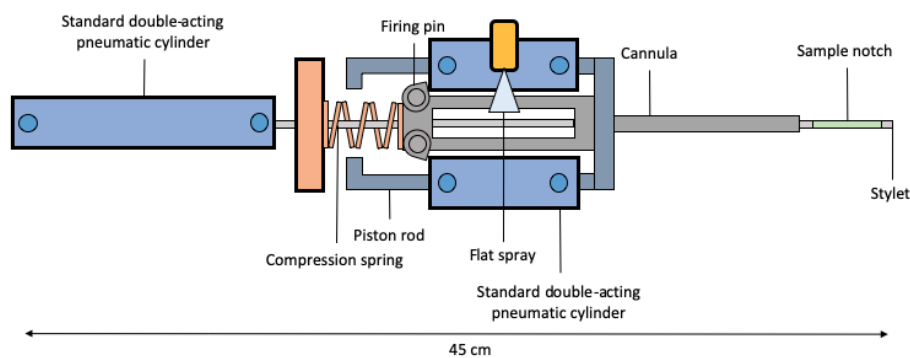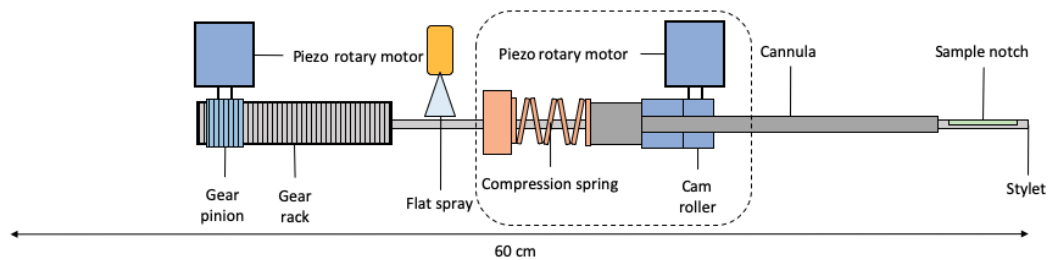

FIGURE 11.14: This figure shows a front-view sketch of concept 5. The components with a thick border-line were fixed. The remaining components could move with respect to the fixed components. In this sketch, the cannula was reloaded and the stylet was fired. The estimated length was shown at the bottom. A top-view sketch of the parts enclosed by the dotted-line box was shown in 11.15.
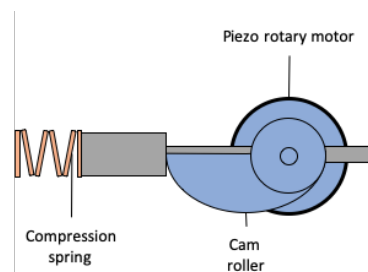
FIGURE 11.15: This figure shows front-view sketch of the parts enclosed by the dotted-line box in Figure 11.14

11.7 Harris profile

A Harris profile is constructed to highlight the strong and weak points of the concepts. A four-point scale is used, where – scored -2 points and ++ scored +2 points. Six criteria are selected from the requirement and specification lists. For each criteria, the values of the four level scale are determined (see Table 11.2). These values are based on the acceptance criteria of the requirement or specification. Section 11.6 consists of all the information that is required to score the concepts. The concepts are scored in Table 11.3.

TABLE 11.2: The scoring of criteria for a Harris profile are explained in this table. Criteria based on the user-requirements (UR) or product specifications (PS) are listed in the first column.

	Score			
UR or PS	–	-	+	++
Dimensions	>>600x200x400 mm	>600x200x400 mm	600x200x400 mm	<600x200x400 mm
Weight	>3 kg	2 to 3 kg	2 kg	<2 kg
Cannula velocity	<1 m/s	3 to 5 m/s	5 m/s	>5 m/s
Standard parts	0%	0 to 50%	50 - 80%	80 - 100%
MRI image distortion	Very likely, metals with high conductivity used at a distance <0.3 m from MRI image iso-center [78]	More likely, metals with high conductivity used at a distance >0.3 m from MRI image iso-center[78]	Not likely, because metals with low conductivity used	None, because no metals used
Costs	>2000	1000 to 2000 euro	500 to 1000 euro	0 to 500 euro

TABLE 11.3: A Harris profile, consisting of 5 concepts, is shown in this table. Criteria based on the user-requirements (UR) or product specifications (PS) are listed in the first column. Their scoring was explained in Table 11.2

	Concept 1				Concept 2				Concept 3				Concept 4				Concept 5			
UR or PS	–	-	+	++	–	-	+	++	–	-	+	++	–	-	+	++	–	-	+	++
Dimensions	–						+					++			+				+	
Weight				++				++				++				++				++
Cannula velocity		-				-					+				+				+	
Standard parts			+					++			+					++				++
MRI image distortion			+				+				+			-				-		
Costs			+				+				+			-				-		
Total score	2				6				8				4				4			

11.8 Selecting final concept

The Harris profile constructed in the previous section, shows that the third concept scores the best in terms of the selected criteria. Concept 2 comes in close second place. The difference in score between these concepts originated from several criteria.

The criteria 'cannula velocity' was the most important. One of the main functions, 'taking a tissue sample', has a higher chance of failure when the cannula velocity is not sufficient. This was the case in concept 2. Though, in contrast to concept 3, concept 2 has the advantages of using more standard parts. However, the custom parts in concept 3 are easy to construct using 3-D printing or conventional machining and, therefore, this was not considered to be a problem. The advantage of the concepts that used pneumatic cylinders to fire the cannula did out weigh to the disadvantage of possibly not reaching the required firing velocity.

Concept 4 and 5 scored rather low compared to concept 3. As described in Section 11.1.3, piezo-electric motors tend to reduce the signal-to-noise ratio and cause artifacts on MRI-images. Pneumatic cylinders on the other hand do not cause distortions on MRI-images of any kind. Besides that, piezo-electric motors are quite expensive compared to pneumatic cylinders. Both these criteria had the most contribution in the difference between scores.

The pneumatic cylinders in concept 3 are discretely controlled. Controlling such movements is rather simple. The piston is fired in or out wards. This means that the controller should only turn the pneumatic valves on or off. Controlling a piezo-electric motor is more complex as it should move to a predefined position, which required a position feedback-loop.

Concept 3 is selected to be the final concept because of the small dimensions, no MRI-image distortion, high cannula velocity and simple control. Also, no show-stoppers were encountered.

Chapter 12

Proof of Principle prototype

This chapter discusses the proof principle prototype of the automatic biopsy system. First, the differences between the final concept and the prototype are discussed in section 12.1. The embodiment of the design is explained in Section 12.2. Finally, the Solid Works model and prototype are presented.

12.1 Differences with final concept

The prototype should provide a way of proving the design principle. Thus, it is not imperative to implement all detailed features of the design in to the prototype. PS-2.1, 2.2, 2.3 and 3.1 do not apply to the proof of principle prototype because it will not be tested in an MRI scanner or with an Ultra-sound prove. This means that expensive or long lead-time MRI-compatible components can be replaced by MRI-unsafe ones. This applies to the pneumatic cylinders and the compression spring. MRI-safe pneumatic cylinders are 10 times more expensive than MRI-unsafe ones. MRI-safe compressing springs are custom made from titanium, which have a long lead-time.
The prototype is not for human use. Thus, sterility, stability and safety (PS-3.2 to 3.4 and 8.1 to 8.3) do not apply in this stage of the design process.
The design principle can be proven by using just a 18G needle with a cutting length of 20 mm. Needles with other diameters and cutting length are not required. PS-5.1, 5.2 and 5.4 are discarded.
PS-6.12 to 6.14 are suspended because knowing the exact position of the biopsy needle in real-time is only of interest for final design and not for the proof of principle prototype.

12.2 Embodiment

Some calculations are required before components can be selected. This applies to the compression spring that is responsible for firing the cannula at the required velocity. Besides that, the pneumatic cylinders should be able to fully compress the compression spring.

12.2.1 Selecting compression spring

In Section 11.1.4, a preliminary calculation of the required advancing force was done. This calculation is updated with the correct cannula mass.

$$F_{Fire} = m_{cannula} a_{cannula} = 0.06 * 1250 = 75 \ N \tag{12.1}$$

$$C_{Spring} = \frac{F_{Fire}}{u_{max}} = \frac{75}{30} = 2.5 \; \frac{N}{mm} \tag{12.2}$$

A spring with a spring constant, stroke length and inner diameter of, respectively, $2.5 \; \frac{N}{mm}$, 31.75 mm and 6.75 mm is considered to be sufficient to fire the cannula at the required speed.

12.2.2 Selecting pneumatic cylinders

An air pressure of 4 bar, which is the air pressure that is available in most operating rooms [75], is used to operate all the pneumatic cylinders. The cylinders have an efficiency of about 90%. The stylet is translated over a distance of 160 mm. Therefore, a pneumatic cylinder with a stroke length of 160 mm is selected. No large forces are subjected on this pneumatic cylinder. The smallest possible cylinder diameter is considered to be sufficient.

With the known cannula advancing force, the required dimensions of the two pneumatic cylinders can be determined.

$$F_{Reload} = \frac{1}{2} F_{Fire} = 37.5 \; N \tag{12.3}$$

$$A_{cannula} = \frac{F_{Reload}}{\rho * \eta} = \frac{37.5}{400.000 * 0,9} = 104 \; mm^2 \tag{12.4}$$

$$d_{cannula} = \sqrt{\frac{A_{cannula} * 4}{\pi}} = \sqrt{\frac{104 * 4}{\pi}} = 11.5 \; mm \tag{12.5}$$

Pneumatic cylinders with a bore diameter of 12 mm and a stroke length of 25 mm are considered to be sufficient to reload the cannula.

The syringe that creates the flat spray, is actuated by a pneumatic cylinder as well. A plunger force of 100 N is required to generate the flat spray.

$$A_{flushing} = \frac{F_{flushing}}{\rho * \eta} = \frac{100}{400.000 * 0,9} = 277 \; mm^2 \tag{12.6}$$

$$d_{flushing} = \sqrt{\frac{A_{flushing} * 4}{\pi}} = \sqrt{\frac{104 * 4}{\pi}} = 14.7 \; mm \tag{12.7}$$

A pneumatic cylinder with a bore diameter of 16 mm and a stroke length of 100 mm is considered to be sufficient to generate the flat spray.

12.2.3 Manufacturing

For the final product, the custom made parts will be manufactured using injection molding. This manufacturing technique has long lead-times and is expensive. Therefore, during the prototype phase, 3D-printing and conventional machining is used instead of injection molding.

12.2.4 Materials

The custom parts are 3D printed in PLA. The standard parts consist of one of the following materials: Stainless Steel, Acrylic, PUN, Rubber, Brass, Polypropylene or PEEK. Only the first one has a high magnetic susceptibility. It is processed in the

pneumatic cylinders, control valves, springs and screws. See Appendix 6.4f for a Bill Of Materials.

12.3   Solid-Works design and prototype

Figure 12.1 and 12.2 shows an isometric and top view of the prototype in Solid Works. Other views can be found in Appendix G. The proof of principle prototype is shown in Figure 12.
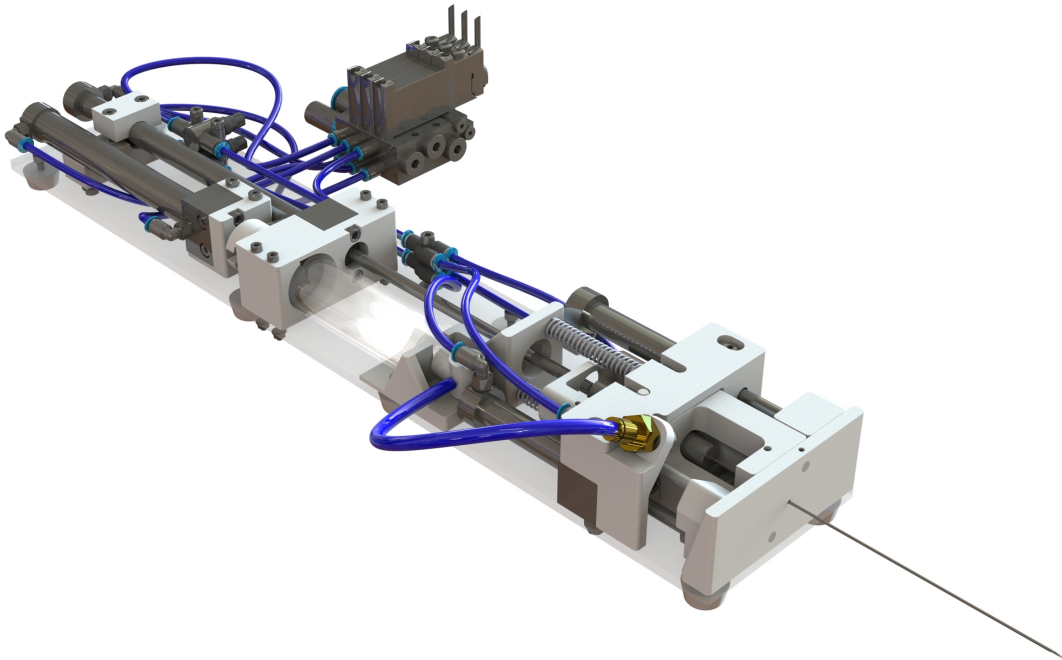
FIGURE 12.1: This figure shows an iso-metric view of the prototype designed in Solid-Works. Here, both the cannula and the stylet are fired.
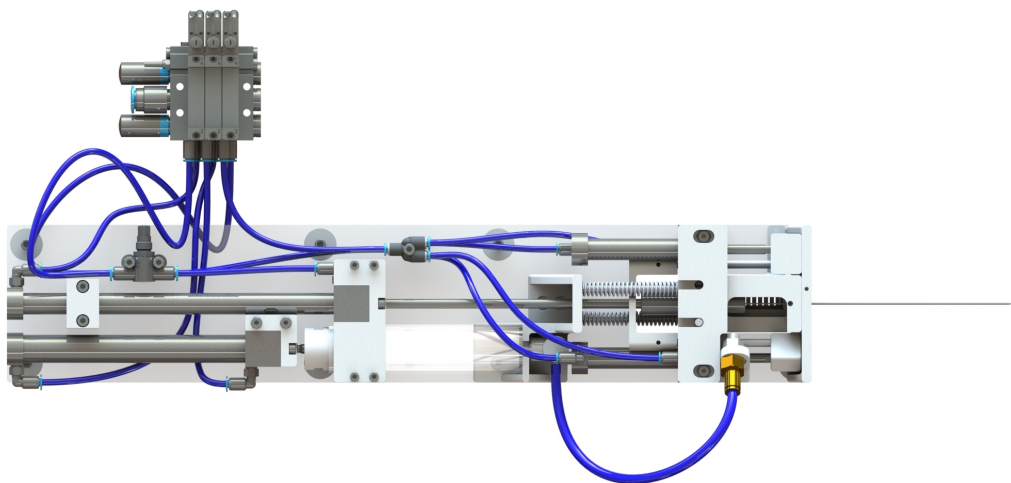
FIGURE 12.2: Top view of the proof of principle prototype in Solid-Works. Figure shows both stylet and cannula in reloaded position.
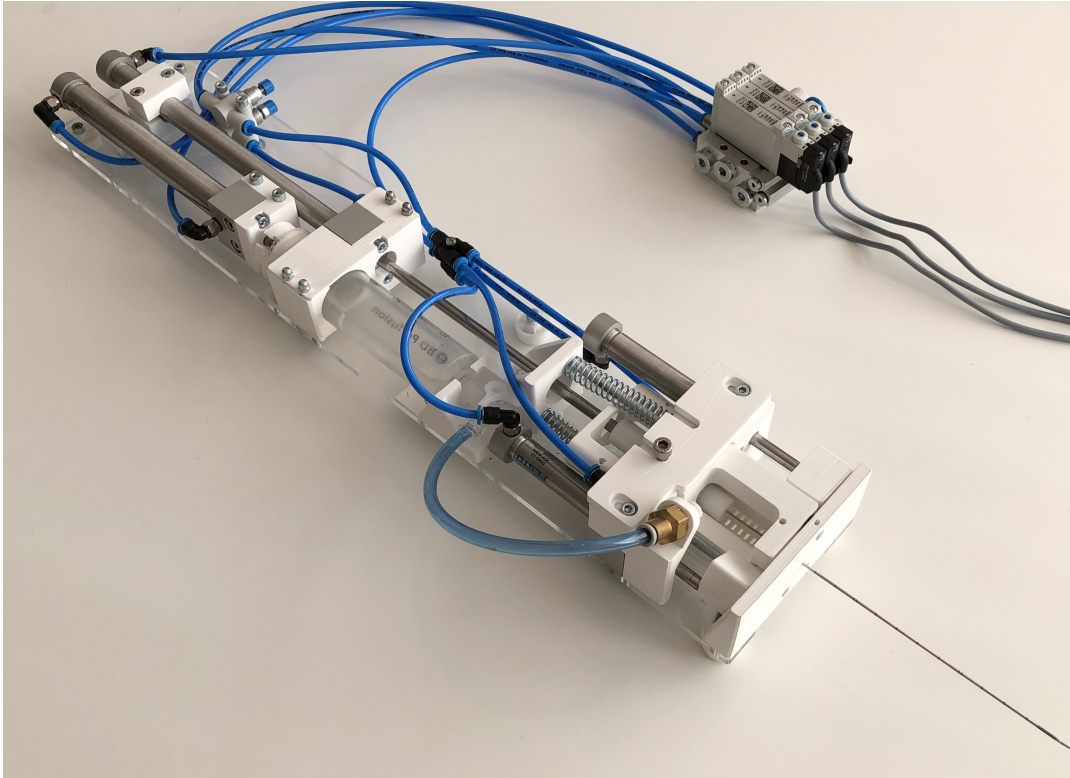
FIGURE 12.3: This figure shows an iso-metric view of the built prototype. Figure shows both stylet and cannula in fired position.
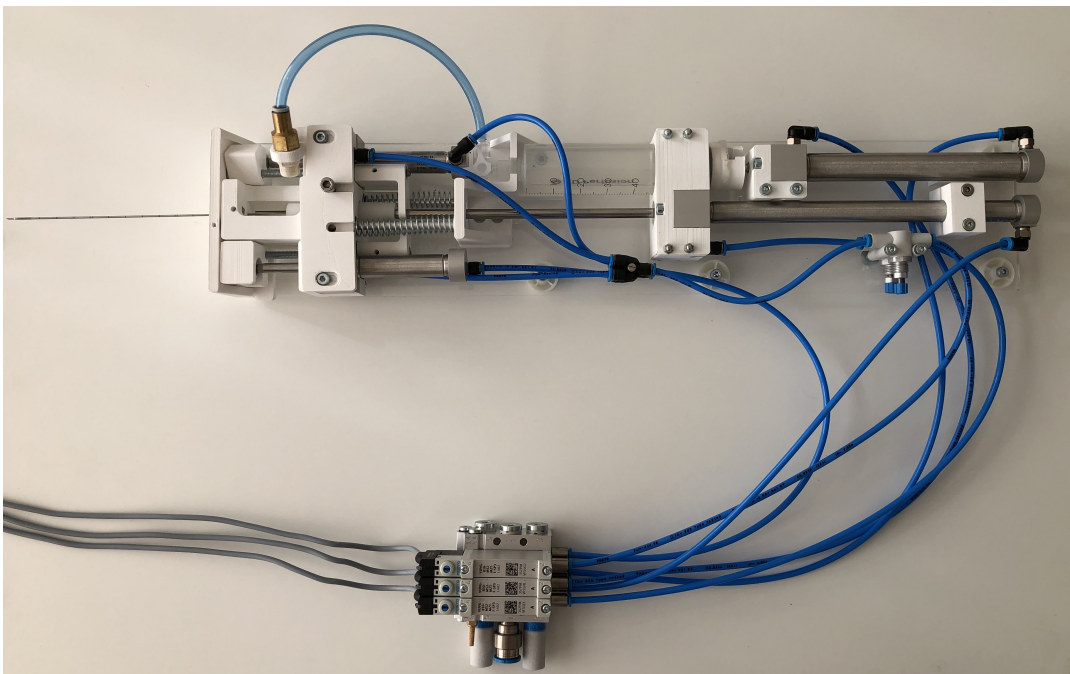
FIGURE 12.4: Top view of the built of principle prototype in. Figure shows both stylet and cannula in fired position.

Chapter 13

Discussion Part C

Part C described the development process of the automatic biopsy system. Based on the clinical workflow, user-input (CoBra project) and literature, user requirements (UR) were determined. Product specifications (PS) were derived from these UR. The PS were quantifiable, verifiable, specific and solution-neutral. Two main functions of the automatic biopsy system were identified: (1) taking a tissue sample with a biopsy needle without human intervention and (2) flush a sample from a biopsy needle. The functions were split into seven sub-functions. Solutions for these sub-functions could be identified and their potential was discussed. Solutions that definitely could not meet the requirements were discarded.

Combining the remaining solutions lead to the construction of five different concepts. A Harris profile showed the strong and weak points of the concept. Of the six criteria used for this profile, MRI image distortion, cannula velocity and costs turned out to differ the most between concepts. The final concept scored high in all the aforementioned criteria. Here, a pneumatic cylinder both reloaded and fired the stylet. While a compression spring and a pneumatic cylinder, respectively, fired and reloaded the cannula, a firing pin mechanism (see Section 11.2 for explanation) decoupled the two actuation methods in between cannula firing and reloading. One of the strong points of this concept was that MRI-safe pneumatic cylinders are commercially available. Also, these cylinders were proven not to distort the MRI-image quality. Finally, the cannula velocity, costs and dimensions were all within limits.

The final concept was realized in a proof of principle prototype. Several differences were made to reduce costs and lead-time. The most important change was that the prototype did not have to meet the MRI-conditional requirement. Hence MRI-safe components could be replaced by MRI-unsafe ones.

Part D

Prototype verification

Chapter 14

Verification Plan

The present part describes the verification of the proof of principle prototype against the product specification. This chapter is focused on the verification plans. In Section 14.1 a distinguish is made between product specifications that require testing and ones that do not. Test plans for testing these PS are discussed next in Section 14.3.

14.1 Categorize product specifications

As is described in Section 12.1, several product specifications are not applicable to the proof of principle prototype. They are once again listed in Table 14.1.

Whether the proof of principle prototype meets the remaining PS is determined in this part. A distinction is made between product specifications that can be evaluated by observation or ones that require some sort of testing (see Table 14.1).

TABLE 14.1: This table is a list of the product specifications (PS). Whether the PS was applicable to the proof principle prototype is indicated here. Also, the method of verification for each PS is determined.

PS	Product Specification	Applicable to prototype	Verification by observation	Verification by testing
1.1	Sampling time	No		
2.1	MR conditional	No		
2.2	Ultrasound compatible	No		
2.3	Local SAR	No		
3.1	Magnetic susceptability	No		
3.2	Chemical stability	No		
3.3	Mechanical stability	No		
3.4	Sterilization	No		
4.1	Maximum operating dimensions	Yes	x	
4.2	Maximum transport dimensions	Yes	x	
4.3	Maximum weight	Yes	x	
5.1	Cutting length biopsy needle	No		

5.2	Needle diameter	No		
5.3	Shaft length	Yes	x	
5.4	Dismountable	No		
6.1	Fire cannula	Yes	x	
6.2	Fire stylet	Yes	x	
6.3	Reload cannula	Yes	x	
6.4	Reload stylet	Yes	x	
6.5	Stylet insertion velocity	Yes		x
6.6	Cannula firing velocity	Yes		x
6.7	Multiple samples	Yes	x	
6.8	Cross contamination	Yes	x	
6.9	Sampling quality	Yes		x
6.10	Detect stylet position	No	x	
6.11	Axial position accuracyof stylet	No	x	
6.12	Detect cannula position	No	x	
6.13	Axial position accuracyof cannula	No	x	
7.1	Removing sample	Yes	x	
7.2	Amount of removal	Yes		x
7.3	Control of depositing	Yes		x
7.4	Fragmentation	Yes		x
8.1	Procedure initiation	No		
8.2	Emergency stop	No		
8.3	Manual retraction	No		

14.2 Verification by observation

There are 10 product specifications that can be verified by observation. Whether these product specifications are met is merely checked by measuring or observing the prototype. Measuring is done using a ruler or scale. The attributed values are compared with the acceptance criteria and this determines whether the product specification passed or failed.

14.3 Verification by testing

Eight product specifications can not be verified by observation but require testing. They are verified by 3 type of tests. The PS that are focused on velocity are to be tested in the first set of tests. PS-6.9 is verified in the second set of tests. The remaining PS, which are focused on sample removal, are verified in the last set of tests.

14.3.1 Test Plan: Velocity

The required velocity of the stylet and cannula during firing is described in PS-6.5 and 6.6. This is tested by making a video with a camera that makes 120 frames per second. Counting the frames from moment of fire phase to end of fire phase gives the time span over a certain distance. The velocity is found by dividing the covered distance by the time span. The test protocol is described in Appendix H

14.3.2 Test Plan: Tissue sample quality

The quality of the tissue sample is described in PS-6.9 and is expressed in terms of tissue sample length. The acceptance criteria were based on literature, which described the required length of prostate tissue samples. Testing the automatic biopsy system on a live human prostate is not possible at this stage of the design process. Therefore, the sample quality is tested using uncooked chicken breasts.
Whether chicken breast tissue resembles prostate tissue was unknown. The initially set acceptance criteria might not apply to chicken breast. Therefore, the automatic biopsy system was not evaluated based on this acceptance criteria but it is compared to the performance of a standard manual 18G Tru-cut biopsy needle (Figure 14.1).
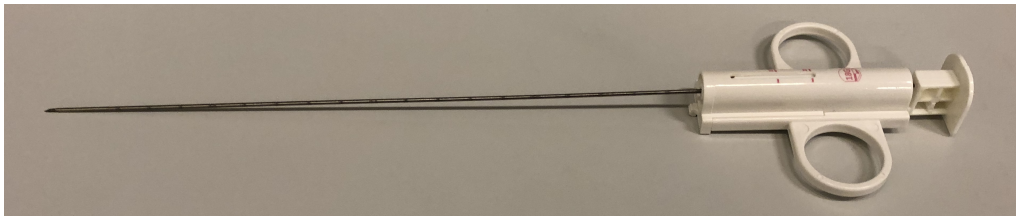
FIGURE 14.1: Semi-automatic 18G Tru-cut biopsy needle (brand).

In the present test plan, the biopsy instrument is the independent variable and the tissue sample length the dependent variable. Equal number of samples are taken with both biopsy needles from three chicken breasts. The samples are taken in a systematic manner to eliminate the influence of previous punctures on the tissue composition. The length of a tissue sample is measured using a caliper (accuracy of ±0.05 mm). The mean tissue sample length are compared using a two-side t-test.
The minimum test size is determined by assuming that the data has a normal distribution. The standard deviation is assumed to be similar to the one that was reported in Kanoa et al. In this study, a standard 18G Tru-cut biopsy needle with a cutting length of 20 mm was used to sample 469 patients. This resulted in an overall standard deviation of 2.9 mm. An acceptable error margin is chosen to be 0.7 mm. The margin of error, standard deviation and confidence interval (95%) are used to determine the minimum sample size of 71 samples per group. The product specification is verified if no significant ($p < 0.05$) decrease in tissue sample length is reported. In Appendix I the test protocol is described in more detail.

14.3.3 Test Plan: Removing a tissue sample

PS-7.2 to 7.4 are verified in the last set of tests. These product specifications describe the tissue sample removing part of the automatic biopsy system. These test are comparable to the ones that are described in Section 8.1.2.

In this test, the same requirements were evaluated. However, the acceptance criteria of PS-7.4, the fragmentation specification, were different. The reason for the alternative acceptance criteria was the use of uncooked chicken tissue instead of live human prostate tissue. For the present test, live human prostate tissue is not available. Therefore, also here, uncooked chicken breast is used. Similar to the test plan described in the previous paragraph, the initially set acceptance criteria might not apply to chicken breast. Therefore, PS-7.4 is updated with the acceptance criteria shown in Table 6.2 for the fragmentation requirement. This acceptance criteria was: tissue sample length after removal should be ≥80% of the length before removal.

The experimental design consists of the following. First, a sample is taken from a chicken breast using the automatic biopsy system. Then it is removed from the stylet by flushing and deposited on the carrier surface, which is the dark surface area in Figure 14.2.

During each run, two measurements were reported: the length of the sample before and after removal. The percentage mentioned in the acceptance criteria of PS-7.4 is the tissue sample length after removing with respect to before removing. Besides that, tissue waste, which potentially remained on the stylet after removing the sample from the stylet, is reported. Finally, the sample depositing location is reported as correct or incorrect.

The samples are taken in a systematic manner to eliminate the influence of previous punctures on the tissue composition.
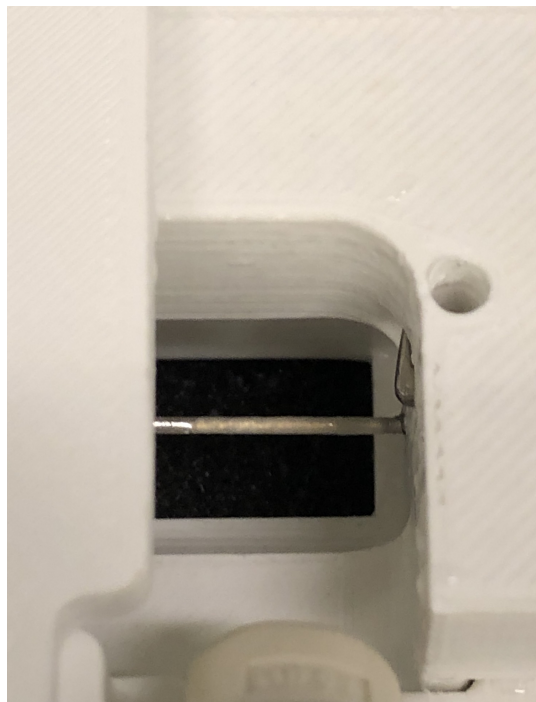
FIGURE 14.2: A close up of the sample just before removal is shown in this figure. The dark surface is the carrier surface at which the sample should be deposited.

A non-parametric binomial model was used to demonstrate a certain probability of conformance to the above-mentioned specifications at a given confidence level for characteristic that had an attributed pass/fail value (Guo et al.). The probability of conformance to a specification (PCS) is related to the risk of the characteristic (major, minor).

Major is associated with a significant degradation of prototype function, while minor only means the prototype functions poorly but still is fit for use. PS-7.2 and PS-7.4 are considered to be a major risk and have a PCS of 97%. Non-conformance to PS-7.3 poses only a minor risk (PCS of 95%).

A 90% confidence level was chosen for both specifications. According to the table shown in Guo et al., zero-failures should appear in a population size of 45 (minor risk) and 76 (major risk).

A more detailed test protocol is described in Appendix J.

Chapter 15

Verification Results

15.1 Verification by observation

Table 15.1 shows the results of the verification by observation. A pass or fail value was attributed by comparing the acceptance criteria with the measured result.

TABLE 15.1: This is a list of product specifications (PS) that were verified by observation. Comparing the results with the acceptance criteria determined whether the PS was met.

PS	Product Specification	Acceptance criteria	Result	Pass/fail
4.1	Maximum operating dimensions	550 x 150 x 300 mm	450 x 140 x 45 mm	Pass
4.2	Maximum transport dimensions	2210 x 1000 x 1000 mm	330 x 100 x 45 mm	Pass
4.3	Maximum weight	2 kg	1.4 kg	Pass
5.3	Shaft length	<200 mm, >100 mm	120 mm	Pass
6.1	Fire cannula	Without manual intervention	Yes	Pass
6.2	Fire stylet	Without manual intervention	Yes	Pass
6.3	Reload cannula	Without manual intervention	Yes	Pass
6.4	Reload stylet	Without manual intervention	Yes	Pass
6.9	Multiple samples	Able to take multiple samples from same lesion without removing of needle.	Yes	Pass
6.10	Cross contamination	A biopsy needle is only used for sampling one lesion.	Yes	Pass

15.2 Verification by testing

15.2.1 Test Result: Velocity

Table 15.2 shows the results of the cannula and stylet velocity tests. A pass or fail value was attributed by comparing the acceptance criteria with the measured result.

TABLE 15.2: These two product specifications focused on the velocity of the stylet and cannula. A pass or fail value was attributed based on the results.

PS	Product Specification	Acceptance criteria	Result	Pass/fail
6.5	Stylet insertion velocity	>50 mm/s	55 mm/s	Pass
6.7	Cannula firing velocity	>5 m/s	3.5 m/s	Fail

15.2.2   Test Result: Sampling quality

The descriptive statistics of the collected are visualized with boxplots in Figure 15.1. See Table 15.3 for a list of several statistic parameters for both type of instruments.
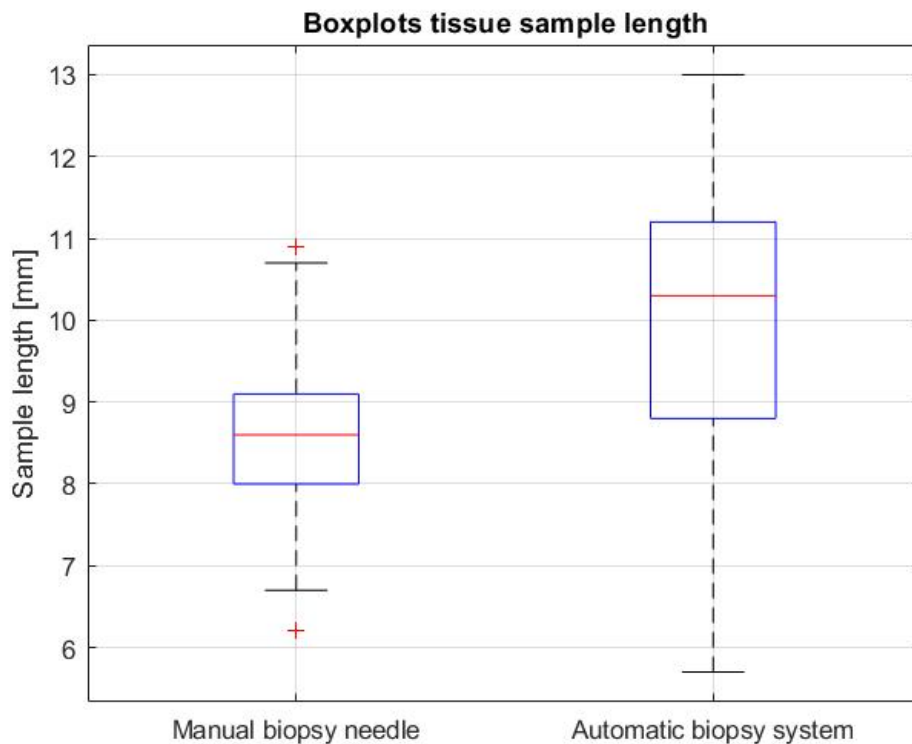
FIGURE 15.1: This figure shows two box-plots. The left one visualizes the data collected with the standard biopsy needle, while the right one does the same for the data collected with the automatic biopsy system.

TABLE 15.3: This table lists the descriptive statistics of the testing done to determine the sampling quality.

Statistic parameter	Manual biopsy needle	Automatic biopsy system
Mean [mm]	8.6	10.2
Median [mm]	8.6	10.4
Standard deviation [mm]	0.9	1.6
Sample variance [mm]	0.9	2.6
Standard error [mm]	0.1	0.2
P-value		3.6e-11

15.2.3 Test Result: Removing a tissue sample

The raw data that was collected in this test, is shown in Figure 15.2. The percentage of length after removing with respect to before is shown as well. A pass or fail value in each run is shown for the product specification 'amount of removal' is shown in Figure 15.3. The same is shown for product specification 'control of depositing' in Figure 15.4.
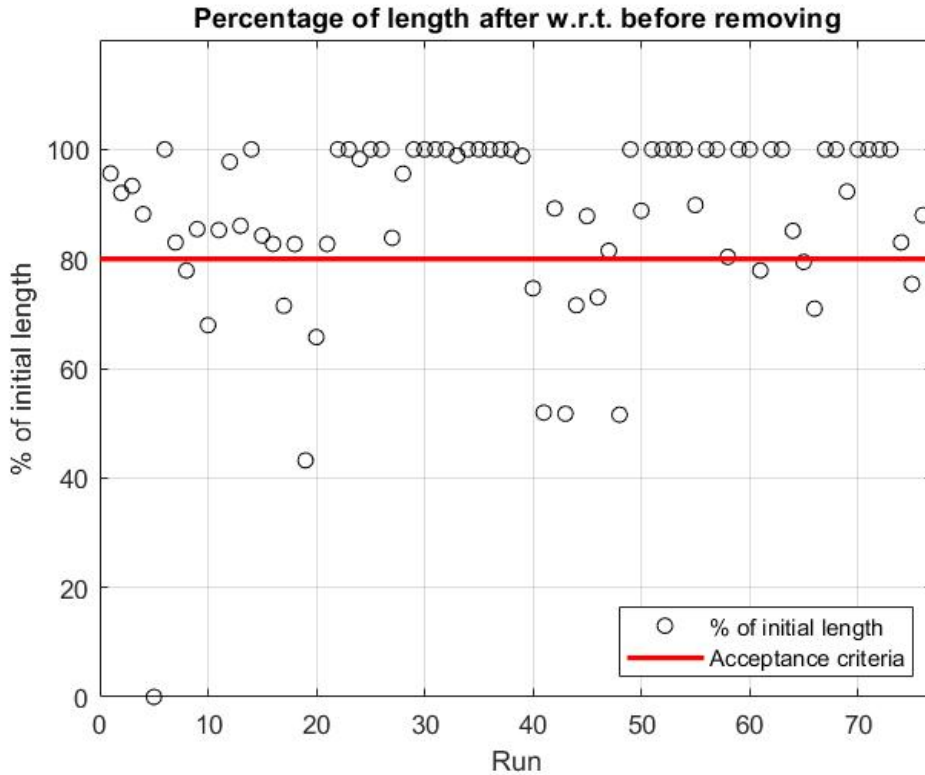
FIGURE 15.2: This figure shows the length reduction of a tissue sample due to the automated removing technique. The red line is the acceptance criteria.
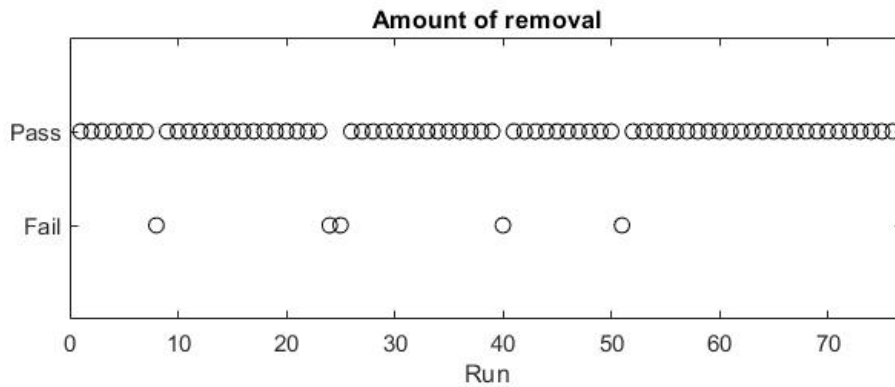
FIGURE 15.3: This figure shows the results of the tests done to verify the product specification 'Amount of removal'.
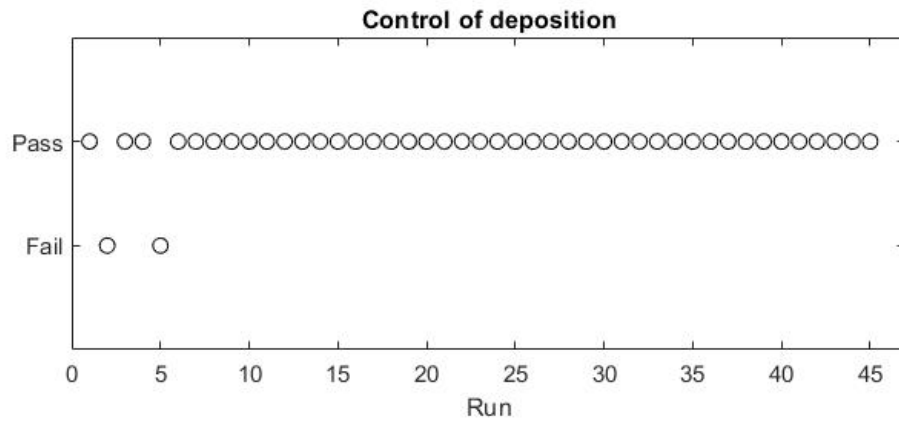
FIGURE 15.4: This figure shows the results of the tests done to verify the product specification 'Control of deposition'.

FIGURE 15.5: This figure illustrates a sample that was properly removed by flushing and deposited correctly in the container.

Chapter 16

Verification Discussion

In the last chapter of Part D, the results of the verification tests are discussed. The discussion is split into two categories. First, the product specifications verified by observation were reviewed. Then, the ones that were required testing were discussed.

16.1 Discussion: verification by observation

The product specifications that could be verified by observation of all passed the acceptance criteria. This means that these PS are met. Only two main-functions were implemented in the proof of principle prototype and other functions such as needle insertion and positioning were out of the thesis scope. Adding these features will most certainly increase the dimensions and weight.

16.2 Discussion: verification by testing

16.2.1 Velocity

The measured velocity of the cannula and stylet was insufficient according to the product specification, which stated that $5 \frac{m}{s}$ is required. This value was based on literature that reported the cannula velocity of five different semi-automatic biopsy needles [72]. The authors did not investigate which cannula velocity was sufficient to sample good quality tissue. Therefore, the initial required velocity should be considered with a degree of caution.

16.2.2 Sampling quality

The sampling quality was tested by comparing tissue samples taken with the automatic biopsy system and a standard 18G biopsy needle. The results showed that significantly longer sample were salvaged with the automatic biopsy system. No trends were visible over the 71 runs. The failed biopsy rate of both instruments was 0%, which is comparable to what was reported in literature.

The results showed that the proof of principle prototype sampled at least as good quality samples compared to a standard biopsy needle. Though, a significant increase in sample length was not expected. Several arguments can explain this suprising increase.
First of all, the manufacturers of both biopsy needles were different. The needles are comparable in diameter, cutting length, tip shape and material. Sufficient sharpness of the cannula can on the other hand be defined or achieved differently. A sharper cannula is expected to cut the tissue more cleanly and, thus, is able to retrieve longer samples.

Secondly, fragmented samples can play a role in tissue sample length. The fragmentation rates of 8 - 36% with standard biopsy instruments have been reported in literature (Inal, cicione). Ergo, sampling fragmented samples with the automatic biopsy system can be expected as well. In case of a fragmented sample, the length of the longest part was measured. During sampling, both instruments fired the cannula and pushed the sample to the distal side of the stylet notch before cutting. However, for sake of sample removal, the stylet was pushed out through the distal end of the cannula with the standard biopsy needle. While with the automatic biopsy system, the stylet was pulled all the way back to the proximal side of the cannula. In case of a fragmented sample, the former way of stylet transportation will expand the distance between the fragmented parts. Whereas, in the latter way, opposite will occur and parts of a fragmented samples will be compressed against one another. Compressed fragmented samples might appear as one and, consequently, may have an increased length. This phenomenon can also explain the increased variance as sampling a fragmented sample was expected happen in up to 36% of the cases.

Despite the suspicion of fragmented samples being compressed together, the quality of the samples was considered to be sufficient. There was concluded that PS-6.9 was met.

16.2.3   Removing a tissue sample

Five out of the 76 samples (6.6%) were not entirely removed from the biopsy needle. In all these cases, the remaining tissue length was <1 mm. Also, in four out of the five runs, the tissue samples had a length before removing that was much lower than the average length before removing. Meaning that these samples were probably fragmented. The problem of residual waste can be solved by flushing with an additional amount of liquid. PS-7.2 was not met but a solution that has a high chance of success is suggested. The solution is simple and no extra risks are involved.

The control of the depositing was not flawless. In two of the 45 samples, the tissue samples were not deposited in the container. One sample was lost and the other adhered to a surface other than the container surface. Creating a funnel, which guides the samples in the direction of the container, might prevent sample loss. The surface of a 3D-printed part is not smooth and to a certain degree, promotes tissue sample adhesion. Applying anti-friction coatings on such surfaces or using alternative machining techniques that results in smoother surfaces can solve the aforementioned problem. Again, the product specification (PS-7.3) was not verified, but solutions were suggested that show serious chance of success.

Finally, 14 of the 76 samples had a length after removing that was <80% of its length before removing. As was mentioned before, one sample was lost, meaning that it had a length reduction of 100%. In the previous section, the results of the sampling quality were discussed. The samples taken with the automatic biopsy system appeared to be significantly longer than those taken with a standard biopsy needle. Fragmented tissue samples that were compressed during transport were considered to have a contribution in the increased sample length. This phenomenon, can also have an influence on the difference between the reported length before and after removal. A fragmented tissue sample that appeared to be one firm sample before removal showed its real consistence only after removal.

The presence of compressed fragmented samples was also proven in the opposite

end of the spectrum. Whereas 13 samples appeared to be longer after removing compared to before. The removing process lengthened the compressed samples and for the reason that the samples were not fragmented, their length appeared to be increased.

There was concluded that PS-7.4 was not met but the results were still promising. Though, testing should be done on human prostate tissue because then the initial set acceptance criteria can be reinstated. Here, the length of the sample after removing is not related to the one before but a minimum sample length of 10 mm determines whether the removing is done properly. This eliminates the influence of compressed fragmented samples.

During testing, some other issues popped up, which lead to recommendation for future research. First and foremost, removed tissue samples were not positioned in a straight line. Pathologists prefer samples to be submitted in a straight line. As this is a requirement before fixation (Literature). Now, the samples are straightened manually, which resulted in damaging several samples.

Secondly, a porous foam sheet was used to embed the tissue sample after removal. However, the foam was not able to drain the excess water quickly. Less dense foam or some other type of draining material should be used.

84

Chapter 17

Discussion Part D

The present part discussed the verification of the proof of principle prototype against the product specifications. Verification was done by observation and testing. The former method verified specifications such as dimensions or weight. All the specifications in this category were met with ease.

Verification by testing required some more attention. Tissue samples were taken from a uncooked chicken breast instead of a live human prostate. First the velocity of cannula and stylet was measured. The stylet reached the required velocity of 50 $\frac{mm}{s}$ but the cannula did not. The compression spring fired the cannula at a velocity of 3.5 $\frac{m}{s}$, which was lower than required. Possible causes of the insufficient velocity can be friction within the system. First of all, friction between cannula and stylet was most likely present because the two metal surfaces slided along another without lubrication. Besides that, two guiding rods constrained the cannula to move only in axial direction. Sliding bearings were used to reduce the friction. Although, they only ensure sliding with negligible friction if the guiding rods are aligned perfectly parallel. There may be assumed that this was not the case in the Proof of Principle prototype. So, these two sources of friction during cannula firing might be a reason for the insufficient velocity.

Surprisingly, the testing done on sampling quality proved that the lower cannula velocity did not result in sampling reduced quality samples. Actually, the exact opposite occurred. Significantly longer tissue samples were retrieved. A reason for this could be related to fragmented samples. With a standard biopsy needle the reloading of the cannula pushed the fragmented parts of the sample away from one another. While, the automatic biopsy system compressed a fragmented sample. In the last case, a fragmented sample appeared to be longer. Ergo, significantly longer samples were taken.

The ability to remove a tissue sample with the automatic biopsy system was tested as well. In some cases, a small amount of tissue remained on the stylet. Flushing with more water might solve this issue.
Furthermore, the sample was deposited correctly in the container in all but two cases. Simple solutions such as other fabrication techniques or anti-friction coatings might do the job.

Finally, the amount of fragmentation due to removing was tested. The flushing technique did not prove to be flawless. 18% of the samples had a length reduction of more than 20% after removal. Again, this issue could be related to the occurance of compressed fragmented samples. A fragmented tissue sample that appeared to be one solid sample before removal showed its real consistence only after removal.

There could be concluded that PS-7.4 was not met but, nonetheless, the results were promising. Testing should be done on human prostate tissue though because this would mean that the initial set acceptance criteria can be reinstated. Here, the length of the sample after removing is not related to the one before but a minimum sample length of 10 mm determines whether the removing is done properly. This eliminates the influence of compressed fragmented samples.

Final discussion

In this thesis project, a biopsy system was developed with the goal of making a trans-perineal prostate biopsy under MRI guidance more time-efficient. Eliminating the manual steps done in between consecutive MRI scans might reduce the procedure time significantly. The time reduction due to this procedural adjustment was merely an assumption, as it was not tested in real-life. Testing was not possible because specialized MRI-safe equipment was not available. Unavailability of equipment highlights why developing an automatic biopsy system was necessary in the first place.

As mentioned in the problem definition, developing such a system poses many challenges. The main challenge was to develop a technique to remove a tissue sample from a biopsy needle without human intervention, whilst preserving the sample quality. A state of the art research on this subject was performed. Here, vacuum-suction showed to be the dominant technique to remove a tissue sample from a biopsy needle. Several studies proved that vacuum-suction was a viable option for larger calibre needles in breast biopsy. A drawback of the method was the high fragmentation rate, which was with an 11G needle already proven to be 43% [3]. The fragmentation rates with a standard biopsy needle rate of up to 36%[61] were reported. Higher fragmentation rate means that automatically a reduction of the quality as well. Biopsy needles used for prostate biopsy have a diameter that is at least twice as small. Samples taken with smaller diameter needles are more fragile. Hence, the already high fragmentation rate with the vacuum method will probably increase even more, which could lead to more tissue loss and lost diagnostic information. This was the main reason for not choosing vacuum to remove the tissue sample from a biopsy needle.

An alternative method was developed that showed promising result in several pilot tests. Here, flushing with water removed the tissue samples entirely and deposited them correctly in most of the runs. This was all done while ensuring a low fragmentation rate. The contact-less nature of the flushing method was one of the reason why it was preferred over other methods such as wiping or pushing. Cross-contamination should be prevented at all costs because contaminating a lesion with previously sampled tissue can induce disease spreading.

Solutions for the two main functions 'automatically taking a tissue sample' and 'removing a tissue sample without human intervention' were combined in several concepts. The final concept was a combination of pneumatic cylinders, compression springs and a syringe pump. These components do not distort the MRI-image quality, are commercially available, can ensure sufficient cannula velocity and, when all combined, are within the dimensional limits. The final concept was realized in a proof of principle prototype that was verified against the product specifications.
The quality of the samples taken with the proof of principle prototype were comparable, if not better, to those taken with a standard biopsy needle. Although, the

velocity of the cannula was lower than what initially was required. Apparently, a lower cannula velocity was sufficient. More research should be done on the required cannula velocity. A pneumatic cylinder was not able to reach the velocity of $5 \frac{m}{s}$ but if a lower velocity would suffice, this type of actuation might be a viable option after all. In the current design, two type of actuators were required to fire and reload the cannula. Eliminating one would make the design less complex.

Removing the tissue sample by flushing with water seemed to be working in most cases. The majority of the tissue samples were removed entirely and deposited correctly in the container. The tests showed already promising results. Some optimization is required to improve the results though. The flat spray fragmented several samples. Slightly decreasing the flow velocity of the spray could solve this problem. Ensuring that all the tissue is removed from the biopsy needle can be realized by flushing with an additional amount of water.
Straightening the tissue samples during depositing can unburden the pathologist. This can be accomplished by for instance guiding the sample through a funnel before dropping them into the container.

In this thesis project, the prototype was verified by taking tissue samples from raw chicken breasts. Whether this type of animal tissue is comparable to live human prostate was unknown. In future research, verification should be done on live human prostate, as only then the real performance of the prototype can be measured.

As mentioned before, the flushing method was preferred over vacuum suction because of high fragmentation rates (43%) [3]. Fragmentation can occur during sampling or removing. If the standard side-cut sampling technique is used, already between 3 - 36% [82][61] of all samples are fragmented before removing.
Unfortunately, the fragmentation rate reported in literature was not clearly defined. So what was considered to be a fragmented sample? The answer to this question varied between studies. Therefore, assumptions were made to be able to compare tissue sample removing methods. There was assumed that sample pieces <2 mm are most likely lost when removed with vacuum suction. Meaning that if the remaining part of the sample was intact, the sample was probably not labelled as fragmented but as firm. Analyzing the data collected with the automatic biopsy system using this new insight showed that only 20% of the samples were fragmented. This figure is twice as low compared to the vacuum-assisted device that sampled with a two times larger biopsy needle.

This thesis project proved that an automatic biopsy system that uses flushing to remove the tissue sample from the biopsy needle has potential. Other techniques such as vacuum-suction or adhesion to a carrier cannot be discarded as their potential is unknown. Comparing the performance of the vacuum-suction with the flushing method was only possible by making some assumptions. Making substantiated conclusions can only be done if both methods are tested with similar specimens and with the same diameter needle.

Appendix A

Literature Study

Biopsy Needle Characteristics and the Prostate Cancer Detection Rate - A Literature Review

Ernst Schillings, *MSc student, TU Delft*

Abstract—**Biopsy needle characteristics such as the cutting length, type of sampling mechanism or needle diameter have in theory influence on the amount of sampled tissue. The effect of changing these biopsy needle characteristics on the detection rate of prostate cancer was reviewed in this literature study. The Web of Science and PubMed databases were searched using a search query that combined the above mentioned biopsy needle characteristics and the cancer detection rate. This resulted in a total of 16 relevant papers. Four papers compared two type of sampling mechanisms: the end-cut and side-cut mechanism. These four studies showed that the prostate cancer detection rate, complication rate and core quality were comparable for these two mechanisms. The side-cut needle was preferred over the end-cut needle because of the significantly lower failed biopsy rate. There were strong indications that the cutting length of a side-cut needle was positively correlated with the prostate cancer detection rate. A side-cut needle with a cutting length of 25 mm was recommended. However, this recommendation should, because of the limited amount of literature, be considered with a degree of caution. More research should be done on this topic. Finally, six studies showed that sampling more tissue with larger diameter needles (16G, 18G and 20G) did not result in an increased prostate cancer detection rate. There were indications that larger calibre needles improved the core quality, although conclusive evidence was not found in literature.**

I. INTRODUCTION

Prostate cancer is the second most common cancer among men around the world. 14.5% of all cancers in men was prostate cancer [1]. Therefore, this type of cancer is considered to be a major health problem [1]. The common practise for diagnosing prostate cancer is by microscopically examining slices of prostate biopsy cores for cancer cells. These biopsy cores are sampled in a systematic way using a core biopsy needle. The sextant method developed by Hodge et al. [2] in 1989 was once the golden standard. However, this method was shown to be insufficient for diagnosing prostate cancer [3]. It was hypothesized that more tissue should be obtained to increase the detection of cancer. Therefore, it was suggested to increase the amount of sampled cores. There seems to be a consensus among scientist that 10 to 12 cores yielded the highest cancer detection rate [4][5][6]. Sampling even more cores did not necessarily result in a higher cancer detection rate. Sampling of specific zones (e.g. peripheral zone, transition zone) was another development in the biopsy of prostate cancer. This resulted in an, compared to the sextant method, increased cancer detection rate [7][8]. The use of MRI for locating cancer and guiding of the needle has been proven to increase the efficiency of prostate

biopsy. The number of clinically significant prostate cancers per number of men biopsied increased from 50% with the standard approach to 70% with MRI [9].

The aforementioned developments in prostate biopsy focused on protocols, sampling schemes and imaging techniques, but changing the biopsy needle itself, or part of the needle, might be just as effective to increase the cancer detection rate. For instance, increasing dimensional characteristics of a biopsy needle should theoretically lead to sampling more tissue per core. Sampling more tissue per core might aid in increasing the detection of cancer. The question is whether changing the characteristics of the biopsy needle will result in the detection of more prostate cancer.

A. Aim

The aim of this study was to review and analyze the literature to show what the effect is of changing biopsy needle characteristics on the detection rate of prostate cancer. The focus was on the following needle characteristics: sampling mechanism, cutting length and needle diameter (see Result section for definitions).

Before the available literature will be discussed, some background on biopsy processing, prostate biopsy procedures and the method for assessing the quality of a biopsy core should be provided.

B. Prostate biopsy processing

Prostate core biopsy is often prescribed when the Digital Rectal Examination (DRE) was positive or Prosate-Specific Antigen (PSA) levels were high. Prostatic glandular tissue, which makes up for 70% of the prostate, is examined and screened for adenocarcinomas (a.k.a. cancer or tumour) [10]. Cancer is diagnosed by histological characterization of the prostatic nuclear and glandular architecture [10]. The prostate has four zones: peripheral, central, transitional and anterior fibromuscular stoma. Only the last zone, which is a very thin layer, does not contain glandular tissue [11]. Prostate biopsy cores are often, immediately after sampling, embedded and flattened in paraffin blocks. At arrival in the laboratory, the samples are straightened and cut into slices with a maximum thickness of 4μ. The processing of prostate biopsy cores was explained in [12]. The pathologist microscopically evaluates the slices and reports the type of cancer, grading of cancer and if possible, the staging. Grading of cancer is done using the Gleason score, which is

composed of the dominant grade and the worst grade present. The Gleason score can range from 6 to 10 [13].

C. Trans-perineal vs. Trans-rectal

Trans-rectal (TR) ultrasound (US) guided biopsy is currently the standard procedure for prostate sampling. During this procedure a probe, with an ultrasound transducer, is inserted into the rectum and produces ultrasound images of the prostate. These images are used to locate the prostate. A biopsy needle is guided through the biopsy probe to the desired location in the prostate. The location of the needle is real-time visible on the ultrasound images. Two type of probes are available: the side-fire (1) and end-fire (2) probe. In the first type, the needle exits the probe through the side. While in the second the needle exits the probe at the end. Studies showed that the type of probe was positively correlated with the detection rate of cancer [14][15]. The effect is most dominant at the lateral and apical regions of the peripheral zone (the squares in Fig. I).

A more recently introduced approach is the trans-perineal

Fig. I: This figure shows the sample location for 12-core prostate biopsy with the trans-perineal (TP) and the trans-rectal (TR) approach. The sampling locations (squares, circles, triangles) and direction of sampling (arrows) were drawn in the transverse, sagittal and coronal plane. The squares, circles and triangles represent respectively sample locations in the peripheral zone, transition zone and apex. Figure retrieved from [16].

(TP) biopsy procedure. Here a biopsy needle is inserted through the perineal path into the prostate under trans rectal US or MRI guidance. Studies have shown that TP results in higher detection rates, mainly for anterior tumours, and has clinical advantages over TRUS guided biopsy [17][16]. Figure I shows the direction of sampling of 12 cores for both the TP and TR approach. Especially with MRI guidance, targeted biopsies can be performed, which leads to less required cores [9] and improved cancer detection rates [18].

D. Quality Evaluation

The quality of biopsy cores is obviously an important factor in the histopathological process. The urologist or radiologist who performs the procedure is responsible for determining the quality of the specimens. Processing of the samples (e.g. embedding on paraffin block, cutting) can directly influence the quality [12]. Factors that determine the quality of the biopsy cores are length of the cores, amount of prostate glandular tissue or absence of extraprostatic connective tissue and degree of fragmentation [12]. A fragmented core is defined as a core that was broken in two or more parts. Cores without glandular tissue are considered to be inadequate [13][12][19]. The presence of glandular tissue can only be defined by microscopic histologic evaluation, which is not always directly possible after sampling [19][20].

The length of a biopsy core is a quality parameter that can be determined more easily. Cores that are shorter than a certain length, also known as the cut-off length, were often marked as being of inadequate quality. The value of this cut-off length varies between studies. Some cut-off values are based on clinical data, others on expert opinions. Boccon-Gibod et al.[19], Bertaccini et al. [20] and Van der Kwast et al. [13] based their cut-off value of 10 mm on expert opinions. Other studies using clinical data reported somewhat higher values, 12,9 mm [21] and 12 mm [22]. According to Obek et al. [21], retrieved cores longer than 11,9 mm resulted in a 2.5 times higher chance of prostate cancer detection. Yilmaz et al. [23] suggested a cut-off value of 6 mm for adequate sampling of glandular tissue. With these varying cut-off values it was still not clear at what length the core quality is sufficient for microscopic evaluation. Therefore, an even lower cut-off value of <5 mm was used to determine which cores should be discarded.

II. METHOD AND MATERIALS

A literature review was conducted to find out if the three selected needle characteristics were positively correlated with the detection rate of cancer. The Web of Science Core collection and PubMed databases were searched using a set of predefined search queries. This set was a combination of keywords that specified the following: the target organ (1), type of biopsy (2), synonyms for cancer (3), synonyms for detection (4), needle diameter (5), cutting length (6) and sampling mechanism (7). The entire search query was: Prostate AND biops* AND needle AND (cancer OR carcinoma*
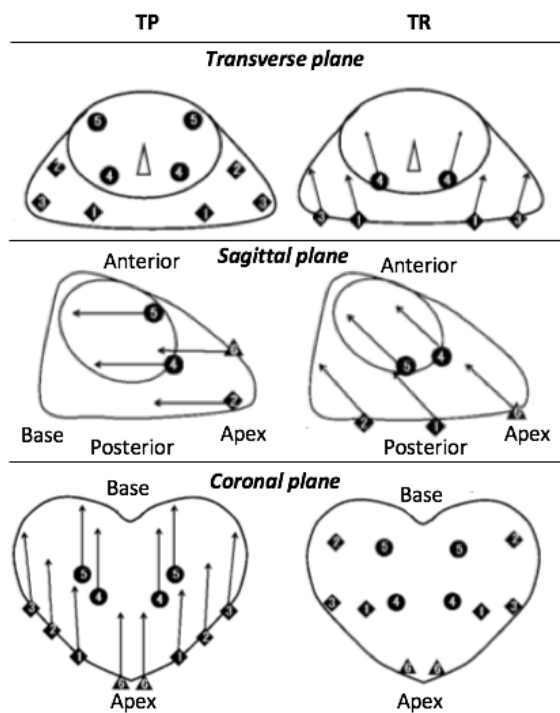
OR tumour*) AND (detection OR diagnosis OR rate OR yield) AND (diameter OR calibre OR cut* OR length OR mechanism*). The databases were searched for papers from the year 2000 to present day.

Exclusion criteria were determined to distinguish between irrelevant and relevant articles. The scope of this literature review was focused on the characteristics of core prostate biopsy needles, therefore other type of biopsy needles (e.g. aspiration needles, fine needles) or other biopsy on other organs were excluded. Papers that reported the correlation between cancer detection rate and a parameter that did not relate to a needle characteristic were excluded as well (e.g. sampling scheme, core number, user experience, imaging technique).

The aforementioned search query yielded 561 articles (13/11/2018). After removing duplicates the total was decreased to 443. The process of selecting relevant papers was performed in steps (see Fig. II). First the articles were scanned for title and abstract, then the entire paper was scanned and finally the entire paper was read thoroughly. This resulted in a total of 16 relevant papers. These papers
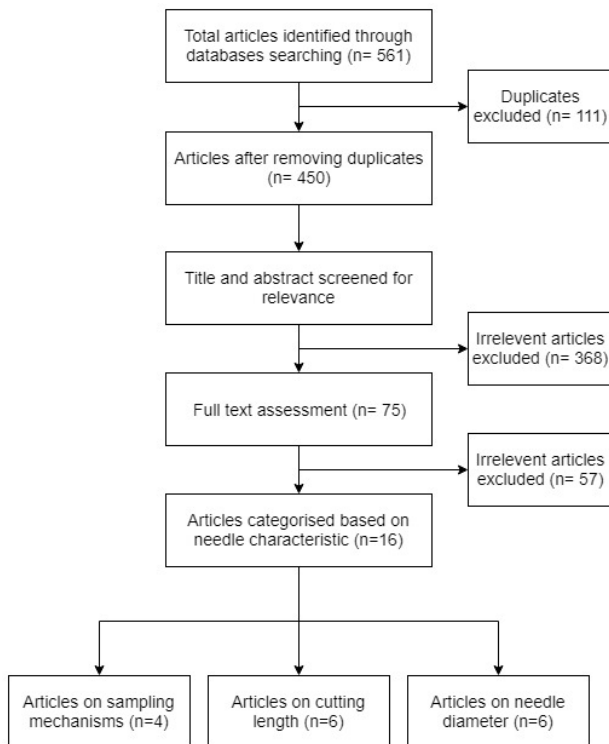
Fig. II: Flowchart of literature selecting process. The Web of Science Core Collection and Pubmed database were searched using the following search query: Prostate AND biops* AND needle AND (cancer OR carcinoma* OR tumour*) AND (detection OR diagnosis OR rate OR yield) AND (diameter OR calibre OR cut* OR length OR mechanism*). The result of this database search was the input for the flowchart.

were categorized in three different groups: sampling mechanisms, cutting length and needle diameter.

III. RESULTS

The selected literature reported about three different biopsy needle characteristics that have been studied for their correlation with the prostate cancer detection rate. One was related to the fundamental mechanism of sampling, while the other two were dimensional characteristics. The three characteristics were: sampling mechanism (Section III-A), cutting length (Section III-B) and needle diameter (Section III-C).

A. Sampling Mechanism

The sampling mechanism defines both the fundamental mechanism that is used to fill the sampling space with target tissue and the mechanism that separates the tissue from surrounding tissue. Several studies have compared the performance of different kind of sampling mechanisms. Two type of sampling mechanisms were reported in literature: the side-cut (Fig. III) and the end-cut (Fig. IV). The side-cut mechanism is the golden standard, while the end-cut mechanism was proposed as an alternative in 1996 by Ascendia AB in Sweden [24]. These mechanisms will be briefly discussed.

Most of the biopsy instruments, manual or automatic, use the side-cut method to cut the tissue and retrieve the sample (see Fig. III). A side-cut instrument consists of an inner needle with a notch that is pushed through an outer sheath.

Fig. III: Mechanism of the side-cut biopsy needle in the open (a) and in the closed (b) position.

Fig. IV: Mechanism of the end-cut biopsy needle in the open (a) and in the closed (b) position.

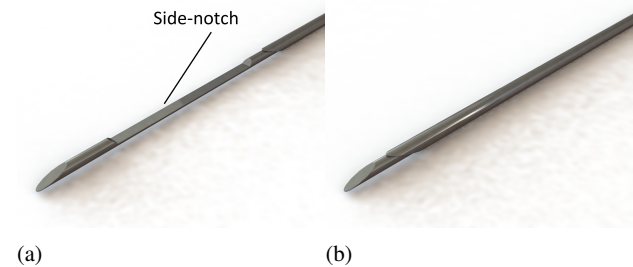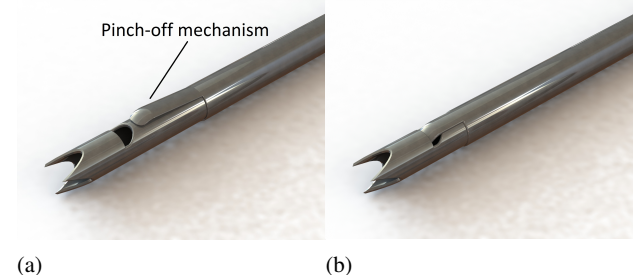The inner needle can axially translate through the outer sheath. A biopsy sample is retrieved by pushing the needle out of the outer sheath into the target tissue. The notch is filled with the target tissue. The tissue is then cut by pushing the outer sheath over the inner needle. The entire needle is pulled from the body and the sample can be collected by pushing the inner needle out. The available side-cut biopsy instruments have a cutting length of 17 - 23 mm [25].

The side-cut technique has two disadvantages. Firstly, only the notch is filled with tissue, meaning that not the entire diameter of the outer sheath is used. Secondly, the first part of the inner needle cuts without being filled with tissue [26]. The end-cut technique has been developed to overcome these disadvantages. Again, the instrument consists of two parts, a hollow inner needle and an outer sheath. The outer sheath has a pinch-off mechanism at the end (see Fig. IV). The inner needle is pushed into the target tissue. After the hollow needle is filled with tissue, the outer sheath is pushed over the inner needle. The pinch-off mechanism cuts the tissue at the end of the inner needle. The entire instrument is pulled back to retrieve the sample. The instrument has three settings for the cutting length: 13, 23 and 33 mm. The end-cut instrument was claimed to have three advantages over the side-cut method. Firstly, a fully cylindrical specimen can be sampled. Secondly, the specimen is cut from point of fire (at the end of needle). Thirdly, the stronger stroke force can cut the tissue more cleanly [34] and can decrease fragmentation [27].

Several studies have compared the performance of the side-cut and end-cut instruments (Table I) in terms of mean length of cores, percentage of the maximum length, mean weight of cores, failed biopsy rate, pain, fragmentation rate, presence of small cores and cancer detection rate. Besides that, two studies reported the type and rate of complication with both the side-cut and the end-cut needle (Table II).

TABLE I: This table lists the results of studies that compared the performance of the end-cut (EC) and the side-cut (SC) needle in prostate biopsy (in *n* patients). The used cutting length was mentioned as well. Small cores were defined as <5 mm. A consultant pathologist evaluated if a core was fragmented. Pain was assessed using the VAS score immediately after the procedure.

Authors	Year	*n*	Needle type	Core length Mean (SD)	S[2]	% ML[3]	Core weight Mean (SD)	S[2]	Failed biopsy %	S[2]	PCa %	S[2]	Frag.[1] %	S[2]	Small cores %	S[2]	Pain VAS[4] (SD)	S[2]
Dogan et al. [25]	2005	25	EC - 23 mm	14.96 (±2.11)		65	5.05 (±0.85)		7		20		6.8		1.8		2.84 (±1.77)	
		25	EC - 33 mm	19.92 (±3.7)	Yes	60	7.25 (±2.61)	Yes	12	Yes	16	No		No		No	2.00 (±0.95)	No
		37	SC - 22 mm	13.31 (±1.63)		60	4.22 (±1.10)		1		25		7.8		2.4		2.43 (±1.64)	
Haggarath et al. [26]	2002	40	EC - 23 mm	17.8		78	6.5		21.9		24.1		N/A[5]		N/A[5]		N/A[5]	
		40	SC -23 mm	17.3	No	75	5.5	Yes	1.9	Yes	23.9	No						
		20	EC - 33 mm	19.9		60	6.53		22.5		N/A[5]							
		20	SC - 22 mm	14.4	Yes	66	4.91	Yes	0	Yes		Yes						
Ubhayakar et al. [27]	2002	15	EC - 33 mm	19.4 (±9.1)		59	N/A[5]		4.4		16		16		4.5		N/A[5]	
		15	SC - 18 mm	14.7 (±5.2)	Yes	82			0	Yes	23	No	46	Yes	3.3	No		
Ozden et al. [28]	2004	43	EC - 13 mm	7.53 (±2.31)		58	N/A[5]		26.42		15		41.02		21.42		N/A[5]	
			EC - 23 mm	13.5 ±6.67	Yes	59			17.81	Yes	19	No	30.05	No	19.44	Yes		
			EC - 33 mm	23.11 ±6.62		70			10.08		22		24		2.4			
		43	SC - 20 mm	15.7 ±3.58		80			0		17		24.12		0.87			

1: Fragmentation
2: Statistical Significant Difference (p<0.05)
3: % ML: Percentage of maximum length.
4: Visual Analogous Scale (0-10) in which 0 reflects the state of no pain and 10 the state of unbearable pain.
5: Data not provided in paper.

TABLE II: This table lists the studies that reported the complication rate of end-cut (EC) or side-cut (SC) needles with different cutting lengths and 16G or 18G calibre needles.

Author	Instrument	Complication							
		Hematuria %	S[1]	Hematospermia %	S[1]	Rectal bleeding %	S[1]	Fever %	S[1]
Dogan et al. [25]	EC	63.2	No	48.9	No	16.3	No	2.0	No
	SC	72.2		44.4		30.6		2.8	
Ubhayakar et al. [27]	EC	67	No	30	No	40	No	20	No
	SC	60		30		20		0	
Kanao et al. [29]	SC 20 mm	15.8	No		N/A[5]			0.2	No
	SC 25 mm	13.7						0.2	
Cicione et al. [30]	16G		N/A[4]			6.4	No	N/A[4]	
	18G					4.8			
McCormack et al. [31]	16G		N/A[4]			10.5	No	4	No
	18G					13		3.8	
Inal et al. [32]	16G	18.5	No		N/A[4]	8.7	No	1.0	No
	18G	12.9				6.9		0	
Wang et al. [33]	18G	61.3	Yes		N/A[4]	14.5	Yes	6.5	No
	20G	26.7				3.4		1.7	

1: Statistical Significant Difference, p<0.05
2: Data not provided in paper.

B. Core length

Biopsy instruments can take a sample of a certain maximum length and this length is determined by the cutting length of the biopsy needle. Theoretically, longer cores can be sampled with an increased cutting length and thus more tissue can be obtained. Kanao et al. [35] showed in a 3D simulation that using instruments with a longer cutting length could result in the detection of more anterior tumours. This might result in a higher cancer detection rate. Whether this claim was supported by clinical data was up for debate.

Several studies directly compared biopsy needles with different cutting lengths. Two studies were found in literature that compared two side-cut needles with different cutting lengths (Table III). Kanao et al. [29] prospectively investigated two instruments with a cutting length of 19 and 25 mm. A total of 12 cores per patient ($n = 469$) was sampled under TRUS guidance. The instrument with longer cutting length could take significantly longer samples. This resulted in a significantly higher detection rate. The difference between pain scores on both sides of the prostate was not significant. Furthermore, the complication rate was not significantly different (Table II). Iczkowiski et al. [36] retrospectively

compared the use of a side-cut needle with a 20 mm cutting length (in 205 patients) and one with a 25 mm cutting length (in 45 patients) in sextant (biopsy of six cores) prostate biopsy. Insignificant more cancer was detected with the longer compared to the smaller cutting length needle. Three studies compared the performance of the different cutting lengths of the end-cut instrument. Fink and colleagues [37] showed in ex vivo settings that the end-cut instrument with a longer cutting length lead to a significant increase in the detection of cancer. However, Dogan et al. [25] and Ozden et al. [28] showed otherwise. They both showed that with TRUS prostate biopsy significantly longer and heavier core were sampled. However, no significant differences in the cancer detection rate were observed.

Five studies researched the correlation between core length and the cancer detection rate. While these studies did not directly measure the effect of using different cutting lengths on the cancer detection rate, they did provide data on core length that might support the use of biopsy needles with longer cutting lengths. These five studies can be categorized in two different groups. Studies in group 1 compared the lengths of cores within the group of cancer patients (Table IV), while those in group 2 compared lengths of biopsy cores

between the group of cancer and no cancer patients (Table IV).

1) Group 1: Doluogly and colleagues [38] analyzed the length of biopsy cores sampled during 12-core TRUS-guided prostate biopsy in 512 patients with cancer. The cores with cancer were significantly longer than cores without. Ergun et al. [22] analyzed the data of 216 patients who have had TRUS-guided prostate biopsy. The number of sampled cores per patient varied between 10 and 12. The biopsy cores were divided into 3 groups, based on their length. The first group of cores where smaller than 10 mm, the second between

10 and 19 mm and the last group larger than 20 mm. The results showed that the group 2 and 3 had a significantly higher detection rate compared to group 1. Also, a significant higher detection rate was observed between group 2 and 3.

2) Group 2: The second category consists of studies that compared cores of patients with and patients without cancer. Iczkowski et al. [36] retrospectively surveyed a total of 1847 prostate biopsies in two hospitals. Six cores were obtained per case. The correlation between core length and the probability of cancer detection or nonbenign findings was demonstrated in Fig. V. The positive predictive value of

TABLE III: This table shows the result of two studies that did research on the effect of different cutting lengths of side-cut needles on the cancer detection rate in prostate biopsy (PCa). The studies had a sample size of *n* patients. Pain in the right-lobe (RL) and left-lobe (LL) of the prostate was measured using a FPS score after the procedure.

Authors	Year	*n*	Cutting length [mm]	Core length [mm]		PCa %		FPS[2] score		
				Overall mean (SD)	S[1]	%	S[1]	RL (SD)	LL (SD)	S[1]
Iczkowski et al. [36]	2002	209	20	17.8	Yes	N/A[3]	No		N/A[3]	
		45	25	19.6		N/A[3]				
Kanao et al. [29]	2018	469	19	16.3 ($\pm$2.9)	Yes	42.0	Yes	2.11 ($\pm$1.15)	2.36 ($\pm$1.22)	No
		489	25	22.4 ($\pm$4.0)		52.1		2.15 ($\pm$1.09)	2.41 ($\pm$1.15)	

1: Statistical Significant Difference, p<0.05
2: Six level Face Pain Scale (0-5) in which 0 reflects the state of no pain and 5 the state of worst pain possible.
3: Data not provided in paper.

TABLE IV: The results of the retrospective studies on the correlation between the length of prostate biopsy cores and the cancer detection rate were listed in this table. The studies had a sample size of *n* patients. The prostate cancer detection rate was abbreviated with PCa. The cores were sampled with a side-cut instrument. The studies in the first group compared cores of cancer patients within their own group, while group 2 compared cores of cancer patients with those of no cancer patients.

Group	Authors	Year	*n*	Categorization	PCa %	Mean core length of cancer patients [mm]			
						Overall (SD)	Cancer (SD)	No cancer (SD)	S[1]
1	Doluoglu et al. [38]	2015	512	N/A[2]	36.80	12,9 ($\pm$5)	11.9 ($\pm$4.4)	11,08 ($\pm$5.,1)	Yes
	Ergun et al. [22]	2016	188	<10 mm	26.60	5,9 ($\pm$2,1)	N/A[2]		Yes
				10 - 19 mm	51.80	12.6 ($\pm$2.4)			
				>20 mm	65.10	20,9 ($\pm$1.5)			
						Mean core length of all patients [mm]			
						Overall (SD)	Cancer patients (SD)	No cancer patients (SD)	S[1]
2	Obek et al. [21]	2012	312	N/A[2]	30.20	11.4 ($\pm$2.5)	12.3 ($\pm$2.6)	11.4 ($\pm$2.4)	Yes
	Deliktas et al. [39]	2016	348	N/A[2]	26.00	N/A[2]	10.6	11.0	No
	Lee et al. [40]	2015	3479	N/A[2]	28.5	16.1 ($\pm$1.9)	16.1 ($\pm$1.8)	16.1 ($\pm$1.9)	No

1: Statistical Significant Difference, p<0.05
2: Data not provided in paper.

the biopsy core length for cancer diagnosis was significant at both sides of the apex and base. In the study of Obek et al. [21], 245 patients had TRUS-guided prostate biopsy. Between 12 and 18 cores were sampled per patient. Their results showed a significant correlation between core length and the cancer detection rate. Deliktas et al. [39] focused in their study on the length of cores, cancer detection rate and prostate volume. Again 379 patients had TRUS-guided biopsy. 12 to 16 cores were retrieved per patient. No significant difference was found between patients with and patient without cancer.
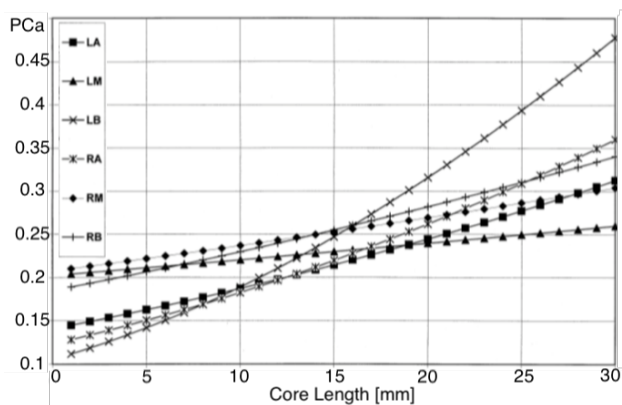

Fig. V: These lines show the probability of prostate cancer detection in the range of core lengths for each sampling site. A total of 6 lines are shown for 6 different sampling sites (LA: left apex, LM: left mid-prostate, LB: left base, RA: right apex, RM: right mid-prostate, RB: right base). The core length ranged between 1 and 28 mm. Figure retrieved from [36]

C. Needle Diameter

Sampling longer cores is not the only method to retrieve more tissue, increasing the diameter increases the available sampling space as well. The needle diameter was the third and last biopsy needle characteristic that was discussed in this literature study. Several studies investigated whether an increased needle diameter resulted in an increased cancer detection rate.

The studies that investigated the correlation between cancer detection rate and the diameter of side-cut biopsy needle were listed in table V. The type and rate of complications was shown in Table II. No studies were found that varied the diameter of end-cut biopsy needles.

Inal et al. [32] showed that with a 16G biopsy needle better specimen quality was obtained compared to 18G in 12 core TRUS guided prostate biopsy. This did not result in significantly higher cancer detection rate. It was concluded that a 16G can be safely used instead of a 18G needle. The difference in the cancer detection rate with 16G and 18G needles in TRUS guided prostate biopsy was also

not significantly different in two other studies [31][30]. Similar results were seen when MRI [41] or trans-perineal [42] approach was used. A thinner needle, which is less invasive, was preferred over a thicker needle. Larger diameter needles resulted in significantly more empty needles [41]. McCormack et al. [31] also did not show that there was a significant difference between 16G and 18G but they did argue that 16G could improve the core quality. This was not supported by clinical data. Wang et al. [33] investigated if a 20G needle had similar cancer detection rates compared to a 18G needle in TRUS guided prostate biopsy. The 20G had similar cancer detection rates and it decreased the local injury and complications. The core quality was evaluated in [30] and [32]. In the former study no difference in quality was observed, where in the latter the larger calibre needle was superior over the smaller one. All of the studies listed in Table V except for one ([31]) were prospective studies.

IV. DISCUSSION

In the past two decades only one alternative to the standard side-cut technique has been introduced into the clinic and subsequently its performance been reported in literature. The four studies on the end-cut vs. side-cut technique gave several reason for the need for an alternative method. First of all, Haggarath et al. [26] reported two major disadvantages of the side-cut as motivation: the distal part of the needle cuts tissue that is not sampled (1) and non optimal use of needle volume (2). Why the first point was claimed to be a disadvantage was not explained nor supported by literature or clinical data. No other studies were found that mentioned this disadvantage. The other three studies mentioned the need for a higher cancer detection rate as motivation [25][27][28]. They hypothesized that more tissue resulted in a higher detection rate. This supports the second disadvantage that was mentioned in Haggarath et al. [26]. More tissue could aid the pathologist in sample evaluation and result in a higher cancer detection rate. Whether the literature supports this hypothesis was investigated in this study. The performance of the end-cut and side-cut instruments were compared in terms of core length, percentage of maximum length, core weight, fragmentation rate, pain, presence of small cores, complication rate and failed biopsy rate.

The end-cut needle can be set at different cutting length, while the side-cut needle has a predetermined cutting length. The cores obtained with both needle set at similar cutting lengths was used to compare the two sampling mechanisms. One reported that 12.3% longer (14.96 mm vs. 13.31 mm, $p < 0.05$ [25]) samples were retrieved with the end-cut instrument compared to the side-cut instrument. Altough, Ozden et al. [28] showed that 16.2% shorter (13.53 vs. 15.7 mm, $p < 0.05$) cores were retrieved. Haggarath et al. [26] did not observe any significant difference. So the end-cut instrument does not always retrieve longer cores compared to the standard side-cut instrument.

The sampled core length can be expressed as a percentage

TABLE V: This table shows the result of the studies that did research on the correlation between needle calibres and the cancer detection rate and fail rate in prostate biopsy. The studies had a sample size of *n* patients. The prostate cancer detection rate was abbreviated with PCa. A consultant pathologist evaluated if a core was fragmented. Small cores were <5 mm. The pain was measured using the VAS[1] score. Where V1 was measured during the procedure, V2 15 to 30 min after the procedure and V3 1 to 2 weeks after the procedure.

Authors	Year	n	Calibre	PCa %	S[3]	Failed biopsy %	S[3]	Frag.[2] %	S[3]	Small core %	S[3]	Pain V1 (SD)	V2 (SD)	V3 (SD)	S[3]
Cicione et al. [30]	2012	125	16G	29.6	No	N/A[4]		5	No	2	No	1.4	1.3	N/A[4]	N/A[4]
		125	18G	20.4				3		5		1.4	1.2		
Durmus et al. [41]	2013	41	16G	22.1	No	12.9	Yes	N/A[4]		N/A[4]		N/A[4]			
		39	18G	24.5		2.1									
McCormack et al. [31]	2012	105	16G	31.4	No	N/A[4]		N/A[4]		N/A[4]		N/A[4]	0.74 (±1.33)	1.03 (±1.86)	No
		105	18G	36.2									0.58 (±1.23)	1.19 (±2.09)	
Inal et al. [32]	2008	103	16G	24.3	No	6.9	Yes	2.8	Yes	Less	Yes	N/A[4]		6.62 (±1.56)	No
		101	18G	15.8		14.1		36		More				5.95 (±1.87)	
Wang et al. [33]	2015	122	18G	40.3	No	N/A[4]		N/A[4]		N/A[4]		N/A[4]			
		122	20G	35.0											
Giovanni et al. [42]	2009	94	16G	28%	No	N/A[4]		N/A[4]		N/A[4]		2.07	N/A[4]	0.06	No
		93	18G	28%								2.34		0.07	

1: Visual Analogous Scale (0-10) in which 0 reflects the state of no pain and 10 the state of unbearable pain.
2: Fragmentation
3: Statistical Significant Difference, $p<0.05$
4: Data not provided in paper.

of the maximum amount of length. This percentage can be seen as a measure of performance. In Ozden et al. [28], only 58% of the available 23 mm is used with the end-cut device while 80% of the 20 mm was used with the side-cut instrument [28]. Dogan et al. [25] and Haggarath et al. [26] showed slightly higher percentages for the end-cut device (65% vs. 60% and 78% vs. 75%, respectively) between instruments. Evaluating the percentages of maximum available length lead to the conclusion that no needle is superior to the other.

The 23 mm end-cut instrument can, in terms of core weight, sample significantly heavier cores than the 22 mm side cut instrument (19.7% [25] and 18.1% [26] heavier). This suggests that the end-cut instrument uses more volume per unit length compared to the side-cut instrument, thus using the available sampling space of the needle more optimal.

A major disadvantage of the end-cut instrument was the occurrence of a failed biopsy or zero biopsy. Biopsy fail rates for the 23 mm end-cut instrument were 7% [25], 21.90% [26] and 17.81% [28]. For the standard side-cut instrument these were all 1% or lower. Similar results were seen with other cutting lengths. These studies show that a significant

difference is observed in terms of the fail rate between these instruments. It was suggested that this problem was caused by the pinch-off mechanism at the end of the needle [25]. Failing a biopsy can be a huge disadvantage because multiple punctures are necessary for taking a sample, which could lead to increased side effects and patient discomfort [28]. A high fail rate is not only disadvantageous for the patient but also for the physician or hospital. Increasing the number of puncture reduces the efficiency of the procedure and moreover raises the operating time and costs. The exact increase of costs due to failed biopsies was unknown.

Studies on the rate of fragmentation, which is one of the core quality indicators, were less unanimous. Ubhayakar et al. [27] reported a significantly lower fragmentation rate with the end-cut compared to the side-cut instrument (16% vs. 46%). Ozden et al. [28] found only a significant difference between the 13 mm end-cut and the side-cut needle. Dogan et al. [25] did not find a significant difference between the two instruments in terms of fragmentation rate. A factor that probably had a huge influence on the results was the subjective method of assessing the fragmentation rate. When a core was defined as fragmented was not provided in the

selected literature. A consultant pathologist reported a core as being 'fragmented' and this observation was solely based on his or her opinion.

One of the other core quality indicators was the presence of cores that were <5 mm. The difference was insignificant in [25] and [27] but significant in [28]. Ozden et al. [28] reported the % of smaller cores for each cutting length of the end-cut needle. The difference was only significant between sampling mechanisms when the end-cut needle had a cutting length of 13 mm and 23 mm. The different presence of smaller cores between [25] and [28] might be attributed to manner of reporting. In the former study the results of the different cutting lengths of the end-cut needle were grouped together while the latter did not. This might have ruled out the possibility of detecting a significant difference. The four studies in Table III reported contradicting results for both quality indicators, meaning that it was not clear what the effect is of the sampling technique on the core quality.

More complications and pain was expected with the end-cut instrument because of the longer cutting length and increased fail rate. This means that the end-cut needle makes deeper incisions and more tissue is separated from surrounding tissue. Only one study measured the pain of the patient following the procedure. The differences were considered to be insignificant [25]. Furthermore, no difference in complication rate was observed (see Table II). Therefore, evidence that substantiate the inferiority of the end-cut needle compared to the side-cut needle in terms of pain and complication rate was non-existent.

It can be concluded that no consensus is found among scientists about which sampling mechanism can sample longer cores when instruments were chosen with similar cutting lengths. Literature indicates that heavier samples can be obtained with the end-cut instrument, which would suggest that more volume is used per unit length. Sampling heavier cores did result in an increase in the detection of cancer [26][28]. However, the difference was not statistically significant. Dogan et al. [25] reported that with the end-cut instrument even a lower cancer detection rate was observed. Meaning that retrieving more tissue with the end-cut instrument did not result in detecting more cancer. The difference was again insignificant. The contradicting results might be explained by the different composition of the test groups. While Haggarath et al. [26] and Ozden et al. [28] selected the cutting length of the end-cut instrument based on the size of the prostate, Dogan et al. did not. This means that on average smaller prostates were sampled with the end-cut compared to those with the side-cut instrument in the former studies and similar size prostates were sampled in the latter study. This might cause the difference between cancer detection rates. All of the aforementioned studies on EC vs. SC suffered from sample size, which may have ruled out detection of significant differences. It can be concluded that, according to literature, sampling more

tissue with the end-cut instrument, compared to the side cut, has not been proven to have an effect on the cancer detection rate. Meaning that both sampling mechanisms can be considered as equally effective. With the major disadvantage of the end-cut instrument failing to take a sample, which is mostly unfavorable for the patient, surgeon and hospital, it was shown that the performance of the end-cut is debatable. Finally, it was not clear which sampling technique sampled the best quality cores. Sampling poor quality cores is undesirable because a pathologist can retrieve less information (e.g. local staging) from the tissue, which makes allocating a Gleason score more difficult. The listed studies in Table I were all published more than a decade ago and no recent studies have been found, which suggests that a consensus has settled among scientists. Therefore to conclude, there are strong indications that the side-cut technique was most suitable for sampling of the prostate.

Cutting length and its correlation to the cancer detection rate was another needle characteristic that was reviewed in this literature study. The cumulative length of tissue cores obtained per patient has a positive influence on the detection rate of prostate cancer [13]. However, the length of single cores is not considered to be of high value in the clinical practise [43]. 3D simulations of TRUS guided prostate biopsy showed that nearly all cancers with a total volume >0.5 ml can be detected by sampling 14-18 cores. Tumours that lay in the anterior zone were considered to be harder to sample with a standard length biopsy needles (see Fig I). It was suggested to increase the cutting length, which could increase the chance of sampling these anterior tumours. Some studies have investigated whether there was a correlation between the cutting length of a biopsy needle and the cancer detection rate.

Studies that directly compared the influence of different cutting lengths on the cancer detection rate were scarce. Kanao et al. [29] concluded that with the 25 mm cutting length side-cut needle significantly longer samples were retrieved compared to the 19 mm cutting length side-cut needle. The increased amount of tissue did result in an increased cancer detection rate, though this difference was only significant in patients with a prostate a volume of 20-40 ml [29]. Iczkowski et al. [36] concluded that also significantly longer cores were sampled with the longer cutting length needle. However, the detection rate of cancer did not significantly increase. The authors hypothesized that this was probably caused by the small sample size. Both studies indicated that sampling more tissue with longer cutting length needles resulted in an increased cancer detection rate but hard evidence was not provided. With the end-cut needle the results were less unified. Setting the cutting length of the end-cut needle on 33 mm instead of 23 mm resulted in significantly longer cores [25][28][37]. Only in the study of Fink et al. [37] sampling longer

cores resulted in a significant increased cancer detection rate. Dogan et al. [25] even reported an insignificantly lower cancer detection rate with the longer cutting length. The positive outcome in [37] was probably caused by the different type of procedure. They performed their biopsy on prostates removed during radical prostectomy. The prostate was pre-treated with formalin to achieve optimal tissue consistency because biopsy in too soft tissue resulted in a failed biopsy. The end-cut needle was tested in more optimal conditions in [37] then in [25][26][27]. This probably had influence on the cancer detection rate.

These contradicting results, the insufficient sample sizes and the limited amount of literature provided insufficient evidence on the correlation between the cutting length and the cancer detection rate. A different approach was used to solve this problem. Literature on the correlation between the biopsy core length and the cancer detection rate was reviewed as well. Increasing the cutting length theoretically increases the maximum biopsy core length. If the correlation between core length and the cancer detection rate is positive, then increasing the cutting length might also have a positive effect on the cancer detection rate. This theory was tested by reviewing the two groups, which were defined in the Result section, of studies on the correlation between the biopsy core length and the cancer detection rate.

In the first group of studies, the biopsy cores of patients with cancer were evaluated within their own group. Ergun et al. [22] showed that longer biopsy cores, >20 mm, resulted in a significantly higher cancer detection rate. Doluogly et al. [38] came to a similar conclusion. The difference was only significant at the right lateral apex when the cores were allocated on anatomical sampling site. This was probably caused by allocating the cores based on their sampling site. This resulted in a declined number of cores per site and finding a significant difference became more difficult.

In the second group, studies were found that contradict each other. Iczkowski et al. [36] showed that there was a significant correlation between core length and the detection of cancer, especially at the apex and base (figure V). Obek et al. [21] concluded that there was a significant difference between the length of biopsy cores of cancer patients and non cancer patients. However, others proved the contrary [39][40]. A difference between the studies that may explain the contradicting conclusions is that Obek et al. [21] disregarded the smaller fragments, which may have resulted in a larger mean core length, while Deliktas et al. [39] did not. Deliktas et al. [39] stated that the cancer detection rate did not depend on core length but on the core length per cc of prostate. Therefore, core length per cc should be a better indicator of cancer. Lee et al. [40] reported an on average longer core lengths compared to the other studies in this group. They hypothesized that a sort of plateau was reached for the detection rate of prostate cancer. Meaning that obtaining more tissue would not result in a higher cancer

detection rate. The same phenomenon was observed when the number of sampled cores was increased to more than 14. This did not result in a higher cancer detection rate either.

The studies in both groups used side-cut needles. All studies except for one indicated that more cancer is detected in longer cores. This supports the hypothesis that increasing the cutting length of a side-cut needle can result in an increased cancer detection rate because longer cores can be sampled. The conclusion of the studies on side-cut instruments with different cutting lengths is now more substantiated [29][36]. Literature on the correlation between core length and the cancer detection rate, while using an end-cut instrument, was non-existent. More research should be done on the effect of cutting length of end-cut needles and the cancer detection rate. Research on the core length at which no more cancer is detected, also known as the saturation core length, should be done too. This can for instance result in a value for the maximum cutting length. Based on the presented literature on the cutting length, the side-cut needle with a cutting length of 25 mm was considered to produce the highest prostate cancer detection rate. The influence of the cutting length of side-cut needles on the core quality was not found in literature. The effect of increasing the cutting length on the pain or complication rate was only reported in [29]. They showed that increasing the cutting length did not increase the pain or complication rate. Therefore, the side-cut instrument with a cutting length of 25 mm was recommended.

The last needle characteristic discussed in this literature review is the needle diameter. Again, only literature that studied the influence of the diameter of side-cut needle was found. A 16G, 18G and 20G needle has, respectively, an outer diameter of 1.65 mm, 1.27 mm and 0.90 mm. About half the cross section of the entire needle makes up the empty notch of the side-cut biopsy needle. The cross section of the sampling space for 16G, 18G and 20G needle is, respectively, 1.07 mm^2, 0.63 mm^2 and 0.32 mm^2. A 16G biopsy needles can, when the cutting length is constant, sample about 1.7 times more tissue compared to a 18G biopsy needle . Compared to a 20G needle, 3.3 times more tissue can be retrieved. Whether this lead to a significant increase in the prostate cancer detection rate was, among others, studied in this literature review.

A clear consensus was found among studies that researched the relationship between the diameter of side-cut needles and the detection of cancer. Needle calibre did not have a significant effect on the detection of cancer in TR ultrasound, TP ultrasound and MRI guided procedures. Some reported insignificant increases in the cancer detection rate with 16G compared to 18G needles, while others showed the contrary. Only one study reported the power and significance level of their randomized controlled trial [30]. This study had the largest sample size of the studies in table V. Increasing the number of patients in the studies with the smaller samples

size might result in a significant difference. The conclusions of the studies with smaller sample size were considered to be of less value. The cancer detection rates in TRUS guided biopsy ranged between 24.5% and 31.4% with the 16G biopsy needle and between 15.8% and 36.2% with the 18G needle. These differences were probably caused by the different composition of the study population. Some included patient that had a PSA of >2.5 mg/L while others used higher cut-off values (>4 mg/L). Again others excluded patients with a too high PSA [31]. The prostate volume varied between studies too. Prostate volume and the cancer detection rate was shown to be negatively correlated [44]. The higher cancer detection rate in [31] compared to the other studies could be caused by the smaller mean prostate volume. The conclusion based on the selected literature is that the diameter of a biopsy needle did not influence the cancer detection rate.

Larger diameter needles did not result in significant difference between pain scores, meaning that the patient experienced equally amount of discomfort with both larger and smaller calibre needles. Between 16G and 18G no significant differences in complication rates were found. But using a 20G needle instead of a 18G significantly reduced the occurrence of hematuria and rectal bleeding. This indicates that using a smaller calibre needle resulted in fewer complications and was favorable over a larger calibre needle. However, the fragmentation or failed biopsy rate was not reported in [33]. Therefore, the performance of the 20G needle compared to the 18G needle is not clear. This should be studied first before a recommendation can be provided.

Inal et al. [32] reported that the smaller calibre (18G) needle had significantly less failed biopsies in TRUS biopsy compared to the larger (16G) needle. Whereas [41] reported the contrary in MRI guided prostate biopsy. This would suggest that the type of procedure might have an influence on the performance of the biopsy needle. The quality of a core was only evaluated in [30] and [32]. The former study did not find a significant difference in fragmentation rate and the presence of small cores, while the latter showed that there definitely was a difference. The fragmentation rate was, similar to the studies shown in III, determined by a subjective consultant pathologist.

Although there were indications that better quality cores could be obtained with a larger calibre needle, hard evidence was not found in literature. The overall conclusion was that needle diameter did not correlate with the cancer detection rate and no needle was favourable over the other.

One of the limitations of this literature review was that the conclusion on core length and prostate cancer detection rate was solely based on retrospective studies, which may have introduced biases. Besides that, an assumption was made that increasing the cutting length would also increase the biopsy core length. Literature on this topic was not found. All of the studies that compared the end-cut with the side-cut needle based their conclusion on somewhat small sample sizes. This could make the detecting of significant differences more difficult. Finally, the amount of literature that studied the effect of the cutting length on the prostate cancer detection rate was limited. Therefore, the conclusion on this topic should be taken with a degree of caution.

V. Conclusion

Literature that studied the correlation between a biopsy needle characteristic and the prostate cancer detection rate was selected. Three needle characteristics were reviewed: sampling mechanism, cutting length and needle diameter.

The type of sampling mechanism did not correlate with the cancer detection rate. Both needles sampled similar quality cores and caused equally amount of complications. However, the end-cut needle showed more failed biopsies. The side-cut method seems to be more suitable then the end-cut method.

There were strong indications that increasing the cutting length of side-cut biopsy needles resulted in an increased cancer detection rate. This was not the case with end-cut biopsy needles. A side-cut needle with a cutting length of 25 mm was recommended. This recommendation can be more substantiated if the influence of the cutting length on core quality will be studied.

Finally, the diameter of the biopsy needle (16G, 18G or 20G) did not correlate with the cancer detection rate. There were indications that a large calibre needle increased the core quality, although hard evidence was not found in literature. No biopsy needle diameter was preferred over the other.

References

[1] F. Bray, J. Ferlay, I. Soerjomataram, R. L. Siegel, L. A. Torro, and A. Jemal, "Global Cancer Statistics 2018: GLOBOCAN Estimates of Incidence and Mortality Worldwide for 36 Cancers in 185 Countries Freddie," *CA: A Cancer Journal for Clinicians*, vol. 00, no. 00, pp. 1–31, 2018.

[2] K. K. Hodge, J. E. McNeal, M. K. Terris, and T. A. Stamey, "RANDOM SYSTEMATIC VERSUS DIRECTED ULTRASOUND GUIDED TRANSRECTAL CORE BIOPSIES OF THE PROSTATE," *Journal of Urology*, vol. 142, no. 9, pp. 71–74, 1989.

[3] M. Norberg, L. Egevad, L. Holmberg, P. Sparén, B. J. Norlén, and C. Busch, "The sextant protocol for ultrasound-guided core biopsies of the prostate underestimates the presence of cancer," *Urology*, vol. 50, no. 4, pp. 562–566, 1997.

[4] R. C. Chambó, F. H. Tsuji, F. de Oliveira Lima, H. A. Yamamoto, and C. M. Nóbrega de Jesus, "What is the ideal core number for ultrasound-guided prostate biopsy?," *Korean Journal of Urology*, vol. 55, no. 11, pp. 725–731, 2014.

[5] M. Ghafoori, M. Velayati, M. A. Ghasabeh, M. Shakiba, and M. Alavi, "Prostate biopsy using transrectal ultrasonography; the optimal number of cores regarding cancer detection rate and complications," *Iranian Journal of Radiology*, vol. 12, no. 2, pp. 0–4, 2015.

[6] J. Irani, P. Blanchet, L. Salomon, P. Coloby, J. Hubert, B. Malavaud, and N. Mottet, "Is an extended 20-core prostate biopsy protocol more efficient than the standard 12-core? A randomized multicenter trial," *Journal of Urology*, vol. 190, no. 1, pp. 77–83, 2013.

[7] M. A. Bjurlin, H. B. Carter, P. Schellhammer, M. S. Cookson, L. G. Gomella, D. Troyer, T. M. Wheeler, S. Schlossberg, D. F. Penson, and S. S. Taneja, "Optimization of initial prostate biopsy in clinical practice: Sampling, labeling and specimen processing," *Journal of Urology*, vol. 189, no. 6, pp. 2039–2046, 2013.

[8] J. L. Wright and W. J. Ellis, "Improved prostate cancer detection with anterior apical prostate biopsies," *Urologic Oncology: Seminars and Original Investigations*, vol. 24, no. 6, pp. 492–495, 2006.

LITERATURE RESEARCH ERNST SCHILLINGS, DEPARTMENT OF BIOMEDICAL ENGINEERING, TU DELFT

[9] C. M. Moore, N. L. Robertson, N. Arsanious, T. Middleton, A. Villers, L. Klotz, S. S. Taneja, and M. Emberton, "Image-Guided Prostate Biopsy Using Magnetic Resonance Imaging-Derived Targets: A Systematic Review," *European Urology*, vol. 63, no. 1, pp. 125–140, 2013.

[10] H. S. Dogan, B. Aytac, Y. Kordan, F. Gasanov, and I. Yavascaoglu, "What is the adequacy of biopsies for prostate sampling?," *Urologic Oncology: Seminars and Original Investigations*, vol. 29, no. 3, pp. 280–283, 2011.

[11] J. E. McNeal, "The zonal anatomy of the prostate," *The Prostate*, vol. 2, no. 1, pp. 35–49, 1981.

[12] T. Van Der Kwast, L. Bubendorf, C. Mazerolles, M. R. Raspollini, G. J. Van Leenders, C. G. Pihl, and P. Kujala, "Guidelines on processing and reporting of prostate biopsies: The 2013 update of the pathology committee of the European Randomized Study of Screening for Prostate Cancer (ERSPC)," *Virchows Archiv*, vol. 463, no. 3, pp. 367–377, 2013.

[13] T. H. Van Der Kwast, C. Lopes, C. Santonja, C.-G. Pihl, I. Neetens, P. Martikainen, S. Di Lollo, L. Bubendorf, and R. F. Hoedemaeker, "Needle Biopsies," *Clin Pathol*, no. 56, pp. 336–341, 2003.

[14] C. B. Ching, A. S. Moussa, J. Li, B. R. Lane, C. Zippe, and J. S. Jones, "Does Transrectal Ultrasound Probe Configuration Really Matter? End Fire Versus Side Fire Probe Prostate Cancer Detection Rates," *Journal of Urology*, vol. 181, no. 5, pp. 2077–2083, 2009.

[15] R. Paul, C. Korzinek, U. Necknig, T. Niesel, M. Alschibaja, H. Leyh, and R. Hartung, "Influence of transrectal ultrasound probe on prostate cancer detection in transrectal ultrasound-guided sextant biopsy of prostate," *Urology*, vol. 64, no. 3, pp. 532–536, 2004.

[16] A. Takenaka, R. Hara, T. Ishimura, T. Fujii, Y. Jo, A. Nagai, and M. Fujisawa, "A prospective randomized comparison of diagnostic efficacy between transperineal and transrectal 12-core prostate biopsy," *Prostate Cancer and Prostatic Diseases*, vol. 11, no. 2, pp. 134–138, 2008.

[17] S. Nafie, M. Wanis, and M. Khan, "The Efficacy of Transrectal Ultrasound Guided Biopsy Versus Transperineal Template Biopsy of the Prostate in Diagnosing Prostate Cancer in Men with Previous Negative Transrectal Ultrasound Guided Biopsy.," *Urologic Oncology*, vol. 14, no. 02, pp. 3008–3012, 2017.

[18] D. T. Chang, B. Challacombe, and N. Lawrentschuk, "Transperineal biopsy of the prostate-is this the future?," *Nature Reviews Urology*, vol. 10, no. 12, pp. 690–702, 2013.

[19] L. L. L. Boccon-Gibod, T. H. Van Der Kwast, R. Montironi, L. L. L. Boccon-Gibod, and A. Bono, "Handling and pathology reporting of prostate biopsies," *European Urology*, vol. 46, no. 2, pp. 177–181, 2004.

[20] A. Bertaccini, A. Fandella, T. Prayer-Galetti, V. Scattoni, A. B. Galosi, V. Ficarra, C. Trombetta, M. Gion, and G. Martorana, "Systematic development of clinical practice guidelines for prostate biopsies: A 3-year Italian project," *Anticancer Research*, vol. 27, no. 1 B, pp. 659–666, 2007.

[21] C. Öbek, T. Doanca, S. Erdal, S. Erdoan, and H. Durak, "Core length in prostate biopsy: Size matters," *Journal of Urology*, vol. 187, no. 6, pp. 2051–2055, 2012.

[22] M. Ergün, E. slamolu, S. Yalçnkaya, H. Tokgöz, and M. Sava, "Does length of prostate biopsy cores have an impact on diagnosis of prostate cancer?," *Turk Uroloji Dergisi*, vol. 42, no. 3, pp. 130–133, 2016.

[23] H. Yilmaz, S. Ciftci, M. Ustuner, U. Yavuz, A. Saribacak, B. Muezzinoglu, and O. Dillioglugil, "Minimum 6mm core length is strongly predictive for the presence of glandular tissue in transrectal prostate biopsy," *World Journal of Urology*, vol. 33, no. 11, pp. 1715–1720, 2015.

[24] A. Weilandt, "WO9622733A1," 1996.

[25] H. S. Dogan, S. Y. Eskicorapci, D. Ertoy-Baydar, B. Akdogan, L. M. Gunay, and H. Ozen, "Can we obtain better specimens with an end-cutting prostatic biopsy device?," *European Urology*, vol. 47, no. 3, pp. 297–301, 2005.

[26] L. Häggarth, P. Ekman, and L. Egevad, "A new core-biopsy instrument with an end-cut technique provides prostate biopsies with increased tissue yield," *BJU International*, vol. 90, no. 1, pp. 51–55, 2002.

[27] G. N. Ubhayakar, W. Y. Li, C. M. Corbishley, and U. Patel, "Improving glandular coverage during prostate biopsy using a long-core needle: Technical performance of an end-cutting needle," *BJU International*, vol. 89, no. 1, pp. 40–43, 2002.

[28] E. Özden, Ç. Göü, Ö. Tulunay, and S. Baltaci, "The Long Core Needle with an End-Cut Technique for Prostate Biopsy: Does It Really Have Advantages When Compared with Standard Needles?," *European Urology*, vol. 45, no. 3, pp. 287–291, 2004.

[29] K. Kanao, K. Kajikawa, I. Kobayashi, S. Morinaga, H. Muramatsu, G. Nishikawa, M. Watanabe, K. Zennami, K. Nakamura, and M. Sumitomo, "Impact of a novel biopsy instrument with a 25-mm side-notch needle on the detection of prostate cancer in transrectal biopsy," *International Journal of Urology*, vol. 25, no. 8, pp. 746–751, 2018.

[30] A. Cicione, F. Cantiello, C. De Nunzio, A. Tubaro, and R. Damiano, "Prostate biopsy quality is independent of needle size: A randomized single-center prospective study," *Urologia Internationalis*, vol. 89, no. 1, pp. 57–60, 2012.

[31] M. McCormack, A. Duclos, L. M, M. H. McCormack, D. Liberman, O. Djahangirian, and J. Bergeron, "Effect of needle size on cancer detection, pain, bleeeding and infection in transrectal ultrasound-guided prostate biopsy: a prospective trial," *Can Urol Assoc J*, vol. 6, no. 2, pp. 97–101, 2012.

[32] G. H. Inal, V. Ç. Öztekin, Ö. Uurlu, M. Kosan, Ö. Akdemir, and M. Çetinkaya, "Sixteen gauge needles improve specimen quality but not cancer detection rate in transrectal ultrasound-guided 10-core prostate biopsies," *Prostate Cancer and Prostatic Diseases*, vol. 11, no. 3, pp. 270–273, 2008.

[33] J. Wang, B. Wan, C. Li, J. Wang, W. Zhao, Q. Fu, and K. Zhang, "Diagnostic yield and complications using a 20 gauge prostate biopsy needle versus a standard 18 gauge needle: A randomized controlled study," *Urology Journal*, vol. 12, no. 5, pp. 2329–2333, 2015.

[34] K. Hopper, C. Abendroth, K. Sturtz, Y. Matthews, J. Hartzel, and P. Potok, "CT Percutaneous Biopsy Guns : Devices in Cadaveric Specimens," *Group*, 1994.

[35] K. Kanao, J. A. Eastham, P. T. Scardino, V. E. Reuter, and S. W. Fine, "Can transrectal needle biopsy be optimised to detect nearly all prostate cancer with a volume of 0.5 mL? A three-dimensional analysis," *BJU International*, vol. 112, no. 7, pp. 898–904, 2013.

[36] K. A. Iczkowski, G. Casella, R. J. Seppala, G. L. Jones, B. A. Mishler, J. Qian, and D. G. Bostwick, "NEEDLE CORE LENGTH IN SEXTANT BIOPSY INFLUENCES PROSTATE CANCER DETECTION RATE KENNETH," *Adult Urology*, vol. 59, no. 5, pp. 698–703, 2002.

[37] K. G. Fink, G. Hutarew, A. Pytel, and N. T. Schmeller, "Prostate biopsy outcome using 29 mm cutting length," *Urologia Internationalis*, vol. 75, no. 3, pp. 209–212, 2005.

[38] O. G. Doluogly, C. N. Yuceturk, M. Eroglu, B. C. Ozgur, A. Demirbas, T. Karakan, S. Bozkurt, and B. Resorlu, "Core Length: An Alternative Method for Increasing Cancer Detection Rate in Patients with Prostate Cancer," *Urologic Oncology*, vol. 12, no. 05, pp. 2324–2328, 2015.

[39] H. Deliktas, H. Sahin, M. Cetinkaya, Y. Dere, O. Erdogan, and E. Baldemir, "Does Core Length Taken per cc of Prostate Volume in Prostate Biopsy Affect the Diagnosis of Prostate Cancer?," *Clinical Genitourinary Cancer*, vol. 14, no. 4, pp. e387–e391, 2016.

[40] S. E. Lee, S. J. Jeong, S. I. Hwang, S. K. Hong, H. J. Lee, S. S. Byun, G. Choe, and S. E. Lee, "Clinical value of core length in contemporary multicore prostate biopsy," *PLoS ONE*, vol. 10, no. 4, pp. 1–9, 2015.

[41] T. Durmus, U. Goldmann, A. D. Baur, A. Huppertz, C. Schwenke, B. Hamm, and T. Franiel, "MR-guided biopsy of the prostate: Comparison of diagnosticspecimen quality with 18G and 16G biopsy needles," *European Journal of Radiology*, vol. 82, no. 12, pp. e749–e754, 2013.

[42] S. Giovanni, M. C. Sighinolfi, F. Francesco, D. S. Stefano, M. Salvatore, M. Paterlini, R. D'Amico, and B. Giampaolo, "Does needle calibre affect pain and complication rates in patients undergoing transperineal prostate biopsy? A prospective, randomized trial," *Asian Journal of Andrology*, vol. 11, no. 6, pp. 678–682, 2009.

[43] A. Descazeaud, M. A. Rubin, Y. Allory, M. Burchardt, L. Salomon, D. Chopin, C. Abbou, and A. De La Taille, "What information are urologists extracting from prostate needle biopsy reports and what do they need for clinical management of prostate cancer?," *European Urology*, vol. 48, no. 6, pp. 911–915, 2005.

[44] S. Al-Khalil, C. Ibilibor, J. T. Cammack, and W. de Riese, "Association of prostate volume with incidence and aggressiveness of prostate cancer," *Research and Reports in Urology*, vol. 8, pp. 201–205, 2016.

Appendix B

Test Protocol: Blowing

B.1   Introduction

Using manually operated biopsy needle in MRI-guided prostate biopsy was shown to be time-inefficient. A system that can automatically take multiple samples without human intervention is a suggested solution. This automatic biopsy system requires the development of a new technique to remove the tissue sample from the stylet. Several techniques are identified. However, finding the best solution is not possible because of their unknown performance.

B.2   Objective

The goal of this experiment is to determine the feasibility of removing a tissue sample from the stylet of a biopsy needle by blowing. Similar experiments are done with other tissue removing techniques. The results of these experiments are used to compare the performance of different tissue sample removing techniques.

B.3   Materials

B.3.1   Specimens

A raw chicken breast (±4 °C) is the specimen source in these tests. The chicken breast is placed against a vertical plate that contains holes, which separated the entry points for each run.

B.3.2   Instruments

A standard 18G Tru-cut Biopsy Needle (Figure D.1) is used to take the tissue samples. This biopsy needle can be fired automatically but is reloaded manually.
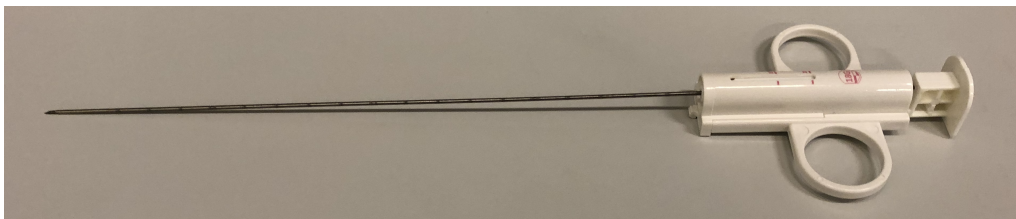

FIGURE B.1: Manually reloaded 18G Tru-cut biopsy needle.

B.3.3 Equipment

The test tool shown in Figure B.2 is used for this experiment. The fan creates the air-flow, while the funnel aims the flow at the specimen. The fan can displace 3 $\frac{m^3}{hr}$ and is powered by a 12V power supply. The funnel can be narrowed near the specimen to increase the air flow velocity.
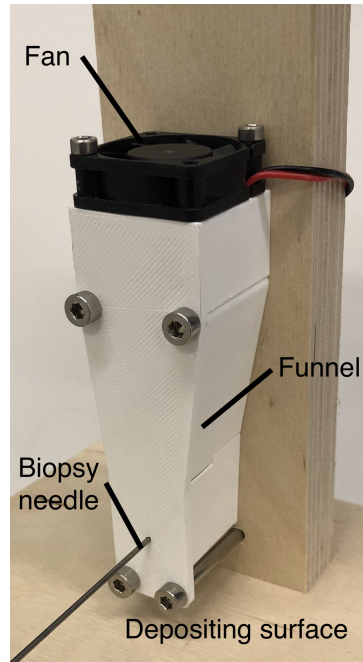

FIGURE B.2: Caption

B.4 Methods

B.4.1 Variables and constants

The dependent variables and their acceptance criteria are listed in Table B.1.

TABLE B.1: Depedent variables and their acceptance criteria for the 'removing by blowing' tests.

#	Requirement	Acceptance criteria
1	Amount of removal	No obvious tissue waste on stylet
2	Fragmentation	Tissue sample length after removal was $\geq$80% of length before removal
3	Control of deposition	Tissue sample deposited on designated surface

The independent variable is the air flow velocity, which is 2.5 $\frac{m}{s}$ or 13 $\frac{m}{s}$. The constants are:

- The funnel shape, which is rectangular
- The direction of gravity with respect to the air flow is parallel.

B.4.2 Experimental Design

The test tool shown in Figure 6.4f creates an airflow and funnels it in the direction of the tissue sample. The test consists of 10 runs. The first 5 runs are done with a low air flow velocity and the remaining runs with a high air flow velocity. The air flow velocity can be controlled by narrowing the funnel near the stylet. A funnel width of 18 mm corresponds to an airflow velocity of 2.5 $\frac{m}{s}$, while one with a width of 4 mm results in an airflow velocity of 13 $\frac{m}{s}$. The length of the tissue sample is measured using a caliper before and after removal from the stylet notch. This was done to determine the amount of fragmentation. The designated depositing area is the horizontal surface directly below the stylet.

B.4.3 Experimental protocol

The experimental protocol of single run is as follows:

1. Reload biopsy needle
2. Insert into specimen
3. Fire and reload biopsy needle
4. Measure length of tissue sample on stylet with caliper
5. If length was « 8 mm, remove sample manually and proceed to step 1.
6. Insert stylet into test tool with stylet notch surface in vertical position
7. Turn on fan and wait for 30 seconds
8. Check whether sample has been removed
9. Check whether sample is on depositing surface
10. Again, measure length of tissue sample on stylet with caliper

B.4.4 Data Processing and Analyses

All the data is reported in Excel. The length of the tissue sample after removal is reported as a percentage of the length before removal. A + means that the acceptance criteria is met and a - that it is not met.

B.5 Results

TABLE B.2: This table lists the results of the blowing tests. Here, V_{low} means low velocity and V_{high} the high velocity of the air flow. The three type of results are explained in B.1.

Run	Amount of removal		Tissue damage		Deposition	
	V_{low}	V_{high}	V_{low}	V_{high}	V_{low}	V_{high}
1	-	-	+	-	-	-
2	-	-	+	+	-	-
3	-	-	+	+	-	-
4	-	-	+	-	-	-
5	-	-	+	+	-	-

Appendix C

Test Protocol: Flushing

C.1 Introduction

Using manually operated biopsy needle in MRI-guided prostate biopsy was shown to be time-inefficient. A system that can automatically take multiple samples without human intervention is a suggested solution. This automatic biopsy system requires the development of a new technique to remove the tissue sample from the stylet. Several techniques are identified. However, finding the best solution is not possible because of their unknown performance.

C.2 Objective

The goal of this experiment is to determine the feasibility of removing a tissue sample from the stylet of a biopsy needle by blowing. Similar experiments are done with other tissue removing techniques. The results of these experiments are used to compare the performance of different tissue sample removing techniques.

C.3 Materials

C.3.1 Specimens

A raw chicken breast (±4 °C) is the specimen source in these tests. The chicken breast is placed against a vertical plate that contains holes, which separated the entry points for each run.

C.3.2 Instruments

A standard 18G Tru-cut Biopsy Needle (Figure D.1) is used to take the tissue samples. This biopsy needle can be fired automatically but is reloaded manually.
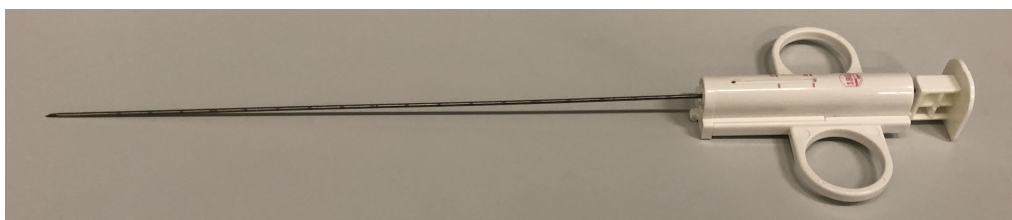
FIGURE C.1: Manually reloaded 18G Tru-cut biopsy needle.

C.3.3 Equipment

A syringe is connected via a tube to a flat spray nozzle. The nozzle is fixed to the test tool shown in Figure C.2. Applying a force on the syringe plunger creates a flat spray jet. Varying the applied force results in different water flow velocities.
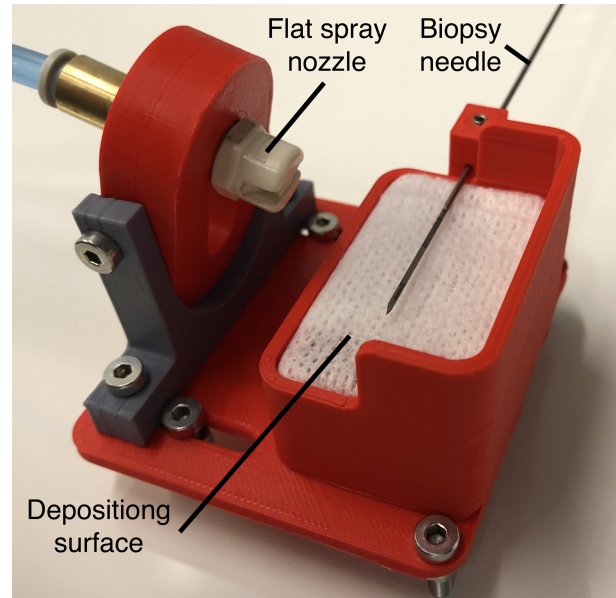

FIGURE C.2: Caption

C.4 Methods

C.4.1 Variables and constants

The dependent variables and their acceptance criteria are listed in Table C.1.

TABLE C.1: Depedent variables and their acceptance criteria for the 'removing by blowing' tests.

#	Requirement	Acceptance criteria
1	Amount of removal	No obvious tissue waste on stylet
2	Fragmentation	Tissue sample length after removal was $\geq$80% of length before removal
3	Control of deposition	Tissue sample deposited on designated surface

The independent variable is the water flow velocity, which is low with a plunger force of 5 N and high with a force of 50 N. The constants are:

- Distribution of jet along tissue sample, which is uniform

- Contact area between water flow and tissue sample, which is the entire front area of the sample.

- Direction of flow, which is 30 °with respect to gravitational force.

C.4.2 Experimental Design

The syringe creates a flat spray jet. The test consists of 10 runs. The first 5 runs are done with a low water flow velocity and the remaining runs with a higher one. The water flow velocity is controlled by changing the force applied on the syringe plunger. The length of the tissue sample is measured with a caliper before and after removal from the stylet notch. This is done to determine the amount of fragmentation. The designated depositing area is shown in Figure C.2.

C.4.3 Experimental protocol

The experimental protocol of single run is as follows:

1. Reload biopsy needle

2. Insert into specimen

3. Fire biopsy needle

4. Reload biopsy needle

5. Measure length of tissue sample on stylet with caliper

6. If length was « 8 mm, remove sample manually and proceed to step 1.

7. Insert stylet into test tool with stylet notch surface facing upwards

8. Apply force on syringe plunger

9. Check whether sample has been removed

10. Check whether sample is on depositing surface

11. Again, measure length of tissue sample on stylet with caliper

C.4.4 Data Processing and Analyses

All the data is reported in Excel. The length of the tissue sample after removal is reported as a percentage of the length before removal. A + means that the acceptance criteria is met and a - that it is not met.

C.5 Results

TABLE C.2: This table lists the results of the blowing tests. Here, V_{low} means low velocity and V_{high} the high velocity of the air flow. The three type of results are explained in C.1.

Run	Amount of removal		Tissue damage		Deposition	
	V_{low}	V_{high}	V_{low}	V_{high}	V_{low}	V_{high}
1	-	-	+	-	-	-
2	-	-	+	+	-	-
3	-	-	+	+	-	-
4	-	-	+	-	-	-
5	-	-	+	+	-	-

Appendix D

Test Protocol: Wiping

D.1 Introduction

Using manually operated biopsy needle in MRI-guided prostate biopsy was shown to be time-inefficient. A system that can automatically take multiple samples without human intervention is a suggested solution. This automatic biopsy system requires the development of a new technique to remove the tissue sample from the stylet. Several techniques are identified. However, finding the best solution is not possible because of their unknown performance.

D.2 Objective

The goal of this experiment is to determine the feasibility of removing a tissue sample from the stylet of a biopsy needle by blowing. Similar experiments are done with other tissue removing techniques. The results of these experiments are used to compare the performance of different tissue sample removing techniques.

D.3 Materials

D.3.1 Specimens

A raw chicken breast (±4 °C) is the specimen source in these tests. The chicken breast is placed against a vertical plate that contains holes, which separated the entry points for each run.

D.3.2 Instruments

A standard 18G Tru-cut Biopsy Needle (Figure D.1) is used to take the tissue samples. This biopsy needle can be fired automatically but is reloaded manually.
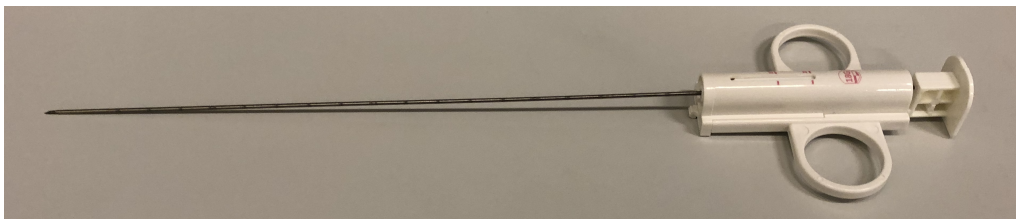
FIGURE D.1: Manually reloaded 18G Tru-cut biopsy needle.

D.3.3 Equipment

The test tool shown in figure D.2 consists of a base and wiper. The shaft of the wiper is connected to a stepper motor (NEMA 17), which is controlled by an arduino with an 12V power supply. The stepper motor rotates the wiper over a fixed range of 120°.
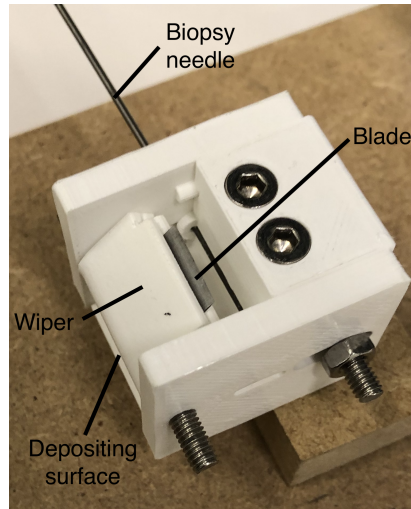

FIGURE D.2: Test tool used to test the wiping technique.

D.4 Methods

D.4.1 Variables and constants

The dependent variables and their acceptance criteria are listed in Table D.1.

TABLE D.1: Depedent variables and their acceptance criteria for the 'removing by wiping' tests.

#	Requirement	Acceptance criteria
1	Amount of removal	No obvious tissue waste on stylet
2	Fragmentation	Tissue sample length after removal was ≥80% of length before removal
3	Control of deposition	Tissue sample deposited on designated surface

The independent variable is the angular velocity of the wiper, which was 8.4 $\frac{rad}{s}$ or 50 $\frac{rad}{s}$. The constants are:

- Minimum distance between blade and stylet notch surface (±0.3 mm)

- Blade width (20 mm)

- The location and orientation of the depositing surface (see Figure D.2

D.4.2   Experimental Design

Moving the wiper over the predefined range should remove the sample from the biopsy needle. The test consists of 10 runs. The first 5 runs are done with a low wiper angular velocity and the remaining runs with a higher one. The length of the tissue sample is measured using a caliper before and after removal from the stylet notch. This was done to determine the amount of fragmentation. The designated depositing area is shown in Figure D.2.

D.4.3   Experimental protocol

The experimental protocol of single run was as follows:

1. Reload biopsy needle

2. Insert into specimen

3. Fire biopsy needle

4. Reload biopsy needle

5. Measure length of tissue sample on stylet with caliper

6. If length was « 8 mm, remove sample manually and proceed to step 1.

7. Insert stylet into test tool with stylet notch surface facing upwards

8. Rotate wiper with predefined angular velocity

9. Check whether sample has been removed

10. Check whether sample was on depositing surface

11. Again, measure length of tissue sample on stylet with caliper

D.4.4   Data Processing and Analyses

All the data is reported in Excel. The length of the tissue sample after removal is reported as a percentage of the length before removal. A + means that the acceptance criteria is met and a - that it is not met.

D.5   Results

TABLE D.2: This table lists the results of the wiping tests. Here, ϑ_{low} means low and ϑ_{high} the high angular velocity of the wi[er. The three type of results were explained in D.1.

Run	Amount of removal		Tissue damage		Deposition	
-----	V_{low}	V_{high}	V_{low}	V_{high}	V_{low}	V_{high}
1	-	-	+	-	-	-
2	-	-	+	+	-	-
3	-	-	+	+	-	-
4	-	-	+	-	-	-
5	-	-	+	+	-	-

Appendix E

Test Protocol: Pushing

E.1 Introduction

Using manually operated biopsy needle in MRI-guided prostate biopsy was shown to be time-inefficient. A system that can automatically take multiple samples without human intervention is a suggested solution. This automatic biopsy system requires the development of a new technique to remove the tissue sample from the stylet. Several techniques are identified. However, finding the best solution is not possible because of their unknown performance.

E.2 Objective

The goal of this experiment is to determine the feasibility of removing a tissue sample from the stylet of a biopsy needle by blowing. Similar experiments are done with other tissue removing techniques. The results of these experiments are used to compare the performance of different tissue sample removing techniques.

E.3 Materials

E.3.1 Specimens

A raw chicken breast (±4 °C) is the specimen source in these tests. The chicken breast is placed against a vertical plate that contains holes, which separated the entry points for each run.

E.3.2 Instruments

A standard 18G Tru-cut Biopsy Needle (Figure D.1) is used to take the tissue samples. This biopsy needle can be fired automatically but is reloaded manually.
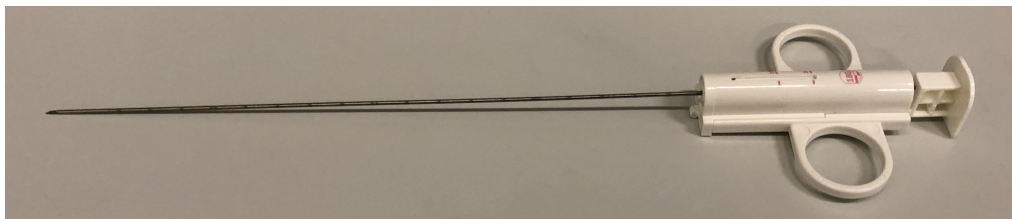
FIGURE E.1: Manually reloaded 18G Tru-cut biopsy needle.
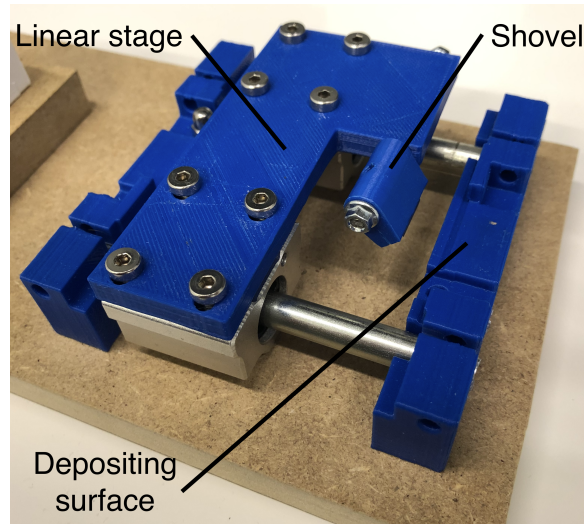
FIGURE E.2: Caption

E.3.3 Equipment

The tool used for in this protocol is shown in Figure E.2. It consists of a linear moving pusher or shovel and a base, in whichthe biopsy needle is fixed with the stylet notch surface facing upwards. The shovelis equipped with a thin blade and is connected to a linear stage that can move onlyalong one axis. This axis is parallel to the stylet notch surface and perpendicular tothe biopsy needle.

E.4 Methods

E.4.1 Variables and constants

The dependent variables and their acceptance criteria are listed in Table E.1.

TABLE E.1: Dependent variables and their acceptance criteria used for the 'removing by pushing' tests.

#	Requirement	Acceptance criteria
1	Amount of removal	No obvious tissue waste on stylet
2	Fragmentation	Tissue sample length after removal was $\geq$80% of length before removal
3	Control of deposition	Tissue sample deposited on designated surface

The independent variable is the linear pushing velocity, which is 10 $\frac{mm}{s}$ or 42 $\frac{mm}{s}$. The constants are:

- Push angle w.r.t. stylet notch surface (40°)

- Minimum distance between blade and stylet notch surface (±0.3 mm)

- Blade width (20 mm)

E.4.2 Experimental Design

Moving the pusher along the stylet notch surface should remove the tissue sample. The test consists of 10 runs. The first 5 runs are done with a low pusher velocity and the remaining runs with a higher one. The length of the tissue sample is measured using a caliper before and after removal from the stylet. This is done to determine the amount of fragmentation. The designated depositing area is shown in Figure E.2.

E.4.3 Experimental protocol

The experimental protocol of single run was as follows:

1. Reload biopsy needle
2. Insert into specimen
3. Fire biopsy needle
4. Reload biopsy needle
5. Measure length of tissue sample on stylet with caliper
6. If length was « 8 mm, remove sample manually and proceed to step 1.
7. Insert stylet into test tool with stylet notch surface facing upwards
8. Move pusher at predefined velocity
9. Check whether sample has been removed
10. Check whether sample is on depositing surface
11. Again, measure length of tissue sample on stylet with caliper

E.4.4 Data Processing and Analyses

All the data is reported in Excel. The length of the tissue sample after removal is reported as a percentage of the length before removal. A + means that the acceptance criteria is met and a - that it is not met.

E.5 Results

TABLE E.2: This table lists the results of the blowing tests. Here, V_{low} means low pusher velocity and V_{high} a high one. The three type of results are explained in E.1.

Run	Amount of removal		Tissue damage		Deposition	
	V_{low}	V_{high}	V_{low}	V_{high}	V_{low}	V_{high}
1	-	-	+	-	-	-
2	-	-	+	+	-	-
3	-	-	+	+	-	-
4	-	-	+	-	-	-
5	-	-	+	+	-	-

Appendix F

Bill Of Materials

TABLE F.1: Bill of Materials of the proof of principle prototype.

Part Name	Amount	Material	Make/buy
0101_BasePlate	1	PLA	Make
0102_LinearGuideFront	1	PLA	Make
0103_LinearGuideMiddle	1	PLA	Make
0104_LinearGuideBack	1	PLA	Make
0105_LinearGuideRod	2	Aluminium	Buy
0106_CannulaCylinderMount	1	PLA	Make
0107_PlungerCylinderMount	1	PLA	Make
0108_193972 GRO-QS-4	2		Buy
0109_StyletCylinderHolder	1	PLA	Make
0110_StyletCylinderHolderTop	1	PLA	Make
0201_193988 DSNU-12-160-P—(AMH—0-ZR)	1	Stainless Steel	Buy
0301_193988 DSNU-12-25-P—(AMH—0-ZR)	1	Stainless Steel	Buy
0401_193989 DSNU-16-100-P—(AMH—0-ZR)	1	Stainless Steel	Buy
0502_CylinderEndBus	1	PEEK	Make
0601_StyletConnector	1	PEEK	Make
0602_Stylet	1	Stainless Steel	Buy
0701_193988 DSNU-12-25-P—(AMH–00–0-KS)	1	Stainless Steel	Buy
0702_CannulaCylinderConnector	1	PLA	Make
0703_CannulaGuideRod	2	Aluminium	Buy
0704_FireEndStop	1	PLA	Make
0801_ CannulaHousing	1	PLA	Make
0802_Cannula	1	Stainless Steel	Buy
0803_FiringPinsShaft	2	Stainless Steel	Buy
0804_SlidingBearing	4	PEEK	Buy
0901_FiringPin	2	PLA	Make
0902_TorsionSpring	2	Stainless Steel	Buy
1001_193989 DSNU-16-100-P—(AMH–00–0-KS)	1	Stainless Steel	Buy
1002_SyringePlungerConnector	1	PLA	Make
1003_SyringePlungerStop	1	PLA	Make
1004_SyringePlunger	1	Rubber	Buy
1101_Syringe	1	Polyprepylene	Buy
1102_ValveL	1	Polyprepylene	Buy
1201_NozzleMount	1	PLA	Make
1202_Flat_spray_nozzle	1	Polyprepylene	Buy
1203_Adapter_R18_6mm	1	Brass	Buy
1300_572230 VTUG-10-SK7-B5T-Q10L-UL-Q4S-3A	1	Stainless Steel	Buy
1500_CannulaCylinderMountRight	1	PLA	Make
1602_ContainerOutside	1	PLA	Make
1701_BoxTop	1	PLA	Make
1801_DoorStop	8	Polyprepylene	Buy
Flat Head Screw M3x14	4	Stainless Steel	Buy
Flat Head Screw M4x14	1	Stainless Steel	Buy
Flat Head Screw M4x18	2	Stainless Steel	Buy
Socket Head Screw M3x30	1	Stainless Steel	Buy

Socket Head Screw M4x14	15	Stainless Steel	Buy
Socket Head Screw M4x18	3	Stainless Steel	Buy
Socket Head Screw M4x20	1	Stainless Steel	Buy
Socket Head Screw M4x22	1	Stainless Steel	Buy
Socket Head Screw M4x25	2	Stainless Steel	Buy
Socket Head Screw M4x30	1	Stainless Steel	Buy
Socket Head Screw M4x40	1	Stainless Steel	Buy
Socket Low Head Screw M3x45	4	Stainless Steel	Buy
Socket Low Head Screw M4x30	1	Stainless Steel	Buy
Socket Low Head Screw M4x45	2	Stainless Steel	Buy
Socket Low Head Screw M4x50	2	Stainless Steel	Buy
Set Screw M3x4	1	Stainless Steel	Buy
Set Screw M3x18	1	Stainless Steel	Buy
M3 Hex nut	6	Stainless Steel	Buy
M4 Hex nut	23	Stainless Steel	Buy
M6 Hex nut	5	Stainless Steel	Buy
M3 Washer	6	Stainless Steel	Buy
M4 Washer	14	Stainless Steel	Buy

Appendix G

Solid Works Figures
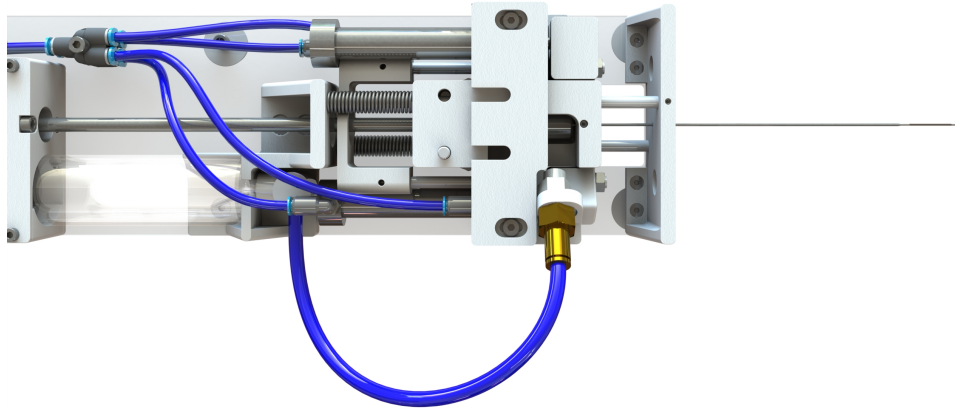
FIGURE G.1: Top view of the proof of principle prototype in Solid-Works. Figure shows stylet in fired and cannula in reloaded position.
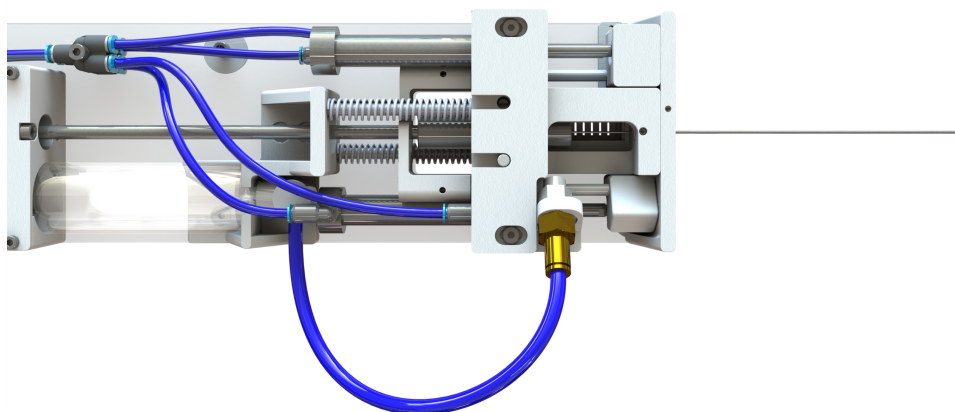
FIGURE G.2: Top view of the proof of principle prototype in Solid-Works. Figure shows both stylet and cannula in fired position.
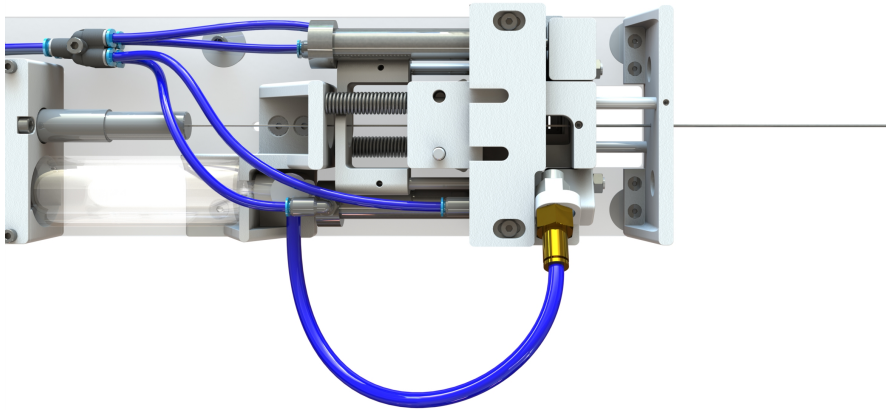
FIGURE G.3: Top view of the proof of principle prototype in Solid-Works. Figure shows both stylet and cannula in reloaded position. Sample can be removed in this position.
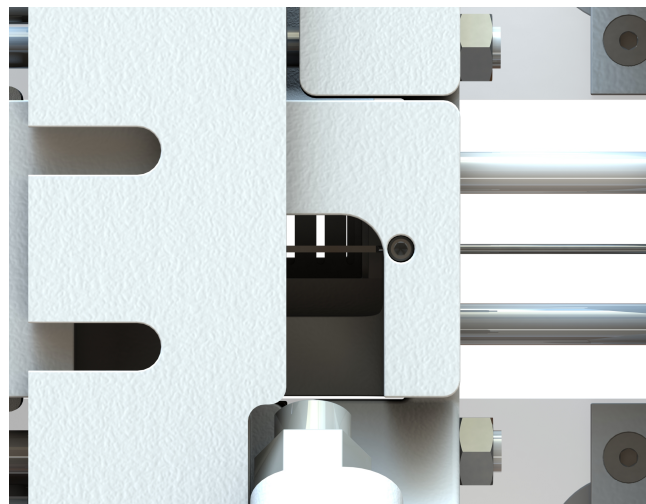
FIGURE G.4: Top view of the proof of principle prototype in Solid-Works. Figure shows both stylet and cannula in reloaded position. Sample can be removed in this position. Figure zooms in on the sample removing location.

(A)   (B) Cation

FIGURE G.5: Top (A) and front (B) view of the proof of principle prototype in Solid-
Works. Figure shows both stylet and cannula in reloaded position.

Appendix H

Verification Protocol: Velocity cannula and stylet

H.1   Introduction

Using manually operated biopsy needle in MRI-guided prostate biopsy was shown to be time-inefficient. A system that can automatically take multiple samples without human intervention is a suggested solution. A prototype of such an automatic biopsy system has been developed.

H.2   Objective

This verification protocol is used to verify whether the automatic biopsy system meets product specification 6.5 and 6.6 (see Table 10.2). These PS describe the required velocity of the stylet and cannula.

H.3   Materials

H.3.1   Instruments

The automatic biopsy system (Figure H.1) is used in this test protocol. The system is fixed to the table with clamps.
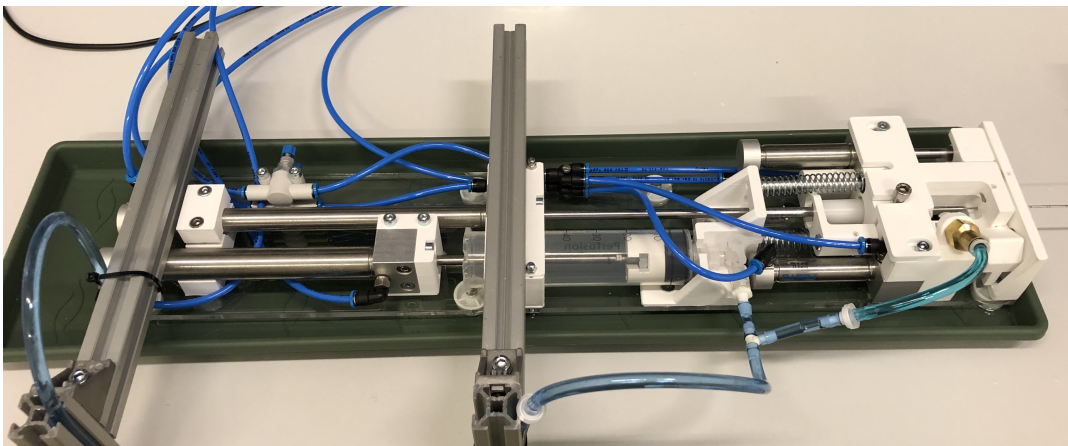
FIGURE H.1: Automatic biopsy system equipped with a standard 18G needle.

H.3.2   Equipment

The required equipment for this verification protocol is the following:

- Camera that is able to record 120 FPS videos
- Clamps

H.4   Methods

H.4.1   Product Specifications

The product specifications listed in Table J.1 are verified with this verification protocol.

TABLE H.1

PS	Product Specification	Acceptance criteria	Measured as
6.5	Stylet insertion velocity	>50 mm/s	Velocity
6.6	Cannula firing velocity	>5 m/s	Velocity

H.4.2   Constants and nuisance factors

The following constants are set:

- Pressure on inlet pneumatic cylinders of 4 bar
- 120 FPS of camera

The following nuisance factors might have an influence of the result.

- Start of movement in between frames

H.4.3   Experimental Design

The firing of cannula and stylet is recorded using the camera. The number of frames from the start to end of fire are counted. The time between two frames is 0.0083 seconds. The distance covered by the cannula and stylet is also known (0.25 mmm). Dividing these two figures results in the velocity. One recording for both the cannula and stylet is considered to be sufficient.

H.4.4   Experimental protocol

1. Start recording
2. Fire stylet
3. Fire cannula
4. Stop recording

H.4.5   Data Processing and Analyses

The recording is analyzed in a video player (e.g. Quicktime Player).

H.5   Results

TABLE H.2

PS	Product Specification	Result	Pass/fail
6.5	Stylet insertion velocity	55 mm/s	Pass
6.6	Cannula firing velocity	3.5 m/s	Fail

Appendix I

Verification Protocol: Sampling quality

I.1 Introduction

Using manually operated biopsy needle in MRI-guided prostate biopsy was shown to be time-inefficient. A system that can automatically take multiple samples without human intervention is a suggested solution. A prototype of such an automatic biopsy system has been developed.

I.2 Objective

This verification protocol is used to verify whether the automatic biopsy system meets the product specification 6.9 (see Table 10.2). Biopsy of a living prostate is not possible at this stage of the project. Therefore, the automatic biopsy system is tested by taking a sample of a chicken breast. Whether the tissue of a chicken breast is comparable to a prostate is unknown. Difference in tissue composition is expected to have an influence on the quality (e.g. length) of the sample. Therefore, the automatic biopsy system is not verified with respect to the initially determined acceptance criteria but the length of the taken samples is compared to samples taken from a chicken breast with a standard 18G Tru-cut biopsy needle.

I.3 Materials

I.3.1 Instruments

A manually reloaded 18G Tru-cut biopsy needle (Figure I.1) and the automatic biopsy system (Figure I.2) are used in this verification protocol. The system is placed on a tray and is fixed to the table with clamps.

I.3.2 Equipment

The equipment used for this verification protocol is a:

- Tray for collecting water
- Specimen holder
- 1L of water
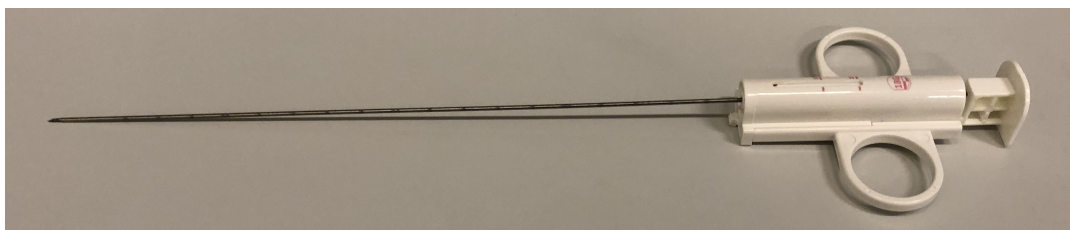
FIGURE I.1: Manually reloaded 18G Tru-cut biopsy needle.
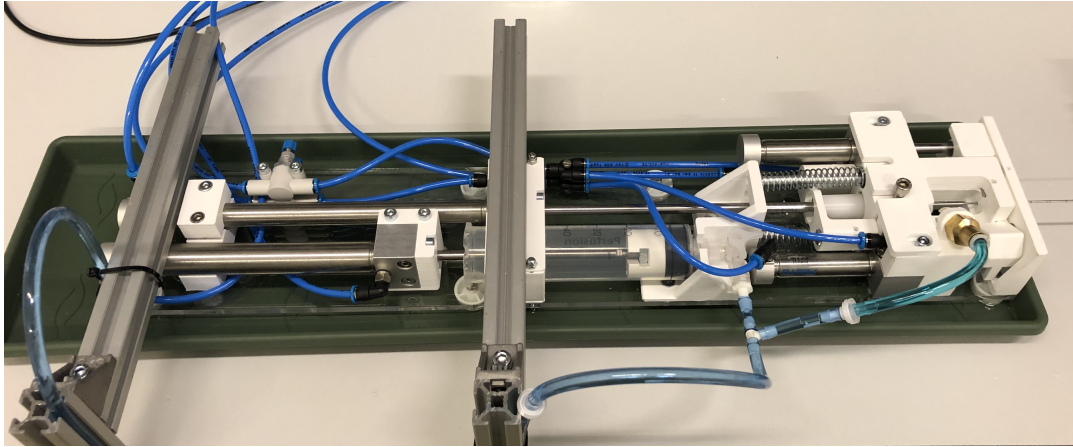
FIGURE I.2: Automatic biopsy system equipped with a standard 18G needle.

- Caliper (accuracy of 0.05 mm)
- Clamps

I.3.3   Specimens

Uncooked chicken breasts are used as specimen. The chicken breasts are cooled to a temperature of 4
°Celcius. The specimen is placed on a slider and against a vertical plate that contains 19 holes (Figure
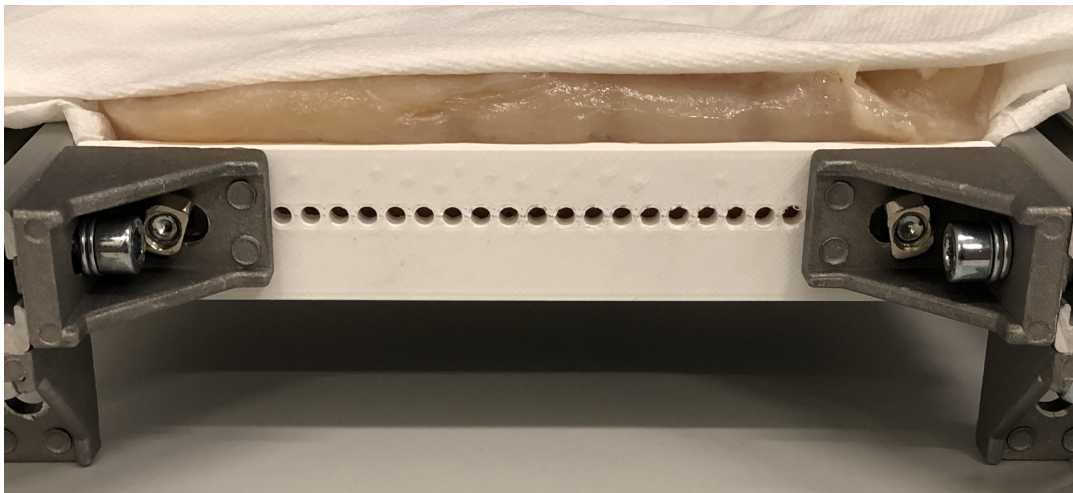I.3).

FIGURE I.3: Chicken breast in specimen holder that contains 19 different entry points
(holes).

Each chicken breast is sampled for a maximum of 38 times. In the first 19 runs the biopsy needle is
inserted into a new hole. Before the second 19 runs are executed, the specimen is rotated for 180°with
respect to the specimen holder.

I.4   Methods

I.4.1   Product Specifications

The product specification listed in Table J.1 is verified with this verification protocol.

TABLE I.1

PS	Product Specification	Acceptance criteria	Measured as
6.9	Sampling quality	Decrease in sample length not significant (p<0.05) compared to standard manual instrument	Sample length

Note: Initial acceptance criteria of PS-7.2 that is shown in Table 10.2 is updated because chicken instead of prostate tissue is sampled.

I.4.2   Constants and nuisance factors

The following constants are set:

- Pressure on inlet pneumatic cylinders of 4 bar
- Specimen temperature of 4 °C
- Insertion depth into specimen of 3 cm
- Flushing volume of 10 ml

The following nuisance factors might have an influence of the result.

- Sharpness of cannula and stylet

I.4.3   Experimental Design

A sample is taken from a chicken breast. Two set of test runs are performed. In the first set, samples are taken using a standard manually operated biopsy needle (18G Tru-cut biopsy needle with a cutting length of 20 mm). The automatic biopsy system is used in the second set of test runs. During each run, one measurement is reported: the length of the sample.

The minimum population size is determined by assuming that the data has a normal distribution. The standard deviation is assumed to be similar to the one that was reported in Kanoa et al. In this study, a standard 18G Tru-cut biopsy needle with a cutting length of 20 mm was used the sample 469 patients. This resulted in an overall standard deviation of 2.9 mm. Besides that, an acceptable error margin is chosen to be 0.7 mm. The margin of error, standard deviation and confidence interval (95%) determine the minimum sample size of 71 samples per group. The product specification is verified if no significant (p<0.05) decrease in tissue sample length is reported.

I.4.4   Experimental protocol

Biopsy using manual 18G Tru-cut needle:

1. Select entry point on specimen.
2. Manually reload biopsy gun.
3. Push stylet into specimen for up to 30 mm.
4. Fire biopsy gun.
5. Remove biopsy needle from specimen.
6. Again, manually reload biopsy gun.
7. Measure and report the length of the sample with caterpillar.
8. Remove sample from stylet.
9. Repeat step 1 to 8 for 71 times.

Biopsy using automatic biopsy system:

1. Select entry point on specimen.
2. Push stylet into specimen for up to 30 mm.
3. Initiate sampling sequence of biopsy system.
4. Measure and report the length of the sample with caterpillar.
5. Remove sample from stylet.
6. Repeat step 1 to 5 for 71 times.

I.4.5 Data Processing and Analyses

All measurements are reported in a vector format in Excel. A two sided t-test compare the means of the sample lengths of standard manual biopsy needle and the automatic biopsy system. Difference are considered to be significant if p<0.05. Box-plots are created to summarize the data.

I.5 Results

The raw data that was collected in this test, is shown in Figure I.4. The descriptive statistics are visualized with boxplots in Figure I.5. See Table I.2 for a list of several statistic parameters for both type of instruments.
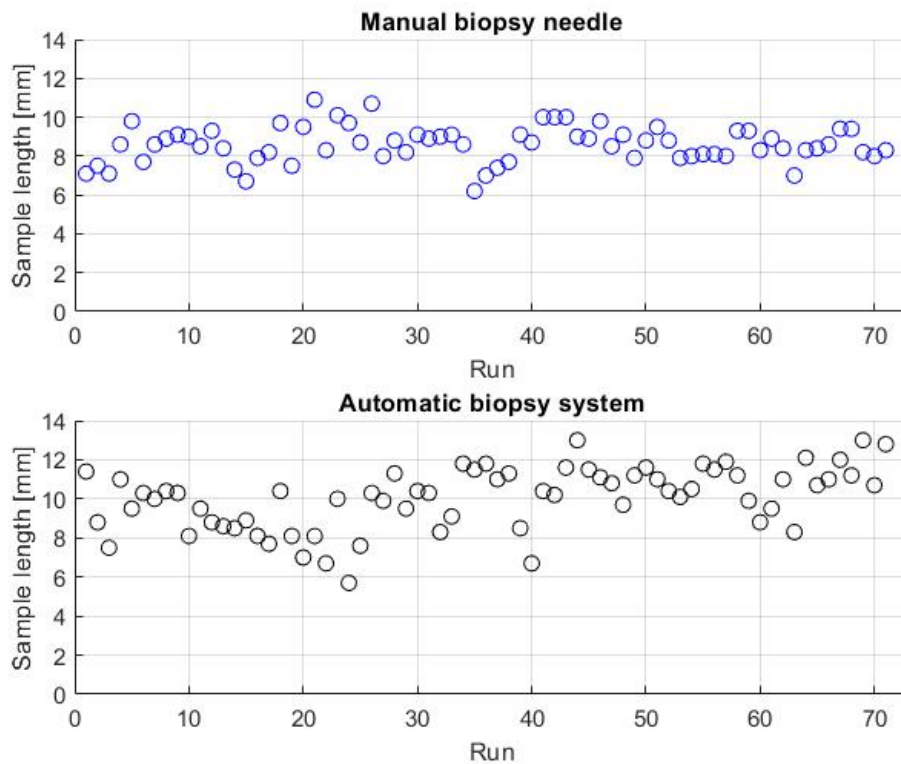
FIGURE I.4: Caption
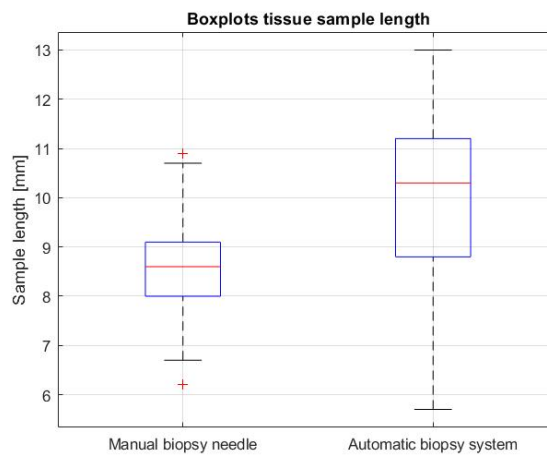
FIGURE I.5: Caption

TABLE I.2

Statistic parameter	Manual biopsy needle	Automatic biopsy system
Mean [mm]	8.6	10.2
Median [mm]	8.6	10.4
Standard deviation [mm]	0.9	1.6
Sample variance [mm]	0.9	2.6
Standard error [mm]	0.1	0.2
P-value	3.6e-11	

Appendix J

Verification Protocol: Removing a tissue sample

J.1 Introduction

Using manually operated biopsy needle in MRI-guided prostate biopsy was shown to be time-inefficient. A system that can automatically take multiple samples without human intervention is a suggested solution. A prototype of such an automatic biopsy system has been developed.

J.2 Objective

This verification protocol is used to verify whether the automatic biopsy system meets product specification 7.2 to 7.4 (see Table 10.2). Biopsy of a living prostate is not possible at this stage of the project. Therefore, the automatic biopsy system is tested by taking a sample of an uncooked chicken breast

J.3 Materials

J.3.1 Instruments

The automatic biopsy system (Figure J.1) is used in this test protocol. The system is placed on a tray and fixed to the table with clamps.
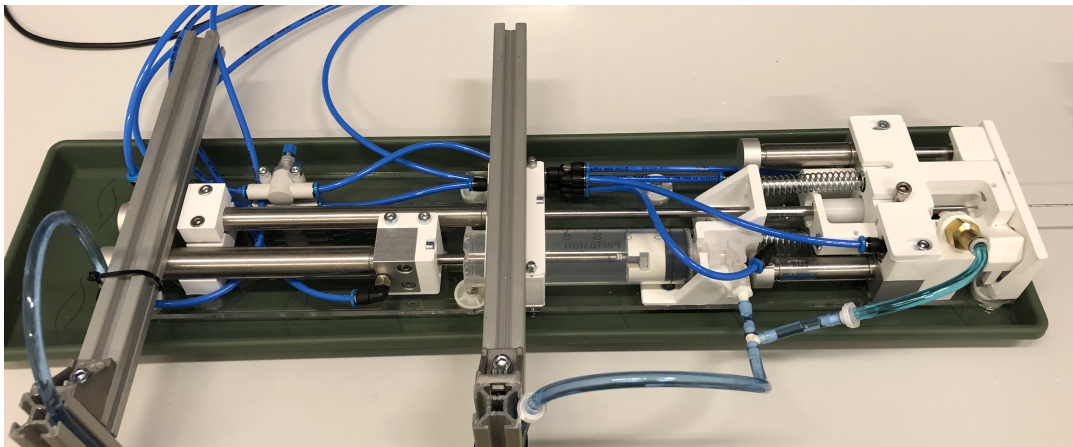
FIGURE J.1: Automatic biopsy system equipped with a standard 18G needle.

J.3.2 Equipment

The equipment used for this verification protocol is a:

- Tray for collecting water

- Specimen holder
- 1L of water
- Caliper (accuracy of 0.05 mm)
- Clamps

J.3.3 Specimens

Uncooked chicken breasts act as specimen. The chicken breasts are cooled to a temperature of 4 °Celcius. The specimen is placed on a slider and against a vertical plate that contains 19 holes (Figure J.2). Each chicken breast is sampled for a maximum of 38 times. In the first 19 runs the biopsy needle is inserted into a new hole. Before the second 19 runs are executed, the specimen is rotated for 180°with respect to the specimen holder.
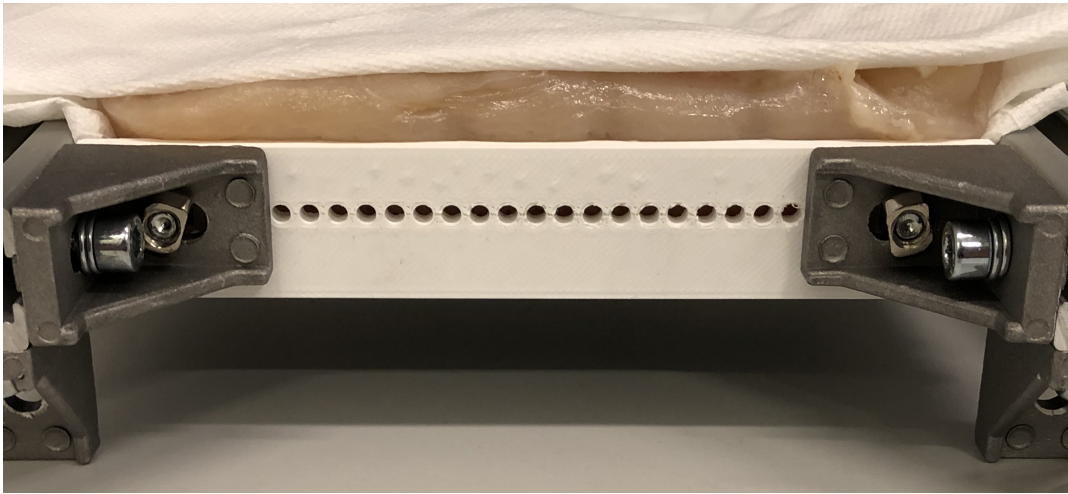
FIGURE J.2: Chicken breast in specimen holder that contained 19 different entry points (holes).

J.4 Methods

J.4.1 Product Specifications

The product specifications listed in Table J.1 are verified with this verification protocol.

TABLE J.1

PS	Product Specification	Acceptance criteria	Measured as	Risk level
7.2	Amount of removal	No obvious parts of tissue sample left on stylet notch	Yes/No	Major
7.3	Control of deposition	Tissue sample deposited on designated surface	Yes/No	Minor
7.4	Fragmentation	Tissue sample length after removal should be 80% of the length before removal	$\frac{L_{after}}{L_{before}}$	Major

Note: Initial acceptance criteria of PS-7.4 that is shown in Table 10.2 is updated because chicken instead of prostate tissue is sampled.

J.4.2 Constants and nuisance factors

The following constants are set:

- Pressure on inlet pneumatic cylinders of 4 bar

- Specimen temperature of 4 °C
- Insertion depth into specimen of 3 cm
- Flushing volume of 10 ml

The following nuisance factors might have an influence of the result.

- Sharpness of cannula and stylet

J.4.3 Experimental Design

Samples of a chicken breast are taken using the automatic biopsy system. They are removed from the stylet by flushing and deposited on the designated surface, which is the black surface area in Figure 14.2.

During each run, two measurements are reported: the length of the sample before and after removal. The percentage mentioned in the acceptance criteria of PS-7.4 is the tissue sample length after removing with respect to before removing. Besides that, tissue waste, which potentially remained on the stylet after removing the sample from the stylet, is reported. Finally, the sample depositing location is reported as correct or incorrect.

The samples are taken in a systematic manner to eliminate the influence of previous punctures on the tissue composition.
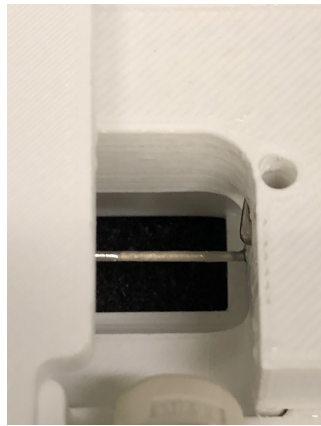
FIGURE J.3: Caption

A non-parametric binomial model is used to demonstrate a certain probability of conformance to the above-mentioned specifications at a given confidence level for characteristic that had an attributed pass/fail value (Guo et al.). The probability of conformance to a specification (PCS) is related to the risk of the characteristic (major, minor).

Major is associated with a significant degradation of prototype function, while minor only means the prototype functions poorly but still is fit for use. PS-7.2 and PS-7.4 are considered to be a major risk and have a PCS of 97%. Non-conformance to PS-7.3 poses only a minor risk (PCS of 95%).

A 90% confidence level was chosen for both specifications. According to the table shown in Guo et al., zero-failures should appear in a population size of 45 (minor risk) and 76 (major risk).

J.4.4 Experimental protocol

Biopsy using manual 18G Tru-cut needle:

1. Select entry point on specimen
2. Push stylet into specimen for up to 30 mm
3. Initiate sampling sequence of biopsy system
4. Measure the length of the sample with caliper.
5. Start flushing
6. Check whether the sample has been removed.

7. Report if obvious waste remained on the stylet.

8. Remove collecting basket with the sample from biopsy system.

9. Report if sample is deposited correctly in container

10. Again, measure and report the length of the sample with caterpillar.

11. Empty collecting basket

12. Repeat step 1 to 9 for 76 times.

J.4.5   Data Processing and Analyses

All measurements are reported in a vector format in Excel. PS-7.2 and 7.4 are verified when zero-failures are reported in 76 runs. Verification of PS-7.3 is proven when zero-failures are absent only in the first 45 runs.

J.5   Results

The raw data that was collected in this test, is shown in Figure J.6. The percentage of length after removing with respect to before is shown as well. A pass or fail value in each run is shown for the product specification 'amount of removal' is shown in Figure J.5. The same is shown for product specification 'control of deposition' in Figure J.4.
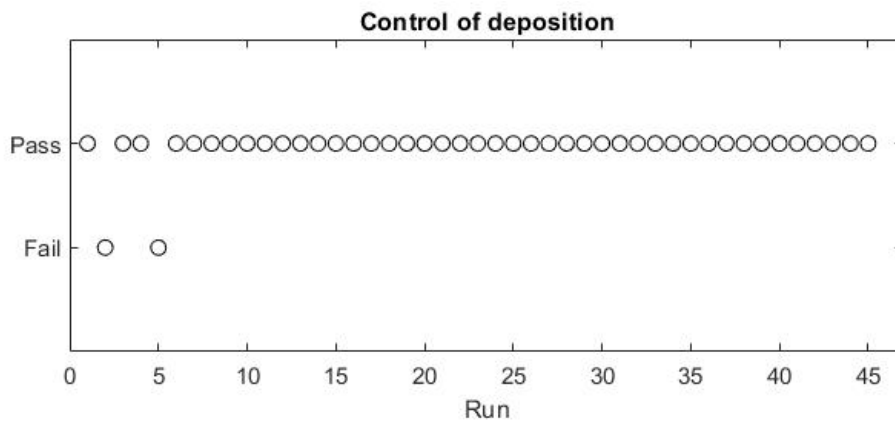
FIGURE J.4: Results of the 'Control of deposition' verification tests.
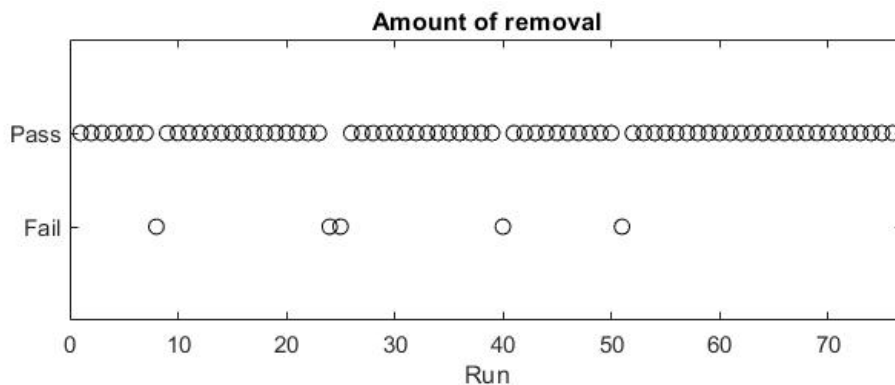
FIGURE J.5: Results of the 'amount of removal' verification tests.
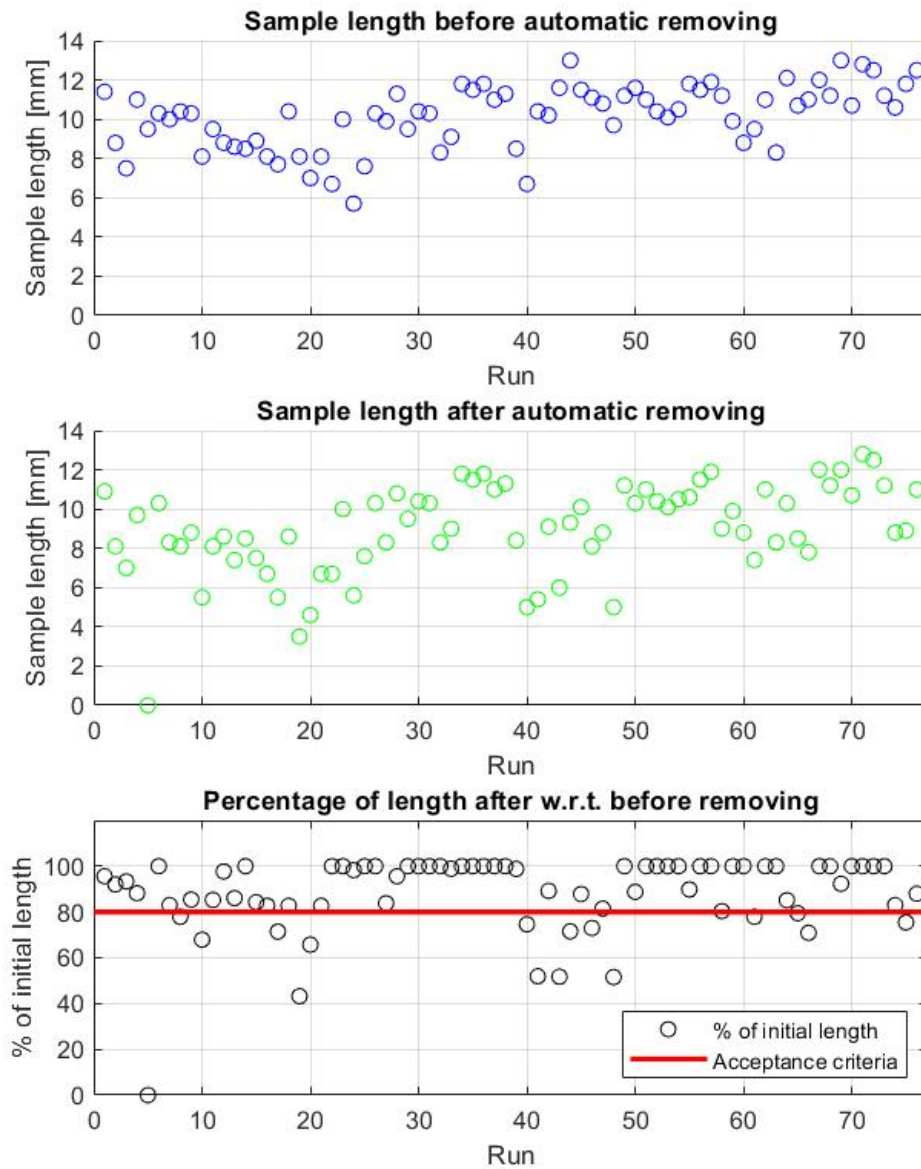
FIGURE J.6: Results of the 'fragmentation' verification tests.

Bibliography

[1] C. K. Kim, "Magnetic Resonance Imaging-Guided Prostate Biopsy: Present and Future", *Korean Journal of Radiology*, vol. 16, no. 1, pp. 90–98, 2009, ISSN: 12296929. DOI: 10.3348/kjr.2009.10.6.635.

[2] C. L. Sistrom and N. L. McKay, "Costs, charges, and revenues for hospital diagnostic imaging procedures: Differences by modality and hospital characteristics", *Journal of the American College of Radiology*, vol. 2, no. 6, pp. 511–519, 2005, ISSN: 15461440. DOI: 10.1016/j.jacr.2004.09.013.

[3] M. El Khoury, B. Mesurolle, A. Omeroglu, A. Aldis, and E. Kao, "Values of pathological analysis of lost tissue fragments in the vacuum canister during a vacuumassisted stereotactic biopsy of the breast", *British Journal of Radiology*, vol. 86, no. 1025, 2013, ISSN: 00071285. DOI: 10.1259/bjr.20120270.

[4] F. Bray, J. Ferlay, I. Soerjomataram, R. L. Siegel, L. A. Torro, and A. Jemal, "Global Cancer Statistics 2018: GLOBOCAN Estimates of Incidence and Mortality Worldwide for 36 Cancers in 185 Countries Freddie", *CA: A Cancer Journal for Clinicians*, vol. 00, no. 00, pp. 1–31, 2018, ISSN: 02507005. DOI: 10.3322/caac.21492.

[5] D. Schipper, *Demcon Web Page*, 2019. [Online]. Available: https://www.demcon.nl/demcon/.

[6] *CoBra-2 Seas Web Page*, 2018. [Online]. Available: https://cobra-2seas.eu.

[7] J. Presti, G. O'Dowd, M. Miller, R Mattu, and R. Veltri, "Extended peripheral zone biopsy schemes increase cancer detection rates and minimize variance in prostate specific antigen and age related cancer rates: results of a community multi-practice study.", *Urology*, vol. 169, pp. 125–129, 2003.

[8] L. Eskew, R. Bare, and D. McCullough, "Systematic 5 region prostate biopsy is superior to sextant method for diagnosing carcinoma of the prostate.", *Urology*, vol. 157, pp. 199–203, 1997.

[9] H Hricak, P. Choyke, S. Eberhardt, S. Leibel, and P. Scardino, "Imaging prostate cancer: a multidisciplinary perspective.", *Radiology*, vol. 243, pp. 28–53, 2007.

[10] S. Marshall and S. Taneja, "Focal therapy for prostate cancer: The current status", *Prostate International*, vol. 3, no. 2, pp. 35–41, 2015, ISSN: 2287903X. DOI: 10.1016/j.prnil.2015.03.007. [Online]. Available: http://dx.doi.org/10.1016/j.prnil.2015.03.007.

[11] R. Pereira, R. Costa, V. Muglia, J. Lajes, R. Dos Reis, F. Silva, and G. B. Silva, "Gleason score and tumor laterality in radical prostatectomy and transrectal ultrasound-guided biopsy of the prostate: a comparative study", *Asian Journal of Andrology*, vol. 0, no. 0, p. 0, 2014, ISSN: 1008-682X. DOI: 10.4103/1008-682x.146970.

[12] S. Nafie, M. Wanis, and M. Khan, "The Efficacy of Transrectal Ultrasound Guided Biopsy Versus Transperineal Template Biopsy of the Prostate in Diagnosing Prostate Cancer in Men with Previous Negative Transrectal Ultrasound Guided Biopsy.", *Urologic Oncology*, vol. 14, no. 02, pp. 3008–3012, 2017.

[13] A. Takenaka, R. Hara, T. Ishimura, T. Fujii, Y. Jo, A. Nagai, and M. Fujisawa, "A prospective randomized comparison of diagnostic efficacy between transperineal and transrectal 12-core prostate biopsy", *Prostate Cancer and Prostatic Diseases*, vol. 11, no. 2, pp. 134–138, 2008, ISSN: 13657852. DOI: 10.1038/sj.pcan.4500985.

[14] D. T. Chang, B. Challacombe, and N. Lawrentschuk, "Transperineal biopsy of the prostate-is this the future?", *Nature Reviews Urology*, vol. 10, no. 12, pp. 690–702, 2013, ISSN: 17594812. DOI: 10.1038/nrurol.2013.195.

[15] J. E. McNeal, "The zonal anatomy of the prostate", *The Prostate*, vol. 2, no. 1, pp. 35–49, 1981, ISSN: 10970045. DOI: 10.1002/pros.2990020105.

[16] *Earthslab Web Page*. [Online]. Available: https://www.earthslab.com/anatomy/prostate/.

[17] Z. Shaikhibrahim, A. Lindstrot, J. Ellinger, S. Rogenhofer, R. Buettner, S. Perner, and N. Wernert, "The peripheral zone of the prostate is more prone to tumor development than the transitional zone: Is the ETS family the key?", *Molecular Medicine Reports*, vol. 5, no. 2, pp. 313–316, 2012, ISSN: 17912997. DOI: 10.3892/mmr.2011.647.

[18] H. S. Dogan, B. Aytac, Y. Kordan, F. Gasanov, and I. Yavascaoglu, "What is the adequacy of biopsies for prostate sampling?", *Urologic Oncology: Seminars and Original Investigations*, vol. 29, no. 3, pp. 280–283, 2011, ISSN: 10781439. DOI: 10.1016/j.urolonc.2009.03.014. [Online]. Available: http://dx.doi.org/10.1016/j.urolonc.2009.03.014.

[19] K. Pandian S, H. Mohammed, C. Ben, P. Rick, and M. Sanjeev, "History of prostatectomy", *Urology news*, vol. 22, no. 2, 2018, ISSN: 00071447. DOI: 10.1136/bmj.2.3681.165-a.

[20] I. M. Thompson, D. P. Ankerst, C Chi, M. S. Lucia, P. J. Goodman, J. J. Crowley, and H. L. Parnes, "Operating Characteristics of Prostate-Specific Antigen in Men With an Initial PSA Level of 3.0 Ng / Ml or Lower", *JAMA - Journal of the American Medical Association*, vol. 294, no. 1, 2006.

[21] A Astraldi, "Diagnosis of cancer of the prostate: biopsy by rectal route", *Urol Cutaneous Rev*, vol. 41, pp. 421–422, 1937.

[22] C. J. Harvey, J. Pilcher, J. Richenberg, U. Patel, and F. Frauscher, "Applications of transrectal ultrasound in prostate cancer", *British Journal of Radiology*, vol. 85, no. SPEC. ISSUE 1, pp. 3–17, 2012, ISSN: 00071285. DOI: 10.1259/bjr/56357549.

[23] C. B. Ching, A. S. Moussa, J. Li, B. R. Lane, C. Zippe, and J. S. Jones, "Does Transrectal Ultrasound Probe Configuration Really Matter? End Fire Versus Side Fire Probe Prostate Cancer Detection Rates", *Journal of Urology*, vol. 181, no. 5, pp. 2077–2083, 2009, ISSN: 00225347. DOI: 10.1016/j.juro.2009.01.035. [Online]. Available: http://dx.doi.org/10.1016/j.juro.2009.01.035.

[24] R. Paul, C. Korzinek, U. Necknig, T. Niesel, M. Alschibaja, H. Leyh, and R. Hartung, "Influence of transrectal ultrasound probe on prostate cancer detection in transrectal ultrasound-guided sextant biopsy of prostate", *Urology*, vol. 64, no. 3, pp. 532–536, 2004, ISSN: 00904295. DOI: 10.1016/j.urology.2004.04.005.

[25] *Cancer Research Web Page*, 2005. [Online]. Available: https://www.cancer.gov/.

[26] H. C. Demirel and J. W. Davis, "Multiparametric magnetic resonance imaging: Overview of the technique, clinical applications in prostate biopsy and future directions.pdf", *TURKISH JOURNAL OF UROLOGY*, vol. 44, no. 2, pp. 93–102, 2018.

[27] M. M. Siddiqui, S. Rais-Bahrami, B. Turkbey, A. K. George, J. Rothwax, N. Shakir, C. Okoro, D. Raskolnikov, H. L. Parnes, W. M. Linehan, M. J. Merino, R. M. Simon, P. L. Choyke, B. J. Wood, and P. A. Pinto, "Comparison of MR/ultrasound fusion-guided biopsy with ultrasound-guided biopsy for the diagnosis of prostate cancer", *JAMA - Journal of the American Medical Association*, vol. 313, no. 4, pp. 390–397, 2015, ISSN: 15383598. DOI: 10.1001/jama.2014.17942.

[28] Y. H. Choi, M. Y. Kang, H. H. Sung, H. G. Jeon, B. Chang Jeong, S. I. Seo, S. S. Jeon, C. K. Kim, B. K. Park, and H. M. Lee, "Comparison of Cancer Detection Rates Between TRUS-Guided Biopsy and MRI-Targeted Biopsy According to PSA Level in Biopsy-Naive Patients: A Propensity Score Matching Analysis", *Clinical Genitourinary Cancer*, vol. 17, no. 1, e19–e25, 2019, ISSN: 19380682. DOI: 10.1016/j.clgc.2018.09.007. [Online]. Available: https://doi.org/10.1016/j.clgc.2018.09.007.

[29] S. Verma, P. L. Choyke, S. C. Eberhardt, A. Oto, C. M. Tempany, B. Turkbey, and A. B. Rosenkrantz, "The Current State of MR Imaging–targeted Biopsy Techniques for Detection of Prostate Cancer", *Radiology*, vol. 285, no. 2, pp. 343–356, 2017, ISSN: 0033-8419. DOI: 10.1148/radiol.2017161684. [Online]. Available: http://pubs.rsna.org/doi/10.1148/radiol.2017161684.

[30] A. E. Pryalukhin, A. Vandromme, A. Dellmann, K. Donhuijsen, and P. G. Hammerer, "Prostate Biopsy Core Handling: Comparison of Contemporary Preembedding Methods", *Urologia Internationalis*, vol. 95, no. 2, pp. 203–208, 2015, ISSN: 14230399. DOI: 10.1159/000375179.

[31] T. Van Der Kwast, L. Bubendorf, C. Mazerolles, M. R. Raspollini, G. J. Van Leenders, C. G. Pihl, and P. Kujala, "Guidelines on processing and reporting of prostate biopsies: The 2013 update of the pathology committee of the European Randomized Study of Screening for Prostate Cancer (ERSPC)", *Virchows Archiv*, vol. 463, no. 3, pp. 367–377, 2013, ISSN: 09456317. DOI: 10.1007/s00428-013-1466-5.

[32] T. H. Van Der Kwast, C. Lopes, C. Santonja, C.-G. Pihl, I. Neetens, P. Martikainen, S. Di Lollo, L. Bubendorf, and R. F. Hoedemaeker, "Needle Biopsies", *Clin Pathol*, no. 56, pp. 336–341, 2003.

[33] L. L. L. Boccon-Gibod, T. H. Van Der Kwast, R. Montironi, L. L. L. Boccon-Gibod, and A. Bono, "Handling and pathology reporting of prostate biopsies", *European Urology*, vol. 46, no. 2, pp. 177–181, 2004, ISSN: 03022838. DOI: 10.1016/j.eururo.2004.04.006.

[34] A. Bertaccini, A. Fandella, T. Prayer-Galetti, V. Scattoni, A. B. Galosi, V. Ficarra, C. Trombetta, M. Gion, and G. Martorana, "Systematic development of clinical practice guidelines for prostate biopsies: A 3-year Italian project", *Anticancer Research*, vol. 27, no. 1 B, pp. 659–666, 2007, ISSN: 02507005.

[35] C. Öbek, T. Doanca, S. Erdal, S. Erdoğan, and H. Durak, "Core length in prostate biopsy: Size matters", *Journal of Urology*, vol. 187, no. 6, pp. 2051–2055, 2012, ISSN: 00225347. DOI: 10.1016/j.juro.2012.01.075.

[36] M. Ergün, E. İslamoğlu, S. Yalçınkaya, H. Tokgöz, and M. Savaş, "Does length of prostate biopsy cores have an impact on diagnosis of prostate cancer?", *Turk Uroloji Dergisi*, vol. 42, no. 3, pp. 130–133, 2016, ISSN: 13084631. DOI: 10.5152/tud.2016.78700.

[37] A. Weilandt, *WO9622733A1*, 1996.

[38] H. S. Dogan, S. Y. Eskicorapci, D. Ertoy-Baydar, B. Akdogan, L. M. Gunay, and H. Ozen, "Can we obtain better specimens with an end-cutting prostatic biopsy device?", *European Urology*, vol. 47, no. 3, pp. 297–301, 2005, ISSN: 03022838. DOI: 10.1016/j.eururo.2004.09.004.

[39] L. Häggarth, P. Ekman, and L. Egevad, "A new core-biopsy instrument with an end-cut technique provides prostate biopsies with increased tissue yield", *BJU International*, vol. 90, no. 1, pp. 51–55, 2002, ISSN: 14644096. DOI: 10.1046/j.1464-410X.2002.02809.x.

[40] G. N. Ubhayakar, W. Y. Li, C. M. Corbishley, and U. Patel, "Improving glandular coverage during prostate biopsy using a long-core needle: Technical performance of an end-cutting needle", *BJU International*, vol. 89, no. 1, pp. 40–43, 2002, ISSN: 14644096. DOI: 10.1046/j.1464-4096.2001.001177.x.

[41] E. Özden, Göğüş, Tulunay, and S. Baltaci, "The Long Core Needle with an End-Cut Technique for Prostate Biopsy: Does It Really Have Advantages When Compared with Standard Needles?", *European Urology*, vol. 45, no. 3, pp. 287–291, 2004, ISSN: 03022838. DOI: 10.1016/j.eururo.2003.10.004.

[42] K. Hopper, C. Abendroth, K. Sturtz, Y. Matthews, J. Hartzel, and P. Potok, "CT Percutaneous Biopsy Guns : Devices in Cadaveric Specimens", *Group*, 1994.

[43] J. Hornak, *Basics of MRI.* 1996.

[44] S. Sammet, "Magnetic resonance safety", *Abdominal Radiology*, vol. 41, no. 3, pp. 444–451, 2016, ISSN: 23660058. DOI: 10.1007/s00261-016-0680-4.

[45] IEC, *Part 2-33: Particular requirements for the safety of magnetic resonance equipment for medical diagnosis*, 2002.

[46] E. Kanal, A. J. Barkovich, C. Bell, J. P. Borgstede, W. G. Bradley, J. W. Froelich, J. R. Gimbel, J. W. Gosbee, E. Kuhni-Kaminski, P. A. Larson, J. W. Lester, J. Nyenhuis, D. J. Schaefer, E. A. Sebek, J. Weinreb, B. L. Wilkoff, T. O. Woods, L. Lucey, and D. Hernandez, "ACR guidance document on MR safe practices: 2013", *Journal of Magnetic Resonance Imaging*, vol. 37, no. 3, pp. 501–530, 2013, ISSN: 10531807. DOI: 10.1002/jmri.24011.

[47] *MRI Questions Web Page*, 2018. [Online]. Available: http://mriquestions.com/acr-safety-zones.html.

[48] A. S.f. T. International and M. (ASTM), *Standard Practice for Marking Medical Devices and Other Items for Safety in the Magnetic Resonance Environment.* 2005.

[49] T. Palmer, P. Wojciech, S. Wilby, D. Hodgson, Y. Nagar, M. Gummerson, A. Labib, D. Jones, J. Benoit, D. Pasquier, and M. Rochdi, "Clinical and Technical Requirement Report", Interreg 2 Seas Mers Zeeën CoBra, Tech. Rep. October, 2018.

[50] M. J. Kim, E. K. Kim, J. Y. Lee, J. H. Youk, B. W. Park, S. I. Kim, H. Kim, and K. K. Oh, "Breast lesions with imaging-histologic discordance during US-guided 14G automated core biopsy: Can the directional vacuum-assisted removal replace the surgical excision? Initial findings", *European Radiology*, vol. 17, no. 9, pp. 2376–2383, 2007, ISSN: 09387994. DOI: 10.1007/s00330-007-0603-4.

[51] M. J. Kim, S. I. Kim, J. H. Youk, H. J. Moon, J. Y. Kwak, B. W. Park, and E. K. Kim, "The diagnosis of non-malignant papillary lesions of the breast: Comparison of ultrasound-guided automated gun biopsy and vacuum-assisted removal", *Clinical Radiology*, vol. 66, no. 6, pp. 530–535, 2011, ISSN: 00099260. DOI: 10.1016/j.crad.2011.01.008. [Online]. Available: http://dx.doi.org/10.1016/j.crad.2011.01.008.

[52] Y. M. Sohn, J. H. Yoon, E. K. Kim, H. J. Moon, and M. J. Kim, "Percutaneous ultrasound-guided vacuum-assisted removal versus surgery for breast lesions showing imaging-histology discordance after ultrasound-guided core-needle biopsy", *Korean Journal of Radiology*, vol. 15, no. 6, pp. 697–703, 2014, ISSN: 12296929. DOI: 10.3348/kjr.2014.15.6.697.

[53] L Tothova, K Rauova, L Valkovic, L Vanovcanova, and V Lehotska, "Stereotactic vacuum-assisted breast biopsy: our experience and comparison with stereotactic automated needle biopsy", *Bratisl Lek Listy*, vol. 114, no. 2, pp. 71–77, 2013.

[54] *Mammotome Elite 13G and 10G Brochure*, 2015.

[55] R. K. Bryan, *US2018242959A1*, 2018.

[56] E. Nevo and Z. Berger, *WO2018127848A1*, 2018.

[57] T. K. Toft, L. U. Nielsen, K. S. Christensen, S. K. K. Hansen, T. Gundberg, H. Harboe, and O. Kjeldsen, *WO2018087367A2*, 2018.

[58] Hologic, *Brevera Web Page*, 2018. [Online]. Available: www.breverabiopsy.com.

[59] TeesuVac, "TeesuVac Web Page", [Online]. Available: https://teesuvac.com.

[60] R. Bard, "MRI Directional Vacuum-Assisted Biopsy Device and Driver", 2015.

[61] G. H. Inal, V. Öztekin, Uğurlu, M. Kosan, Akdemir, and M. Çetinkaya, "Sixteen gauge needles improve specimen quality but not cancer detection rate in transrectal ultrasound-guided 10-core prostate biopsies", *Prostate Cancer and Prostatic Diseases*, vol. 11, no. 3, pp. 270–273, 2008, ISSN: 13657852. DOI: 10.1038/pcan.2008.34.

[62] G. Torlakovic, E. Torlakovic, and V. K. Grover, "Easy method of assessing volume of prostate adenocarcinoma from estimated tumor area: Using prostate tissue density to bridge gap between percentage involvement and tumor volume", *Croatian Medical Journal*, vol. 46, no. 3, pp. 423–428, 2005, ISSN: 0353-9504.

[63] H. Graf, G. Steidle, P. Martirosian, U. A. Lauer, and F. Schick, "Metal artifacts caused by gradient switching", *Magnetic Resonance in Medicine*, vol. 54, no. 1, pp. 231–234, 2005, ISSN: 07403194. DOI: 10.1002/mrm.20524.

[64] B. A. Hargreaves, P. W. Worters, K. B. Pauly, J. M. Pauly, K. M. Koch, and G. E. Gold, "Metal-induced artifacts in MRI", *American Journal of Roentgenology*, vol. 197, no. 3, pp. 547–555, 2011, ISSN: 0361803X. DOI: 10.2214/AJR.11.7364.

[65] M. K. Konings, L. W. Bartels, H. F. Smits, and C. J. Bakker, "Heating around intravascular guidewires by resonating RF waves", *Journal of Magnetic Resonance Imaging*, vol. 12, no. 1, pp. 79–85, 2000, ISSN: 10531807. DOI: 10.1002/1522-2586(200007)12:1<79::AID-JMRI9>3.0.CO;2-T.

[66] S. A. Mohsin, J. A. Nyenhuis, and R. Masood, "Interaction of Medical Implants With the Mri Electromagnetic Fields", *Progress In Electromagnetics Research C*, vol. 13, pp. 195–202, 2010. DOI: 10.2528/pierc10041805.

[67] ISO, *Sterilization of medical devices — Microbiological methods — Part 2: Tests of sterility performed in the definition, validation and maintenance of a sterilization process*.

[68] J. F. Schenck, "The role of magnetic susceptibility in magnetic resonance imaging: MRI magnetic compatibility of the first and second kinds", *Medical Physics*, vol. 23, no. 6, pp. 815–850, 1996, ISSN: 00942405. DOI: 10.1118/1.597854.

[69] S. J. Zhang, H. N. Qian, Y. Zhao, K. Sun, H. Q. Wang, G. Q. Liang, F. H. Li, and Z. Li, "Relationship between age and prostate size", *Asian Journal of Andrology*, vol. 15, no. 1, pp. 116–120, 2013, ISSN: 1008682X. DOI: 10.1038/aja.2012.127. [Online]. Available: http://dx.doi.org/10.1038/aja.2012.127.

[70] M. Mahvash and P. E. Dupont, "Mechanics of Dynamic Needle Insertion", *Biomedical Engineering, IEEE Transactions on*, vol. 57, no. 4, pp. 934–943, 2010.

[71] D. Van Gerwen, *Needle-Tissue Interaction by Experiment*. 2013. DOI: 10.4233/uuid:c2dac8ee-0529-49ae-8374-2d49efd0ba90. [Online]. Available: http://repository.tudelft.nl/view/ir/uuid%3Ac2dac8ee-0529-49ae-8374-2d49efd0ba90/.

[72] O. Wendt, C. Siewert, T. Lüth, R. Felix, and U. Boenick, "Schnittgeschwindig keiten und biopsieerfolg unterschiedlicher stanzbiopsieinstrumente", *Radiologe*, vol. 41, no. 6, pp. 484–490, 2001, ISSN: 0033832X. DOI: 10.1007/s001170051059.

[73] K. Spanner and B. Koc, "Piezoelectric Motors, an Overview", *Actuators*, vol. 5, no. 1, p. 6, 2016. DOI: 10.3390/act5010006.

[74] *Festo Web Page*. [Online]. Available: https://www.festo.com/cms/nl-be_be/15945.htm.

[75] ISO, *Medical gas pipeline systems - Part 1: Pipeline systems for compressed medical gases and vacuum*.

[76] "Ultrasonic Piezomotors", PI, Tech. Rep.

[77] *Piezomotor Web Page*.

[78] G. S. Fischer, I. Iordachita, C. Csoma, J. Tokuda, S. P. Dimaio, C. M. Tempany, and N. Hata, "MRI-Compatible Pneumatic Robot for Transperineal Prostate Needle Placement", vol. 13, no. 3, pp. 295–305, 2008.

[79] P. Shokrollahi, J. M. Drake, and A. A. Goldenberg, "A study on observed ultrasonic motor-induced magnetic resonance imaging (MRI)artifacts", *Biomedical Journal*, vol. 42, no. 2, pp. 116–123, 2019, ISSN: 23194170. DOI: 10.1016/j.bj.2018.12.007. [Online]. Available: https://doi.org/10.1016/j.bj.2018.12.007.

[80] Y. Wang, G. A. Cole, H. Su, J. G. Pilitsis, and G. S. Fischer, "MRI compatibility evaluation of a piezoelectric actuator system for a neural interventional robot", *Proceedings of the 31st Annual International Conference of the IEEE Engineering in Medicine and Biology Society: Engineering the Future of Biomedicine, EMBC 2009*, pp. 6072–6075, 2009, ISSN: 1557-170X. DOI: 10.1109/IEMBS.2009.5334206.

[81] *Blue white Web Page*. [Online]. Available: https://www.blue-white.com/peristaltic-pump-wear-factors/.

[82] A. Cicione, F. Cantiello, C. De Nunzio, A. Tubaro, and R. Damiano, "Prostate biopsy quality is independent of needle size: A randomized single-center prospective study", *Urologia Internationalis*, vol. 89, no. 1, pp. 57–60, 2012, ISSN: 00421138. DOI: 10.1159/000339250.